1980

Transport of ozone across an air/water interface coupled with aqueous decomposition

Ahmad Ali Mehrabzadeh
Portland State University

AN ABSTRACT OF THE THESIS OF Ahmad Ali Mehrabzadeh for the Master of Science in Chemistry presented July 25, 1980.

Title: Transport of Ozone Across an Air/Water Interface Coupled with Aqueous Decomposition

APPROVED BY MEMBERS OF THE THESIS COMMITTEE:

[redacted]

Robert J. O'Brien, Chairman

[redacted]

Bruce W. Brown

[redacted]

David K. Roe

Photoacoustic spectroscopy was used to analyze the transport of ozone through the air/water interface. Experimental results showed that the ozone transport rate is similar to rates measured for other gases of low solubility and low reactivity. The transport rate increases with increasing pH. The decomposition rate of ozone was studied in solutions. The decomposition rate also depends on the pH of the solution, and in high pHs both the deposition velocity and the decomposition rate constant of ozone have larger values. The value of the deposition velocity (K_d) is $3.7\pm.9\times10^{-3}$ cm/sec and the decomposition

rate constant is $5.3 \pm 0.6 \times 10^{-5}$ sec^{-1} for distilled water. For ocean water, the respective values are $5.2 \pm 0.4 \times 10^{-3}$ sec^{-1} and $7.8 \pm 0.4 \times 10^{-4}$ cm/sec respectively.

Previous studies of ozone transport into natural water bodies are apparently incorrect. These studies ignored ozone solubility and considered ozone to be destroyed upon surface contact. The ozone flux rates currently used for the ocean are apparently 10 to 100 times too great. These lower ozone fluxes should have a significant impact on tropospheric/stratospheric photochemical models. Ozone concentrations predicted for surface waters of the earth in unpolluted regions are predicted to range from 20 ng/L to 2 ng/L. Surface water ozone levels in areas suffering from photochemical air pollution may be 10 to 15 times higher than these levels at times. The ecological impact of these ozone levels is apparently unrecognized but may be significant.

TRANSPORT OF OZONE ACROSS AN AIR/WATER INTERFACE COUPLED WITH AQUEOUS DECOMPOSITION

by

AHMAD ALI MEHRABZADEH

A thesis submitted in partial fulfillment of the requirements for the degree of

MASTER OF SCIENCE
in
CHEMISTRY

Portland State University

1980

TO THE OFFICE OF GRADUATE STUDIES AND RESEARCH:

The members of the Committee approve the thesis of Ahmad Ali Mehrabzadeh presented July 25, 1980.

[redacted]

Robert J. O'Brien

[redacted]

Bruce W. Brown

[redacted]

David K. Roe

APPROVED:

[redacted]

Bruce W. Brown, Acting Department Chairman, Dept. of Chemistry

[redacted]

Stanley Rauch, Dean of Graduate Studies and Research

ACKNOWLEDGEMENTS

I would like to thank Dr. David Roe, as my first advisor, for his help throughout the course of this research. Also, I wish to thank Jim Sweet, Mario Aparicio-Razo and Jane McDowell for helping me with my thesis.

My appreciation and gratitude are extended to Dr. Robert O'Brien, my research advisor, for his help and patience throughout the duration of this project.

And I extend my special thanks to my wife, Manijeh.

TABLE OF CONTENTS

LIST OF TABLES

LIST OF FIGURES

FIGURE PAGE

FIGURE PAGE

FIGURE PAGE

CHAPTER I

INTRODUCTION

Ozone is formed by the absorption of far ultraviolet solar radiation by oxygen in the middle and upper stratosphere. Ozone in the troposphere has traditionally been attributed to two different sources--injection from the stratosphere and photochemical oxidation processes. The ozone concentration in clean air is typically 35 ppb (1). In polluted air it varies from 0 to 800 ppb (2).

The possible mechanisms for destruction of tropospheric ozone are the following:

1. Thermal decomposition
2. Photochemical reaction
3. Reaction with other gases
4. Reaction with earth surfaces
5. Reaction with atmospheric aerosols.

Thermal decomposition of ozone is too slow to be important (3). Photolysis of ozone is followed by rapid recombination of O and O_2.

$$O_3 + h\nu \rightarrow O_2 + O(^3P) \qquad \lambda > 309 \text{ nm}$$

$$O_2 + O(^3P) + M \rightarrow O_3 + M$$

So this process is not important in the destruction of ozone. However the production of $O(^1D)$ from uv photolysis of ozone leads to production of hydroxyl radical. Crutzen (4) proposed a large photochemical sink for ozone of the order of 10^{11} molecules cm^2 sec^{-1} in the troposphere

via this reaction sequence:

$$O_3 + h\nu \rightarrow O(^1D) + O_2 \qquad \lambda > 309 \text{ nm}$$

$$O(^1D) + H_2O \rightarrow 2\ OH$$

Inclusion of methane oxidation by OH is capable of enough catalytic production of ozone in the troposphere to compensate to some extent for the amount of ozone destroyed photochemically (4, 5).

$$CH_4 + 4\ O_2 \xrightarrow{\text{OH catalyzed}} H_2O + H_2 + 2\ O_3 + CO$$

Ozone can also be destroyed by reaction with NO_x (6).

$$NO + O_3 \rightarrow NO_2 + O_2$$

$$NO_2 + O_3 \rightarrow NO_3 + O_2$$

$$O + NO_2 \rightarrow NO + O_2$$

Chameides (7) estimated that photochemical processes produce about 0.6×10^{11} and destroy about 1.4×10^{11} ozone molecules $cm^{-2}sec^{-1}$, while mixing processes transport about 1.4×10^{11} ozone molecules $cm^{-2}sec^{-1}$ from the stratosphere into the troposphere and ground level flux destroys about 0.6×10^{11} ozome molecules $cm^{-2}sec^{-1}$. Singh (8), by considering some recent models (7), concluded that photochemistry involving natural hydrocarbons (including CH_4 and CO) and NO_x plays at best a relatively insignificant role in determining the net tropospheric O_3 balance, so important sinks are O_3 destruction near the earth's surfaces and to a less certain degree the gas phase photolysis that results in some net O_3 destruction.

Experimental measurements of Aldaz (9) and theoretical calculations by Fabian (10) of the earth's sink strength for atmospheric

ozone shows 3.3 to 6 x 10^{10} molecules $cm^{-2}sec^{-1}$. The rates of O_3 destruction depend on the surface conditions. For instance, sea water surface seems about 5 times less effective than grassland (11,12).

Comparison of various figures for the rate of O_3 destroyed in the troposphere and rate of destruction of O_3 on various earth surfaces indicates that the reaction at the earth's surface is an important sink for ozone.

In 1969 Aldaz (9, 13) by using the "box method" experimentally measured the destruction rate of ozone on natural land and water surfaces. Briefly the procedure consists of using a cubic box (1 m^3) open on the bottom and covered with mylar film, which was considered to be nearly inert to ozone. A small amount of ozone was injected, and chemical reaction with the surface was observed by measuring the decrease of the ozone concentration as a function of time with a chemiluminescent detector (14).

He assumed that ozone will be destroyed at the time of collision on the surface of the earth (land or water). The flux (F) of ozone is obtained from the expression

$$F = k_d(O_3) \qquad \text{molecules/cm}^2\text{-sec}$$

where (O_3) is the ozone concentration in molecules/cm^3 and k_d is the deposition velocity. Thus k_d has dimensions of velocity

$$k_d = \frac{F}{[O_3]} = \frac{\text{molecule/cm}^2\text{-sec}}{\text{molecule/cm}^3} = \frac{\text{cm}}{\text{sec}}$$

He measured a deposition velocity of 0.60 cm/sec over grassland and desert, 0.04 cm/sec over seawater, and 0.02 cm/sec over snow.

In 1970, P. Fabian and E. Junge (10) developed a mathematical model to estimate the vertical ozone transport in the lower troposphere due to turbulence as a function of wind velocity and surface roughness. They obtained good agreement with previous estimates of the ozone global rate by Aldaz, but they suggested a possible source of error in the ozone deposition velocity on the ocean surface. The value of k_d = .04 cm/sec that Aldaz obtained from the box method may perhaps be too low due to chemically active particles of the ocean spray layer.

In 1972 H. Tiefenau and P. Fabian (15) and later in 1973 H. Tiefenau (16), estimated the deposition velocity of ozone on ocean surfaces from profile measurements between 1 and 20 m height above the open ocean at a lighthouse on the North Sea. The yield of k_d = $8 - 17 \times 10^{-3}$ cm/sec was about four times smaller than Aldaz's results ($k_d = 4 \times 10^{-2}$). They suspected that the discrepancy between their result and the laboratory data of Aldaz was that the box method is not applicable for true natural conditions.

In 1974 V.H. Regener (17) suggested a theoretical procedure for evaluation of the deposition velocity of ozone at earth surfaces. The method is applicable when the ozone profile on one hand and the wind speed at a fixed level on the other hand, are measured simultaneously. He calculated the differential ozone profile as a function of deposition velocity k_d. Unknown k_d can now be determined by a best fit of the differential function (given by Regener) to the measured vertical distribution of ozone density. Application of this method to some ozone profiles by Tiefenan and Fabian leads to k_d = 0.1 cm/sec at the surface of water which is about two to four times larger than the value obtained in the "flux method" by Aldaz.

Liss (18) suggested the use of a two layer model to estimate the flux of various gases across the air-sea interface. He described the deposition velocity for gases as an exchange constant, and the reciprocal of the exchange constant is a measure of the "resistance" to gas transfer. The total resistance to the exchange of any gas will be due to a combination of the resistance of the gas and liquid phases (Fig. 1). He showed that liquid phase resistance will dominate for all sparingly soluble gases which are not chemically reactive, for example, O_2, N_2, CO, CH_4, and N_2O. Thus all resistance to transfer across the interface occurs in the liquid phase. The value for the liquid phase exchange constant appropriate to sea surface is .0056 cm/sec (18). Although Liss did not consider the case for ozone, the situation should be almost the same because of low solubility (19, 20) and reactivity.

Junge (21) has used a model similar to the Liss (18) model to estimate halocarbon transport into the sea. He assumed the ocean can be subdivided with sufficient approximation into two reservoirs, the mixed layer and the deep sea. Then he determined the flux of gas across the interface by molecular diffusion through the laminar surface layer of thickness δ. Thus deposition velocity is the ratio of diffusion coefficient (D) of the gas to δ, the thickness of the laminar layer (D/δ). The values of D and δ were reported by Broeker and Peng (22). (Liss, also, in his calculation referred to these data.) $D = 1.57 \times 10^{-5}$ cm^2/sec for O_2 and $\delta = 7 \times 10^{-3}$ cm. δ was measured by the escape rate of radon formed in the mixed layer by decay of dissolved radium. By using these values of D and δ, $k_d = D/\delta = 2 \times 10^{-3}$ cm/sec.

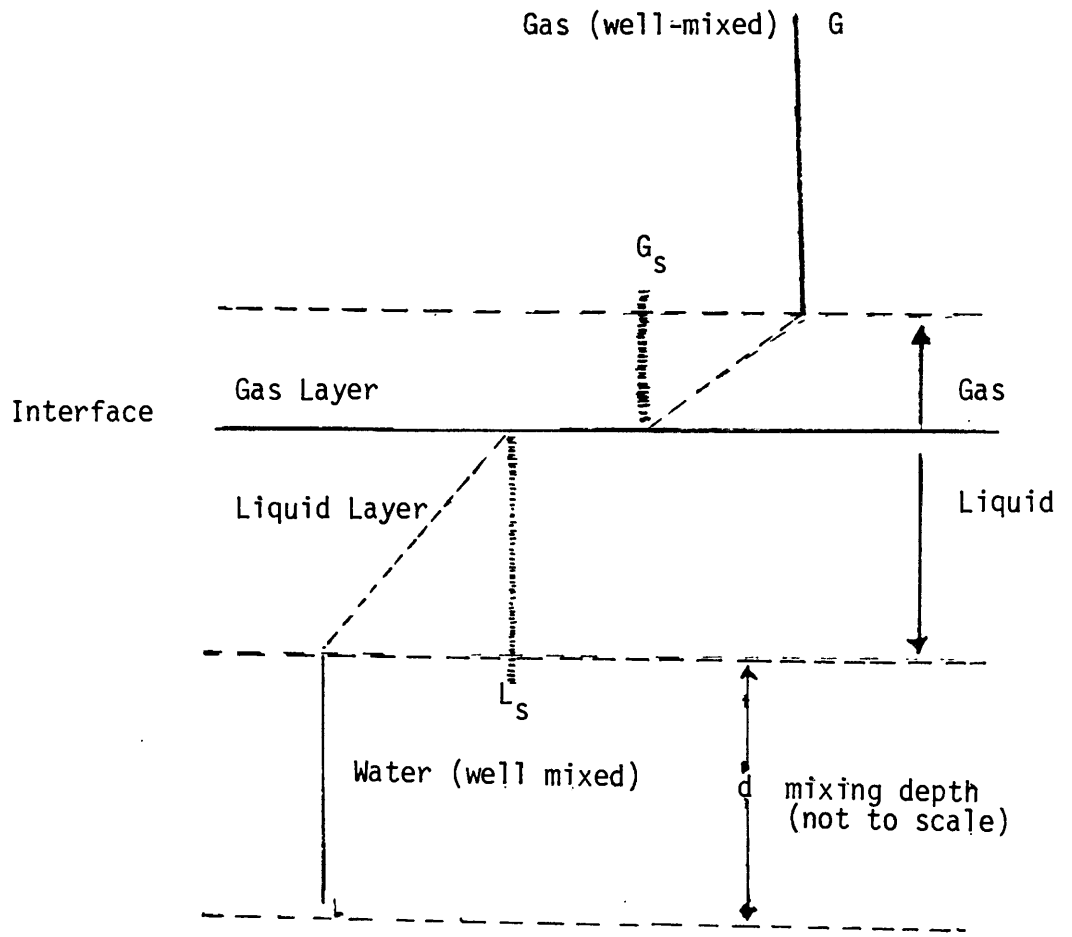

Figure 1. Two-layer model of a gas-liquid interface.

Thus, according to measurement and theoretical calculation, the value of the specific exchange constant or deposition velocity of ozone on water surfaces ranges between 8×10^{-3} and 1×10^{-1} cm/sec (Table I).

Most current global ozone models refer to the value of $k_d = .04$ obtained by Aldaz. Crutzen estimated the natural and man-caused ozone perturbations due to NO_x (11), by using a two-dimensional photochemical model and he used the value of k_d measured by Aldaz. He also used Aldaz's k_d value in his numerical study of the troposphere using a one-dimensional model (12). Chameides (23) used a photochemical model to calculate significant rates of photochemical production and destruction of ozone for background tropospheric conditions. This model also used the results of Aldaz.

As oceans cover about 70% of the earth's surface, an increase or decrease in the ozone decomposition velocity could mean a significant change in the calculated global ozone sink and in the concentration of ozone above ocean surfaces.

Aldaz and other authors in their study assume that ozone is destroyed at the time of collision at the surface, and didn't consider any diffusion of ozone into the water or decomposition in water. Ozone has a Henry's Law coefficient in distilled water of 3.3 at $25^{o}C$ (19, 20). Weiss (24), Alder (25), and Kilpatrick (26) studied the destruction rate of ozone in solutions. They found the reaction of ozone with water had an order of 1, 3/2, or 2 depending on the concentration of ozone in solution and the pH of the solution. The rate of decomposition of ozone increased at increasing pH (25, 26), but at pH around neutral,

TABLE I

DEPOSITION VELOCITY (k_d) VALUES AS REPORTED BY DIFFERENT METHODS AND AUTHORS

Author	Method	Deposition Velocity k_d (cm/sec)	Date	Reference
Aldaz	"Box Method"	0.04	1969	(9)
Fabian and Junge	Theoretical Calculation	suggests $k_d < 0.04$	1970	(10)
Tiefenau and Fabian	Lighthouse	0.0018 to 0.017	1972 1973	(15) (16)
Regener	Theoretical Calculation	0.1	1974	(17)
Liss	"	0.0056	1974	(18)
Junge	"	0.002	1976	(21)

decomposition is relatively slow ($T \approx$ several hours).

Since all previous geophysical work assumed ozone was destroyed at the surface of the ocean, the possibility of dissolved ozone in the surface water of the ocean has apparently never been raised. This possibility may have significant ecological implications. This research is an attempt to study more carefully ozone destruction on and below water surfaces.

CHAPTER II

THEORY

Theoretical study and calculation of the decomposition velocity (k_d) of ozone on water surfaces and the rate constant of decomposition of ozone in water was done by considering the following model.

If ozone flows through a well-mixed reactor vessel, then some of the ozone will enter solution through the surface. The ozone may either re-evaporate or be destroyed. Finally, the undestroyed ozone will flow out. The reaction for each step is:

1) Flow in

$$G_0 \xrightarrow{k_1} G \qquad (1)$$

where G_0 = initial concentration of ozone which is entering the reactor

G = concentration of ozone in the gas phase of the reactor

2) Flow out

$$G \xrightarrow{k_2} \text{Loss} \qquad (2)$$

3) Diffusion of ozone from gas phase to liquid phase

$$G_1 \xrightarrow{k_3} L \qquad (3)$$

where L = concentration of ozone in the liquid phase.

4) Diffusion of ozone from liquid phase to gas phase

$$L \xrightarrow{k_4} G_1 \qquad (4)$$

5) Decomposition of ozone in water

$$L \xrightarrow{k_5} \text{Loss} \tag{5}$$

6) Decomposition of ozone on surface of glass of gas phase part of reactor

$$G \xrightarrow{k_6} \text{Loss} \tag{6}$$

Diffusion of ozone in the gas and liquid phases will be assumed to be rapid in this model. The rate for each step is given by the following expressions:

$$\text{Reaction 1} = k_1 G_0 = \frac{F}{V_g} G_0 = R_1 \tag{7}$$

where F = flow rate of the input ozone

V_g = volume of the gas phase

$$\text{Reaction 2} = k_2 G = \frac{F}{V_g} G = R_2 \tag{8}$$

$$\text{Reaction 5} = k_5 L^n = R_5 \tag{9}$$

where k_5 = rate constant of decomposition of ozone in the liquid phase

n = order of reaction.

The decomposition of ozone in aqueous media has been found to be represented by first (25), 3/2 (26) and second order (24) dependence on ozone concentration. Alder and Hill (25) had reported that 10^{-4} M ozone in 0.1 M $HClO_4$ solution. The decomposition of ozone follows the first order law. Kilpatrick (26) repeated Alder's measurement with 10^{-2} M O_3 in 0.1 M $HClO_4$ solution, and found that the decomposition of ozone follows the 3/2 order law. Also, Kilpatrick (26) did the experiment in NaOH solution. The NaOH solutions were prepared by

dilution of carbonate-free 0.1 M NaOH with CO_2-free water. The rate of decomposition was found to be second order.

$$\underline{\text{Reaction 6}} = k_6 G = R_6 \tag{10}$$

where k_6 = the rate constant of decomposition of ozone on the glass of the gas phase reaction vessel (assumed to be first order).

Reactions 3 and 4. For calculation of the rates of reactions 3 and 4, which represent transfer of ozone between the gas and liquid phases, a two layer film system is used (27). This system was described by Liss (18). The main body of each fluid is assumed to be well mixed. The main resistance to gas transport comes from the gas and liquid phases' interfacial layers, across which the exchanging gases transfer by molecular processes (Fig. 1). Assuming transport through the layer system is by molecular diffusion, Fick's First Law in the one-dimensional form (with z as the vertical direction) is applicable.

$$F = -D \frac{\partial c}{\partial z} \tag{11}$$

where F is the flux of gas through each layer; D the coefficient of molecular diffusion of gas in the layer material and c the gas concentration.

The more usual form of equation (11) for gas exchange studies is:

$$F = k_d \times \Delta c \tag{12}$$

where Δc is the concentration difference across the layer and k_d the exchange constant or deposition velocity because it has dimensions of velocity (cm/sec). It is a measure of the flux of gas per unit concentration gradient.

Applying equation (12) to the two-layer situation shown in Fig. 1, and assuming that transport of gas across the interface is a steady state process, it follows that

vertical flux of ozone from the gas phase = $F_g = k_g(G - G_s)$ (13)

vertical flux of ozone in the liquid phase = $F_\ell = k_\ell(L_s - L)$ (14)

$$F = F_g = k_g(G - G_s) = F_\ell = k_\ell(L_s - L)_s \quad (15)$$

where G_s and L_s are the concentration of ozone at the interface of each phase. k_g and k_ℓ are the exchange constant (deposition velocity, for gas and liquid phases), respectively. Assuming the interface itself has no resistance, then the exchanging gas obeys Henry's Law, and

$$G_s = HL_s \quad (16)$$

Solving for G_s and L_s between equations (15) and (16) leaves

$$F = k_g(G - HL_s) = k_\ell(L_s - L) \quad (17)$$

$$k_gG_g - k_gHL = k_\ell L_s - k_\ell L$$

$$kgG + k_\ell L = k_\ell L_s + k_gHL_s = L_s(k_\ell + k_gH)$$

$$L_s = \frac{k_gG + k_\ell L}{k_\ell + k_gH} \quad (18)$$

$$G_s = H\,\frac{k_gG + k_\ell L}{k_\ell + k_gH} \quad (19)$$

Thus

$$F_g = k_g(G - G_s) = k_g\left(G - \frac{Hk_gG + Hk_\ell L}{k_\ell + k_gH}\right)$$

$$= k_g\,\frac{Gk_\ell + Gk_gH - Hk_gG - Hk_\ell L}{k_\ell + Hk_g}$$

$$= (G_g - HL)\,\frac{k_gk_\ell}{k_\ell + Hk_g} = (G - HL)\left(\frac{1}{k_g} + \frac{H}{k_\ell}\right)^{-1} \quad (20)$$

$$F_L = k_\ell(L_s - K) = \frac{k_gg + k_\ell L}{k_\ell + Hk_g} - L$$

$$= (G/H - L)\left(\frac{1}{k_\ell} + \frac{1}{Hk_g}\right)^{-1} \quad (21)$$

The reciprocal of the exchange constant is a measure of "resistance" to gas transfer. The total resistance to exchange of any gas will be due to a combination of the resistance of the gas and liquid phases, so

$$\text{resistance of the gas phase} = r_g = \frac{1}{k_g} \tag{22}$$

$$\text{resistance of the liquid phase} = r_\ell = \frac{1}{k_\ell} \tag{23}$$

$$\text{Total resistance of gas phase} = R_g = \frac{1}{K_g} = \frac{1}{k_g} + \frac{H}{k_\ell} \tag{24}$$

$$\text{Total resistance of liquid phase} = R_\ell = \frac{1}{K_\ell} = \frac{1}{k_\ell} + \frac{1}{Hk_g} \tag{25}$$

Thus equations (20) and (21) can be written as

$$F_g = K_g(G - HL) \tag{26}$$

$$F_L = K_\ell(G/H - L) \tag{27}$$

For sparingly soluble gases which are not chemically reactive $r_\ell >> r_g$ so

$$K_g = \frac{k_\ell}{H} \tag{28}$$

$$K_\ell = k_\ell \tag{29}$$

so

$$F = F_g = \frac{k_\ell}{H}(G - HL) \tag{30}$$

$$F = F_L = k_\ell(G/H - L) \tag{31}$$

Equations (30) and (31) can be applied to reactions (3) and (4), thus

$$\text{for gas phase} = \frac{dG}{dt} = -R_3 + R_4 = -F_g \times \frac{Ag}{Vg} \tag{32}$$

$$\text{for liquid phase} = \frac{dL}{dt} = R_3 - R_4 = F_\ell \frac{A_\ell}{V_\ell} \tag{33}$$

where Ag and Vg are the surface and volume of the gas phase and A_ℓ and V_ℓ are the surface and volume of the liquid phase, respectively. In the case of the cylindrical reactor,

$$\frac{A_g}{V_g} = h_g \qquad h_g = \text{height of the gas phase} \tag{34}$$

$$\frac{A_\ell}{V_\ell} = h_\ell \qquad h_\ell = \text{height of the liquid phase} \tag{35}$$

Thus (32) and (33) are

$$(-R_3 + R_4) = \frac{-F_g}{h_g} = \frac{-k_\ell}{Hh_g}(G - HL) \tag{36}$$

$$(R_3 - R_4) = \frac{F_\ell}{h_\ell} = \frac{-k_\ell}{Hh_\ell}(G - HL) \tag{37}$$

Now by considering all 6 reactions for ozone,

$$\frac{dG}{dt} = R_1 - R_2 - R_3 + R_4 - R_6 \tag{38}$$

$$\frac{dL}{dt} = R_3 - R_4 - R_5 \tag{39}$$

$$\frac{dG}{dt} = \frac{F}{V_g}G_0 - \frac{F}{V_g}G - \frac{k_\ell}{Hh_g}(G - HL) - k_6G \tag{40}$$

$$\frac{dL}{dt} = \frac{k_\ell}{Hh_\ell}(G - HL) - k_5L^n \tag{41}$$

These two differential equations may be solved by numerical integration (appendix A).

A subcase of equations (40) and (41) is a stop flow experiment ($F_1 = 0$). Since $R_1 = R_2 = 0$,

$$\frac{dG}{dt} = \frac{-k_\ell}{Hh_\ell}(G - HL) - k_6G \tag{42}$$

$$\frac{dL}{dt} = \frac{k_\ell}{Hh_\ell}(G - HL) - k_5L^n \tag{43}$$

if the concentration of the liquid phase (L) = 0 (i.e., $V_\ell >> V_g$). Then equation (42) can be written as:

$$\frac{dG}{dt} = \frac{-kL}{Hh_g} G - k_6 G = \left(- \frac{k_\ell}{Hh_g} + k_6 \right) G$$

Thus the slope of a plot of ln G vs. time is given by

$$\text{slope} = \frac{k_\ell}{Hh_g} + k_6 \qquad (44)$$

or

$$k_\ell = (\text{slope} - k_6)\, H \cdot h_g \qquad (45)$$

This allows calculation of the value of k_ℓ, the ozone transfer coefficient.

If the concentration of ozone in the liquid phase is not zero, then both differential equations must be solved simultaneously. By using measured values for the deposition velocity, k_5 (the rate constant of decomposition of ozone in solution) can be determined by using the computer program (Appendix B) to reproduce the gas phase data.

The rate constant of destruction of ozone on the glass surface (k_6) can be determined from equation (45) if the liquid phase is absent. It can be shown that k_6 measured in a dry spherical vessel is the same k_6 operating in the vessel half-filled with water. Furthermore, a hemispherical gas phase vessel will give the lowest possible contribution of ozone decomposition on glass to overall ozone loss. The volume or radius of such a vessel is not a factor.

CHAPTER III

EXPERIMENTATION, RESULTS AND DISCUSSION

DETECTION OF OZONE IN THE GAS PHASE

Photoacoustic Spectroscopy (PAS)

In photoacoustic spectroscopy, light energy is first converted into sound and then into an electrical signal (28). A modulated beam passes through a container that holds a gas sample. Energy absorbed by the gas from the beam heats the gas and causes its pressure to rise. Since the beam is modulated, this pressure rise is periodic at the beam modulation frequency. It is detected by a microphone and converted into an electrical signal.

Ozone can absorb light and decompose via the reaction sequence

$$O_3 + h\nu\ (\lambda = 254) \rightarrow O_2 + O('D) - 42.2\ \text{kcal/mol}$$

$$O('D) + M \rightarrow O(^3P) + M - 45.25\ \text{kcal/mol}$$

$$O(^3P) + O_2 + M \rightarrow O_3 + M - 25.5\ \text{kcal/mol}$$

overall process $h\nu = -112.9$ kcal/mol

Thus light absorbed by O_3 heats its surroundings slightly. This small temperature rise causes a corresponding pressure increase which can be detected by the microphone of the photoacoustic system.

The photoacoustic system was developed by Cary (29) for measurement of mercury. This system was modified for detection of ozone in this research (Fig. 2). The light pulse controller, which was a

SC/mp microprocessor system was replaced by a simple digital phase shifter (Appendix C). The circuit assured that only signals with exactly the frequency and phase of the light source were amplified. The best frequency, which was applied by a square wave generator, was 289 Hz and the phase delay was 10.8 degrees to get the maximum sensitivity of PAS for ozone.

For producing ozone, a 4-watt mercury lamp was placed in a glass container (Fig. 2) and supplied by two 18-volt DC power supplies and a 15-volt regulator (Appendix D). The intensity of the lamp was controlled by a photocell, which is able to provide ozone concentration ranges between 0 and 200 ppm (at the maximum intensity of the lamp) for a flow rate of input air into the glass container of 100 cc/min. By decreasing the flow rate of input air to 1 cc/min., the concentration of the ozone generator vessel can go up to 1000 ppm.

The 0.5 ml ozone sample was taken by a glass syringe and injected through a rubber septum that was close to the sample cell (Fig. 2). Air was passed continuously through the sample cell as a carrier gas.

An estimate of the detection limit where the signal is equal to the lowest peak-to-peak noise level is about 0.8 ppm. Signal response vs. ozone concentration is shown in Figure 3, as well as the noise level.

The ozone generator was calibrated by a single beam spectrophotometer with a pathlength of 64.8 cm (30) using an ozone molar absorptivity at 253.7 nm of .186 cm^{-1} $(moles/liter)^{-1}$ (31).

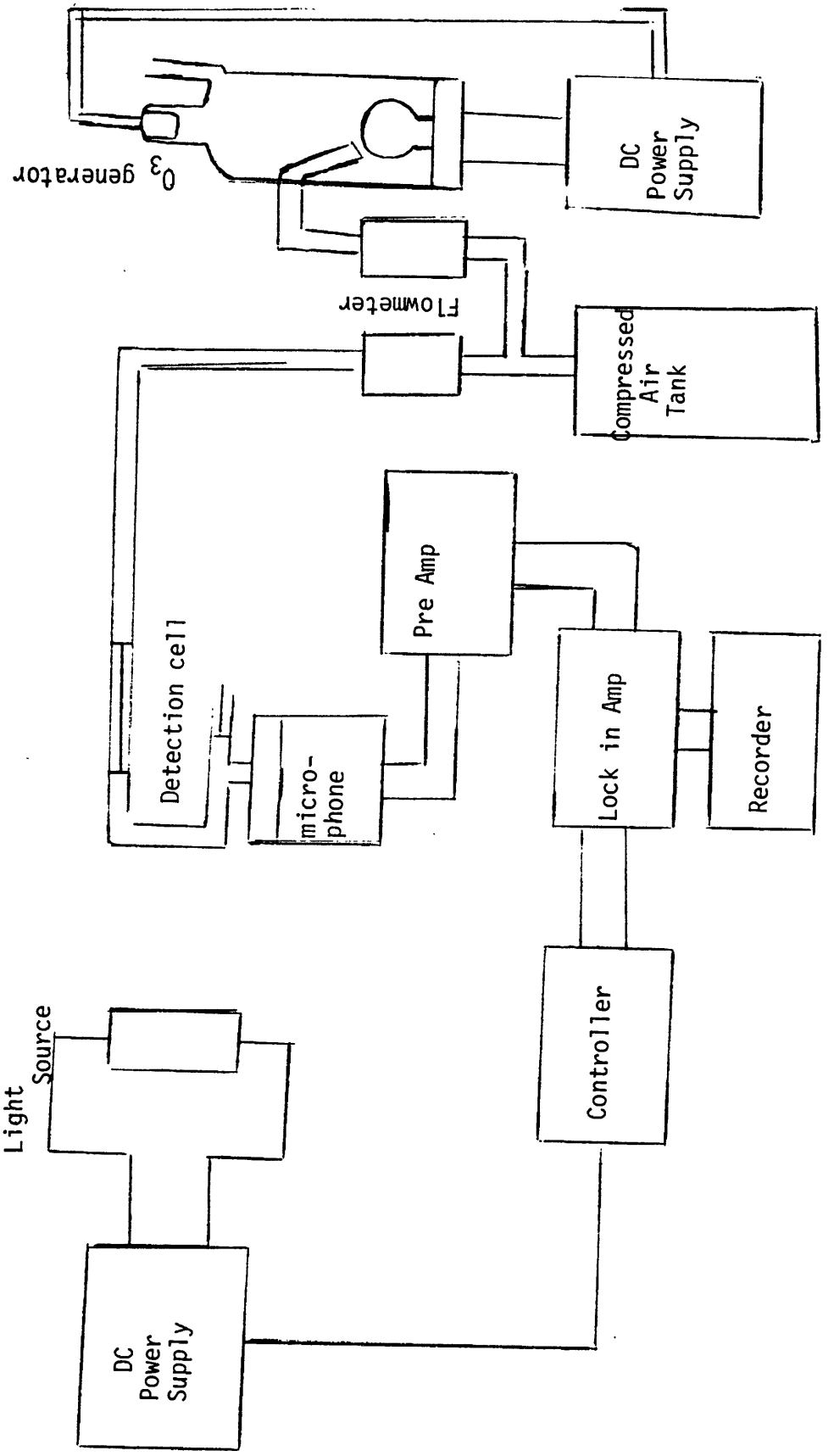

Figure 2. Schematic diagram of apparatus.

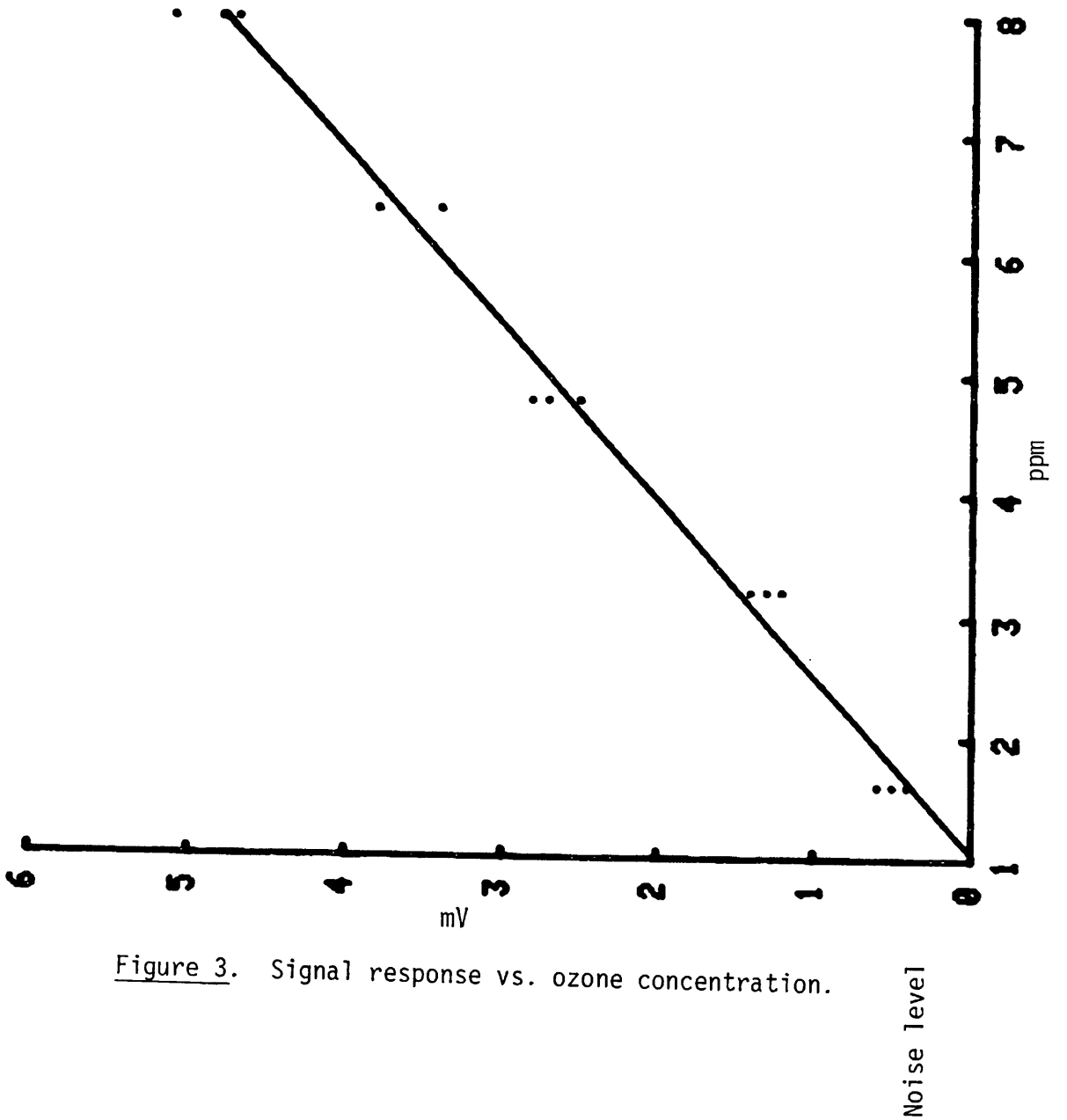

Figure 3. Signal response vs. ozone concentration.

STUDY OF OZONE LOSS THROUGH LIQUID SURFACES

Glass Tube Reactor Method

Preliminary experiments were carried out to assess the decomposition of O_3 on liquid surfaces in a glass tube (2.5 cm I.D. and 70 cm long) (Fig. 4). The reactor was filled halfway with the proper solution (distilled water, H_2SO_4, NaOH). The O_3 stream was passed above the solution in the reactor and then passed through a small trap which was cooled by dry ice and methanol before entering the detection cell. The trap prevented introduction of water vapor into the detection cell which would influence the response of the detector. For comparison of the input and output of the O_3 concentration, ozone was passed straight through a teflon tube and then into the detector (Fig. 2). With this technique it was possible to compare the output and the input, and to check for any destruction. The reactor was filled with several solutions, distilled water, concentrated H_2SO_4, and various NaOH solutions. The results (Table II) show that the destruction of ozone is a function of the pH of the solution and by increasing

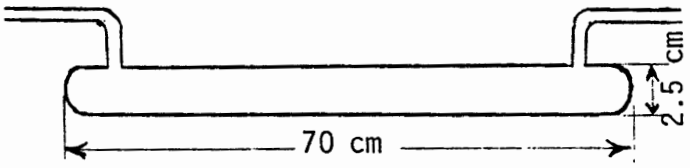

Glass tube reactor

Tank reactor

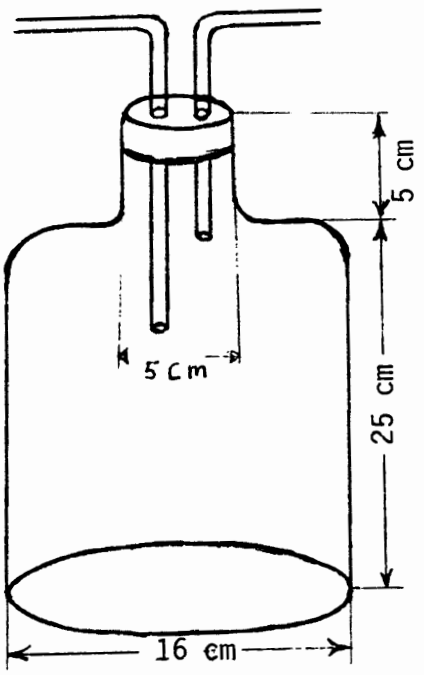

Figure 4. Reactor apparatus used.

TABLE II

PERCENT DESTRUCTION OF OZONE IN DIFFERENT pH SOLUTIONS (IN THE GLASS TUBE REACTOR)

Solution	pH	Percent destruction of ozone	Predicted from Aldaz k_d
H_2SO_4 (concentrated)	<<1	0	
Distilled water	5.5	0	100
NaOH	10	40	
NaOH	12	75	
Saturated NaOH solution	>14	100	
NaOH	14	100	

G_o = 60 ppm, flow rate = 5 cc/min

length = 70 cm

I.D. = 2.5 cm

the pH, the destruction was also increased. There was almost no destruction by distilled water. By using the Aldaz number for the deposition velocity of ozone, $k_d = 4 \times 10^{-2}$ (9), on the surface of the water, the expected percent destruction of ozone in the reactor can be calculated as follows:

ozone input = $F \times G_{in}$

G_{in} = O_3 input concentration

F = flow rate of input ozone

ozone output = $F \times G_{out}$

G_{out} = output of ozone concentration

flux of O_3 into surface of water = $k_d \times G$

G = O_3 concentration in contact with surface of water

O_3 destroyed = $k_d \times G \times dA$

dA = surface in contact = rdL

where

r = radius of glass tube

L = length of glass tube

$$F \times G_{in} - F \times G_{out} = k_d \times G \times 2r \times dL$$

$$\frac{G_{in} - G_{out}}{G} = \frac{dG}{G} = \frac{2k_d \times r}{F} dL$$

$$\int_{G_o}^{G} \frac{dG}{G} = \frac{k_d \times r}{F} \int_{o}^{L} dL$$

$$\ln \frac{G}{G_o} = \frac{k_d \times r \times L}{F}$$

$$\frac{G}{G_o} = \exp \frac{2k_d \times r \times L}{F}$$

$$\frac{G}{G_o} = \exp \frac{4\times10^{-2} \text{ cm/sec} \times 1.25 \text{ cm} \times 70 \text{ cm}}{5 \text{ cm}^3/60 \text{ sec}} = 3.3 \times 10^{-7}$$

$$\frac{G_o - G}{G} \times 100 = 100\%$$

Thus, according to the Aldaz value of k_d, the experiment should have given 100% destruction. But the experimental result showed almost no destruction on distilled water (Table I). Thus, Aldaz's result must be wrong. This error could have been anticipated by the failure of Aldaz to consider the destruction of ozone in solution rather than at the surface.

To study the effects of the contact surface between the liquid and gas phases and also the effect of the volume of the liquid phase on the destruction of ozone, the tube reactor was replaced by a tank reactor.

Tank Reactor Vessel Methods

In this method the glass tube was replaced by a sealed Pyrex tank (Fig. 4). The mouth of the tank was covered by a rubber stopper which was covered by teflon tape. Two teflon tubes were inserted through the stopper into the tank as input and output for ozone.

The tank was filled with distilled water up to 4 liters and ozone was bubbled into the solution without stirring. The experiment was repeated, stirring the solution with a teflon stirring bar. The experiment was again repeated by passing ozone above the surface of the water. In eacy case, the output of the tank was passed through the trap, then into the detector. The initial concentration of ozone was

measured by passing the input stream of ozone directly to the detector. The flow rate = 100 cc/min; the surface between the gas and liquid phases = 200 cm^2; ozone concentration = 65 ppm; and the volume of the gas phase = 1 liter.

The results in Table III show, in the case of bubbling through the solution, that stirring of the liquid phase did not change the destruction of ozone. The only effect of stirring was on the time to achieve a steady state between the gas and liquid phases, which reduced the time to approximately half of what it was with no stirring. This was obviously because of the faster distribution of ozone in solution.

When ozone was passed above the water, stirring the water caused more destruction. This can be explained as faster diffusion and a smaller concentration gradient in the solution with stirring.

To study the effect of the volume of the liquid phase on the destruction of ozone, the tank was filled with differing amounts of distilled water. Ozone was passed above the water, and the destruction was measured relative to the input ozone concentration (Table IV). The liquid phase was stirred for all cases.

Aldaz (9) and others (10, 14, 15) assumed ozone was destroyed at contact with the liquid phase surface. According to their assumption, the expected percent destruction can be claculated as:

amount ozone in - amount ozone out = amount ozone destroyed

$$FG_o - FG = k_d GA$$

$$\frac{G_o - G}{G} = \frac{k_d \times A}{F}$$

$$\text{percent destruction} = \left(\frac{G_o - G}{G_o}\right) \times 100 = \frac{k_d \times A}{F}$$

TABLE III

PERCENT OZONE DESTRUCTION UNDER DIFFERENT CONDITIONS IN THE TANK REACTOR

Conditions	Percent destruction of O_3
Stirring and Bubbling O_3 through liquid phase	27.5 ± 2.4
No stirring, but bubbling O_3 through liquid phase	26.2 ± 1.9
Stirring liquid phase and passing O_3 above liquid phase	15.5 ± 1.3
No stirring but passing O_3 above liquid phase	11.5 ± 1.5

Thus the percent of ozone destruction is only a fraction of the surface contact area. For constant contact area but with different liquid phase volumes (Table IV), different percent destruction was measured. Therefore the percent of destruction is not only a function of contact surfaces, but is also dependent on the liquid phase volume. The explanation is that a larger volume of water dissolves more ozone, and more decomposition of ozone in water leads to a higher percent of destruction.

Although the model of surface destruction only is clearly wrong, we may use it to calculate an "apparent" value of k_d:

$$k_d = \left(\frac{G_o - G}{G}\right) \times 100 \quad \frac{F}{A}$$

$$k_d = (\text{percent destruction}) \times \frac{F}{A}$$

k_d is a function of the destruction constant $\frac{G_o}{G}$ at a constant flowrate and the contact surface area (Table IV). In Table IV apparent values of the deposition velocity are seen to vary from 7×10^{-4} to 6×10^{-3} cm/sec, much smaller than those reported by Aldaz. Table IV shows, at a constant surface of contact, that the destruction of ozone depended on the volume of the liquid phase. A larger liquid phase gives more destruction, which shows ozone is destroyed in the water. Two last measurements show that the destruction of ozone also depends on the surface of contact; decreasing the surface causes less destruction. The change of ozone destruction with liquid phase volume is not linear (Fig. 5).

Injection Method

In this method of the reaction vessel was the same as in the previous experiment, but instead of passing the output of the tank through the detector as before, a 1 cc syringe was used. The sample from the output of the tank was injected into the PAS detector. Injections were

TABLE IV

PERCENT OZONE DESTRUCTION AT DIFFERENT GAS AND LIQUID VOLUMES AND CONTACT SURFACES

Volume of liquid phase (cm^3)	Volume of gas phase (cm^3)	Contact Surface between phases (cm^2)	Percent destruction of O_3	Calculated k_d assuming surface destruction only
0	5050	--	1 ± 0.6	
100	4950	200	3.6 ± 0.9	7.2×10^{-4}
1000	4050	200	12.5 ± 1.8	2.5×10^{-3}
2000	3050	200	20.8 ± 2.1	4.16×10^{-3}
3000	2050	200	26.2 ± 1.6	5.2×10^{-3}
4000	1050	200	28.5 ± 2.5	5.2×10^{-3}
4800	250	160	20.0 ± 1.8	---
5000	50	12.5	14.0 ± 1.2	---

Liquid phase was stirred in all cases.

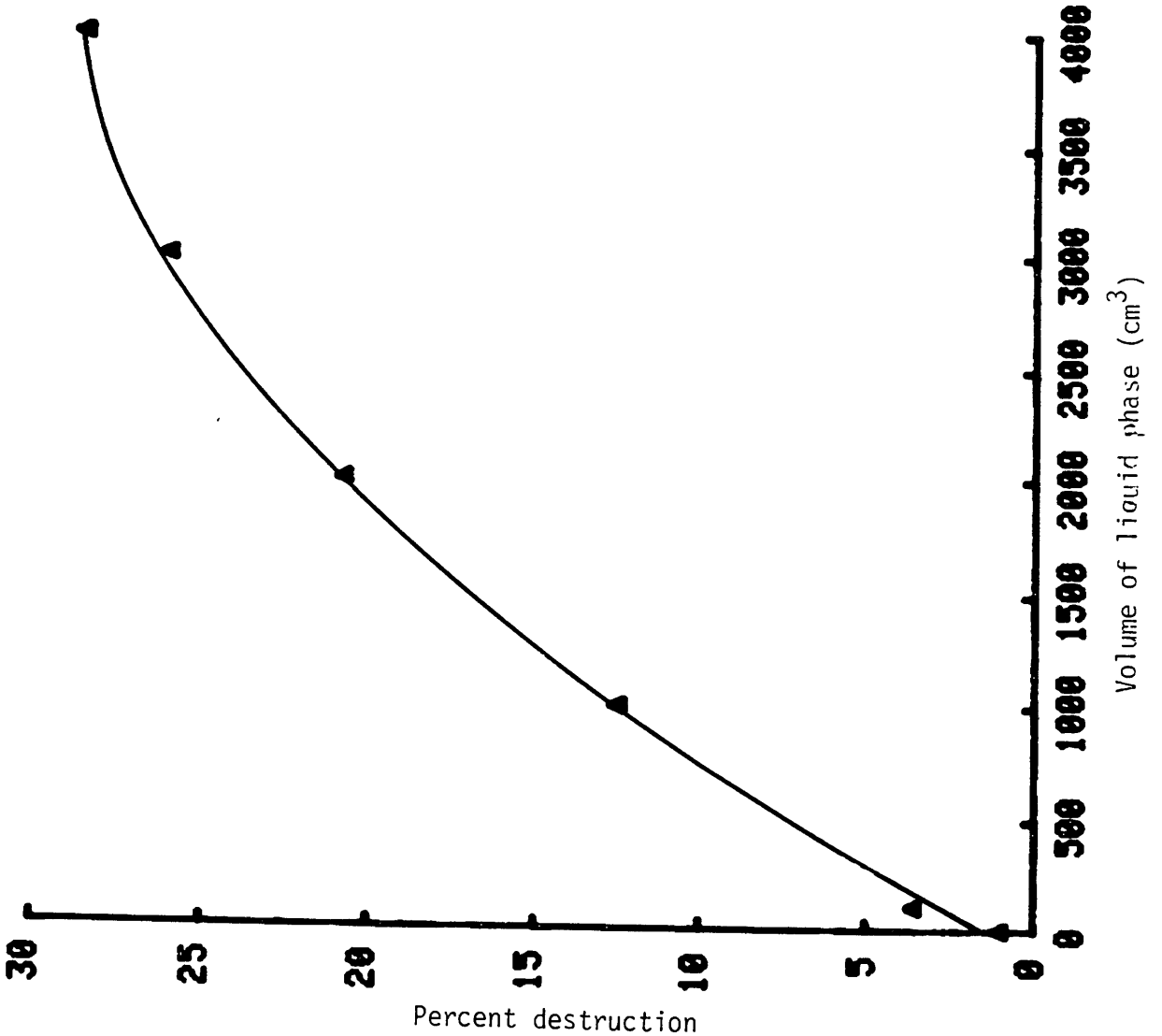

Figure 5. Change of ozone destruction with volume.

continued until the sample approached a steady state (constant response of PAS to the injection), and then compared with the response of the PAS to the ozone sample before it entered the tank. The percent destruction was then calculated (Table V).

Results are comparable with the continuous method (previous experiment) and show a dependency of the destruction of ozone on the surface area and pH of the solution.

The tank mouth was stoppered with a rubber stopper which was covered by teflon tape (rubber destroys ozone very quickly). Later the stopper was replaced by a teflon sheet. The experiment was repeated on distilled water with the injection method (Table VI).

Stop Flow Method

In this method ozone was first passed above the solution to reach a steady state, then the flow was stopped and the rate of disappearance of ozone was measured. This was done in two ways:

1) After steady state was reached, the flow was stopped for a certain time. Then renewed air flow through the tank and detector measured the decreased concentration of ozone. The experiment was repeated for different times of exposure of the liquid phase. The concentration of ozone vs. time was plotted, using a computer for numerical integration, to get the proper rate constant of decomposition in water and transfer rate of ozone (Table VII and Figs. 13 and 14).

2) The experiment was repeated with the injection method. After steady state was reached, the flow was stopped, samples taken at different times, and injected into the PAS. These data were analyzed by plotting the concentration vs. time and using the computer model. A gas phase volume of 50 cc and a volume of 5000 cc for the liquid phase

TABLE V

PERCENT OZONE DESTRUCTION WITH DIFFERENT pH SOLUTIONS AND CONTACT SURFACES

Volume of liquid phase (cm^3)	Volume of gas phase (cm^3)	Contact Surface (cm^3)	pH	Percent Destruction of O_3
4000	1000	200	5.5	28
5000	50	12.5	5.5	13
5000	50	12.5	1.3	7.2

TABLE VI

PERCENT OZONE DESTRUCTION IN THE CASES OF BUBBLING OZONE THROUGH AND PASSING OZONE ABOVE LIQUID PHASE (H_2O) WITH DIFFERENT CONTACT SURFACES

Conditions	Volume of liquid phase (cm^3)	Volume of gas phase (cm^3)	Contact Surface (cm^3)	Percent Destruction of O_3
Bubbling O_3 through liquid phase	5050	50	12.5	26.5
Bubbling O_3 through liquid phase	4850	200	160	21.2
Passing O_3 above liquid phase	4850	200	160	14.3

TABLE VII

TRANSFER RATE AND DECOMPOSITION OF OZONE THROUGH WATER (TANK REACTOR)

Volume of liquid phase (cm^3)	Volume of gas phase (cm^3)	Contact Surface (cm^2)	Transfer Rate cm/sec	Rate Constant of Decomposition (sec^{-1})
5000	50	12.5	9×10^{-3}	3×10^{-4}
4000	200	100	6×10^{-3}	3×10^{-4}

gave a rate constant of decomposition of ozone in water of $K_5 = 8 \times 10^{-4}$ sec^{-1} and a transfer rate of 3×10^{-2} cm/sec (Fig. 6).

Comparing the results of 1) and 2) showed a significant difference in the values of $K_d = 5 \times 10^{-3}$ to 3×10^{-2}. Also, considering all previous values for K_d, there is a large uncertainty. This may be due to ignoring the destruction of ozone on the glass surfaces. For measurements of the rate constant K_6 (see "Theory") for ozone on glass, different sized beakers were taken and the mouths were covered by teflon sheets. The ozone was introduced into the beakers by taking the sample at different times (injection methods) (Figs. 16-21). Later, the teflon cover was replaced by milar film because the mylar is less reactive to ozone than teflon, to get a more accurate rate constant for glass (Table VIII).

Since mylar caused less destruction of ozone than the teflon cover, a more accurate K_6 for glass was obtained, decreasing the surface area of the cover resulted in a smaller K_6, meaning that the rate of destruction on glass is smaller than teflon or mylar. So to get a more accurate value of K_6 for glass, the surface area of the cover must be decreased.

The surface contact with mylar was minimized to obtain a constant value of K_6 for glass. Then to get a more accurate K_d for water, a glass tube form, with a small hole (1 mm diameter) was used for introducing ozone (Fig. 7). First, the tube was placed on a glass plate and the K_6 was measured on a glass surface (Fig. 8). The tank was then filled to the glass tube with solution, assuming that all the ozone enters into the solution will be diluted away by the large liquid volume. Ozone was introduced into the gas phase and the concentration

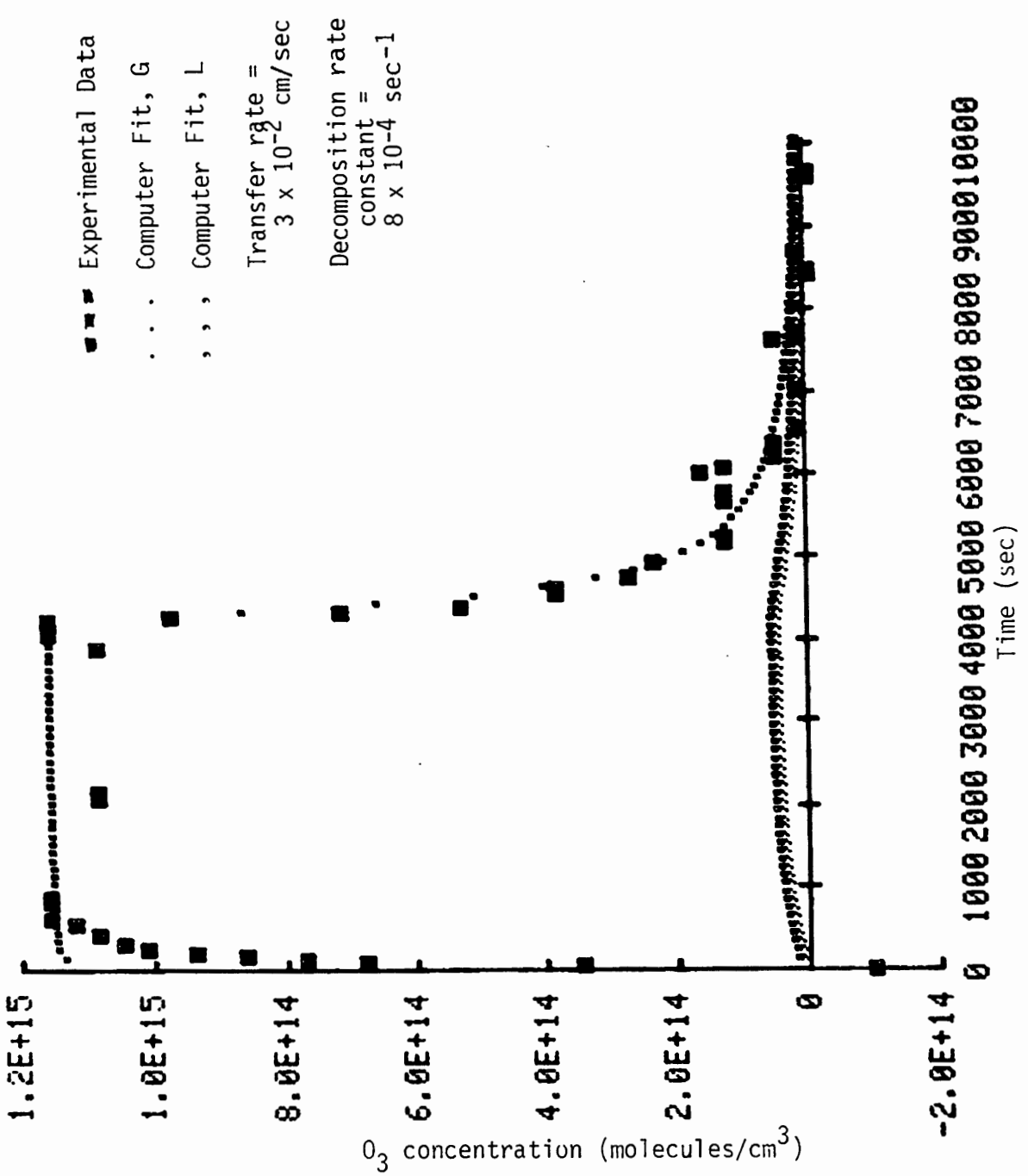

Figure 6. Loss of ozone through distilled water.

TABLE VIII

RATE CONSTANT OF DESTRUCTION OF O_3 IN DIFFERENT GLASS REACTORS

Type of Reactor	Type of cover on mouth of Reactor	Volume of liquid phase cm^3	Volume of gas phase cm^3	Total Surface Area of Glass cm^2	Surface Area of Cover cm^2	Rate Constant of Destruction of O_3 on glass (sec^{-1})	Reference Figure Number
250 ml beaker	Teflon	0	250	108	28	1.6×10^{-3}	16
400 ml beaker	"	0	400	280	38	5.7×10^{-4}	17
250 ml beaker	Mylar	0	250	180	28	2.0×10^{-4}	18
400 ml beaker	"	0	400	280	38	1.3×10^{-4}	19
500 ml glass bottle	"	0	500	335	3.2	6.1×10^{-5}	20
50 ml beaker	"	0	50	66.1	13.8	8.2×10^{-4}	21

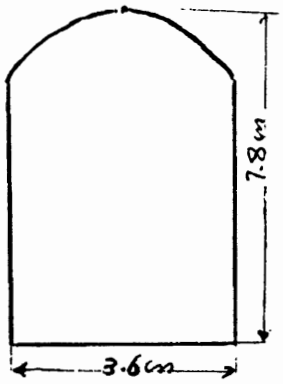

Glass tube

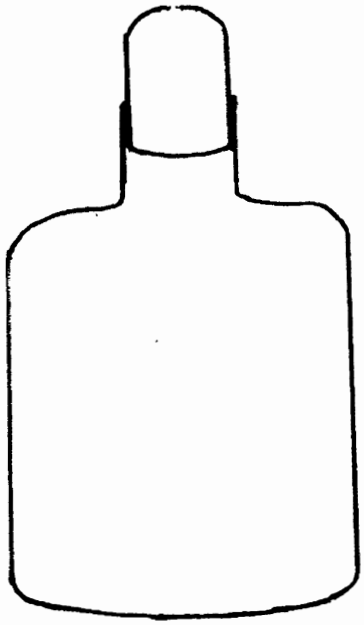

Figure 7. Glass tube as gas phase part of reactor.

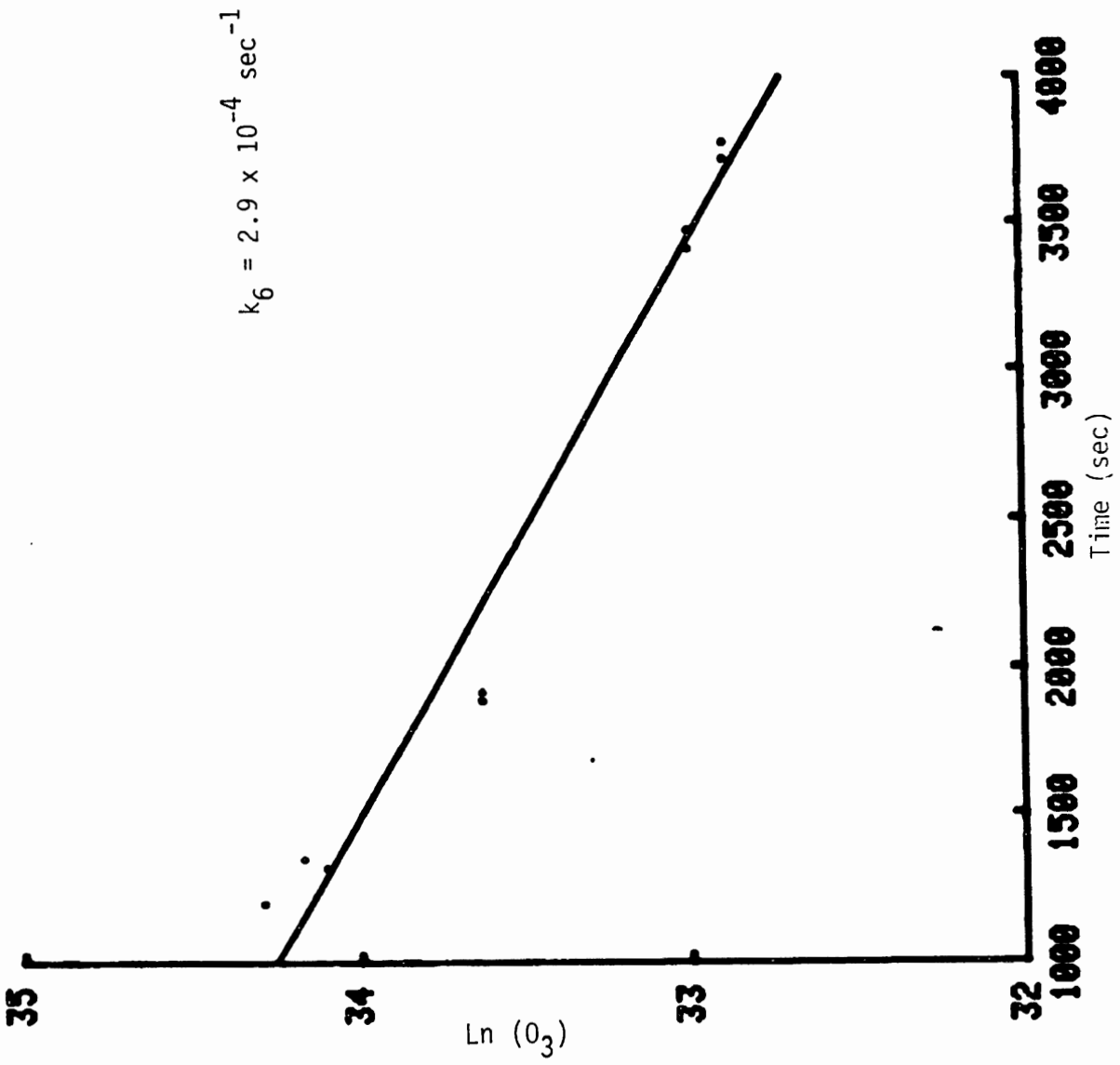

Figure 8. Graphic presentation of destruction of O_3 on glass surfaces.

was measured at different times with the injection method. The natural log of ozone concentration was plotted vs. time, and the slope was calculated (Table IX) to give K_6 and k_d. The K_6 values on the glass were subtracted to give k_d. Experiments were done for different pH values and solutions were not stirred (Fig. 22-29).

Data in Table X again shows the transfer rate increasing with pH. The only exception was the value at pH = 9, which was about equal to the value at pH = 5.5. There is no explanation for this.

Hemisphere Gas Phase Reactor

For increasing the probability of collision of ozone molecules to water over that of glass surfaces, a hemisphere glass vessel was made. The destruction rate of ozone on the surface of the hemisphere was measured (Fig. 30), and then by using the hemisphere as a gas phase part of the reaction vessel, the transfer rate was measured at different pHs (the injection method was used without stirring) (Table X and Figs. 31-34).

A problem with the hemisphere was a difficulty in using it as a gas phase part for the tank reactor. So again the glass tube, as was used before, was selected for the gas phase. The tank was filled up to the neck and up to about 2 cm in the gas phase reactor (for complete sealing and to prevent ozone from escaping). A small hole was made on top of the glass tube for introducing or removing ozone. An experiment was done to measure the transfer rate into distilled water and NaOH solutions with different pHs while stirring the solutions (Table XI). For each case, also, the experiment was done for different initial ozone concentrations, but the results (Figs. 35-42) showed the rate transfer to be independent of the initial O_3 concentration.

TABLE IX

TRANSFER RATE OF OZONE ON DIFFERENT pH SOLUTIONS (WITHOUT STIRRING) USING GLASS TUBE, GAS PHASE

pH	Transfer rate of ozone on surface of liquid phase (cm/sec) Trial 1	Trial 2	Reference Figure Number
1.3	5.8×10^{-4}	5.3×10^{-4}	22, 23
5.5	1.3×10^{-3}	9.9×10^{-4}	24, 25
9	1.9×10^{-3}	1.2×10^{-3}	26, 27
13	1.1×10^{-2}	1.2×10^{-2}	28, 29

Gas phase volume = 80 cm^3

Liquid phase volume = 5000 cm^3

$K_6 = 2.9 \times 10^{-4}$ sec^{-1}

TABLE X

TRANSFER RATE OF O_3 ON DIFFERENT pH SOLUTIONS
(USING HEMISPHERE, NO STIRRING)

pH	Transfer Rate Constant (sec^{-1})	Transfer Rate (cm/sec)	Reference Figure Number
1.3	2.24×10^{-4}	4.02×10^{-4}	31
5.5	3.34×10^{-4}	6.01×10^{-4}	32
9	1.2×10^{-4}	2.16×10^{-4}	33
13	1.03×10^{-2}	1.88×10^{-2}	34

Gas phase volume = 45 cm^3

Liquid phase volume = 2000 cm^3

$K_6 = 2.9 \times 10^{-4}$ sec

TABLE XI

TRANSFER RATE OF OZONE ON DIFFERENT pH SOLUTIONS
(USING GLASS TUBE FOR GAS PHASE AND
STIRRING THE LIQUID PHASE)

pH	Transfer rate constant (sec^{-1})		Transfer rate cm/sec		Reference Figure Number
	Trial 1	Trial 2	Trial 1	Trial 2	
3.5	1.22×10^{-3}	1.21×10^{-3}	8.06×10^{-3}	8.25×10^{-3}	35, 36
5.3	3.22×10^{-4}	1.6×10^{-4}	2.21×10^{-3}	1.1×10^{-3}	37, 38
11.5	1.44×10^{-3}	1.45×10^{-3}	9.99×10^{-3}	9.98×10^{-3}	39, 40
14	3.78×10^{-3}	4.82×10^{-3}	2.59×10^{-2}	2.63×10^{-2}	41, 42

Liquid phase volume = 5000 cm^3

Gas phase volume = 70 cm^3

Contact phase = 10.2 cm^2

$K_6 = 2.7 \times 10^{-4}$

By comparing Tables IX and XI, results show that in the case of stirring the solution, the transfer rate increased. This can be explained again by the decreasing concentration gradient in the liquid phase caused by stirring.

Deposition Velocity of Ozone on Ocean Surfaces

To find a more realistic number for the deposition velocity, the experiment was repeated for seawater and also for distilled water for various concentrations of O_3 in the gas phase, both with stirring and not stirring the liquid phase (Fig. 43-54 and Tables XII and XIII). It was assumed that the concentration of ozone in the liquid phase for the measurement of k_d (see "Theory") was almost zero. For checking this assumption for both distilled water and seawater, the experiment was repeated using 21 liters of the liquid phase (Table XIV and Figs. 54-58). Data showed the k_d for seawater to be 2 times larger than the k_d for distilled water (Table XIII), which can be explained by the higher pH of seawater (pH = 8.5) than that of distilled water (pH = 5.5). Previous experimental results showed that k_d has a larger value for higher pHs. The k_d values were independent of the initial ozone concentration in the gas phase (Figs. 43-50). The results also showed that the k_d values were larger in stirred solutions than in those that were not stirred (Tables XII-XIV).

Measurement of the Decomposition Rate Constant of O_3 in Solution

Voltammetry. For measurement of the rate of destruction of ozone in solution, a differential pulse polarograph (DPP) (Model 174A Polarographic Analyzer, Princeton Applied Research Co.) was used. The electrochemical reduction of ozone in an acidic medium has been reported using a platinum electrode and a rotated gold disc electrode (32-35). The

TABLE XII

DEPOSITION VELOCITY OF OZONE ON DISTILLED WATER AND OCEAN WATER

	Trial 1		Trial 2		Trial 3		Trial 4		Average
Liquid	Transfer Rate Constant (sec^{-1})	Deposition Velocity (cm/sec)	Transfer Rate Constant (sec^{-1})	Deposition Velocity (cm/sec)	Transfer Rate Constant (sec^{-1})	Deposition Velocity (cm/sec)	Transfer Rate Constant (sec^{-1})	Deposition Velocity (cm/sec)	Deposition Velocity (cm/sec)
Distilled Water* (Stirred)	1.19×10^{-4}	2.73×10^{-3}	1.17×10^{-4}	2.69×10^{-3}	2.27×10^{-3}	5.17×10^{-3}	1.78×10^{-4}	4.10×10^{-4}	$3.67 \pm 1 \times 10^{-3}$
Ocean Water** (Stirred)	4.36×10^{-4}	5.38×10^{-3}	4.82×10^{-4}	5.96×10^{-3}	4.14×10^{-4}	5.3×10^{-4}	4.12×10^{-4}	6.10×10^{-4}	$5.69 \pm .4 \times 10^{-3}$

$K_6 = 2.7 \times 10^{-4}$

Gas phase volume = 70 cm^3

Liquid phase volume = 5000 cm^3

Contact phase = 10.2 cm^2

* Reference figure numbers: 43, 44, 45, 46

** Reference figure numbers: 47, 48, 49, 50

TABLE XIII

DEPOSITION VELOCITY OF OZONE ON DISTILLED AND OCEAN WATER

Liquid Phase	Trial 1 Transfer Rate Constant (sec^{-1})	Trial 1 Deposition Velocity (cm/sec)	Trial 2 Transfer Rate Constant (sec^{-1})	Trial 2 Deposition Velocity (cm/sec)	Average Deposition Velocity (cm/sec)	Reference Figure Number
Distilled Water*	1.56×10^{-4}	5.2×10^{-4}	1.48×10^{-4}	4.46×10^{-4}	$4.83 \pm 0.5 \times 10^{-4}$	51, 52
Ocean Water*	3.13×10^{-4}	5.82×10^{-4}	2.68×10^{-4}	5.22×10^{-4}	$5.52 \pm 0.4 \times 10^{-4}$	53, 54

Gas phase volume = 70 cm^3

Liquid phase volume = 5000 cm^3

Contact phase = 10.2 cm^2

* Liquid phase not stirred.

TABLE XIV

DEPOSITION OF OZONE ON DISTILLED WATER

Condition of Liquid Phase	Trial 1		Trial 2		Average Deposition Velocity (cm/sec)	Reference Figure Number
	Transfer Rate Constant (sec^{-1})	Deposition Velocity (cm/sec)	Transfer Rate Constant (sec^{-1})	Deposition Velocity (cm/sec)		
Stirred	4.02×10^{-4}	9.2×10^{-4}	3.21×10^{-4}	7.33×10^{-4}	8.2×10^{-4}	55, 56
Not Stirred	1.93×10^{-4}	5.3×10^{-4}	1.89×10^{-4}	4.47×10^{-4}	4.9×10^{-4}	57, 58

Gas phase volume = 70 cm^3

Liquid phase volume = 2100 cm^3

Contact surface = 10.2 cm^2

$K_6 = 2.7 \times 10^{-4}$

electrochemical reduction of ozone is as follows:

$$O_3 + 2\ H^+ + 2\ e^- \rightarrow H_2O + O_2$$

In this study, DPP was used with an indicator electrode of platinum foil having a surface area of about 1 cm. The ozone solution was made by bubbling ozone into a 0.1 M NaCl solution for 2 hours to get a saturated solution of ozone and equilibrium between the gas and liquid phases. Then, measuring the gas phase by PAS and using the solubility of ozone in water, the concentration was calculated in solution. Next, solutions were made with different concentrations of ozone and analyzed by DPP at different times (Fig. 59 and 61).

The response of DPP due to reaction of ozone at the platinum electrode was proportional to the ozone concentration. From the slope of log ozone vs. time (Fig. 60-62), the rate of decomposition was determined. The results are shown in Table XIV.

A problem with this method was poor reproducibility of the slope (order of reaction); in some cases the order was 1 and in others less than 1. Another problem was that the experiment was not sensitive to low concentrations of ozone. This is more important because Hill (25) measured a reaction order of 1 for the decomposition of ozone at a concentration of about 10^{-4}M. But Kilpatrick (26), repeating Hill's experiment with higher concentrations of ozone, found a reaction order of 1.5. So, the order of decomposition is dependent upon the ozone concentration in the solution.

PAS. Because results from the voltammetry method had an uncertainty in the value of the decomposition constant, the value was measured in another way.

TABLE XV

DECOMPOSITION RATE CONSTANT OF OZONE
AS MEASURED BY VOLTAMMETRY
(SEC^{-1})

Initial O_3 Concentration (M)	Slope of ln O_3 vs. time	Shape of Curve
1×10^{-4}	1.6×10^{-3}	Linear
1.6×10^{-4}	1.95×10^{-3}	Linear
4×10^{-4}	9.05×10^{-4}	Not linear
3.2×10^{-4}	1.15×10^{-3}	" "
4.8×10^{-4}	1.23×10^{-3}	" "
2.4×10^{-4}	1.2×10^{-3}	" "
1.6×10^{-4}	4.38×10^{-4}	" "

According to theory, if the concentration of ozone in the liquid phase is large enough, the rate of change of gas phase ozone depends on both the deposition velocity and the decomposition constant in the liquid phase. A 100 cm^3 10^{-4} M solution solution of ozone was made and diluted to 5 liters in the tank reactor, using the glass tube for the gas phase part in stirring the solution. The gas phase ozone increased to reach equilibrium with the liquid phase, which was observed by taking gas samples and using the injection method (0.5 ml sample). Ozone first reached equilibrium after about 40-70 minutes, and then started to decrease and took about 4-7 hours to be completely destroyed, depending on the initial concentration of ozone in the liquid phase. The concentration of ozone vs. time was then plotted. By using the computer model and the previous measured values for deposition velocity on water and glass, the rate constant of the destruction of ozone in solution (K_5) was determined (Figs. 64-70). To determine an accurate initial concentration of ozone in the liquid phase, it was calculated by extrapolating the decreasing part of the plot of $Ln(O_3)$ vs. time (Fig. 65) Results are shown in Table XV.

The experiment was repeated for seawater (Table XV). The results show the rate constant of decomposition of ozone in seawater to be about 10 times larger than in distilled water. This is to be expected because seawater has a pH of 8.5, compared with a pH of 5.5 for distilled water. Also K_5 was determined by using 3/2 order reactions for the decomposition reaction of ozone in water. The ocean water showed a better fit of numerical integration with experimental data (Figs. 69, 70). Thus, it might be that the decomposition reaction of ozone in the ocean follows the 3/2 order law.

TABLE XVI

DECOMPOSITION RATE CONSTANT OF OZONE (K_5) IN DISTILLED WATER AND OCEAN WATER

Conditions	Trial 1	Trial 2	Trial 3	Average	Reference Figure Number
Decomposition rate constant of ozone in distilled water $(sec^{-1})^a$	6.0×10^{-5}	5.0×10^{-5}	5.0×10^{-5}	5.3×10^{-5}	63, 65, 66
Decomposition rate constant of ozone in ocean water $(sec^{-1})^a$	7.5×10^{-4}	8.0×10^{-4}	--	7.78×10^{-4}	67, 68
Decomposition rate constant of ozone in ocean water $(molecule)^{-\frac{1}{2}}(cm^{3\frac{1}{2}}\text{-}sec)^{-1}$	2.50×10^{-11}	5.40×10^{-11}	--	3.95×10^{-11}	69, 70

Gas phase volume = 70 cm^3

Liquid phase volume = 5000 cm^3

All solutions stirred

[a] Decomposition rate constant using first order reaction

[b] Decomposition rate constant using 3/2 order reaction

Measurement of ozone in solution with the PAS. Iodometric and spectrophotometric analyses are common methods for measurement of ozone. Both have some difficulty and error, especially at low concentrations. Production of H_2O_2 in the iodometric method oxidizes iodine, and also ozone is destroyed during the analysis. Voltammetry is a more sensitive method, which was done for ozone in an acidic medium (31-33), at concentrations between 10^{-3} and 10^{-4} M. Recently, Smart et al (34), by using a voltammetric membrane electrode, detected between 50 and 100 ppb. Smart's group used a three electrode voltammetric cell and a gas permeable membrane.

Because of the simplicity of the PAS, an attempt was made to use PAS to detect ozone in the liquid phase. By providing a fast equilibrium between the gas and liquid phases, and then by measuring the gas phase by PAS, the concentration of ozone in solution can be calculated from the solubility of ozone in the liquid phase.

For the experiment, a stock solution of ozone was made with a known concentration. Then, using several volumetric flasks, dilutions were made. To reach a fast equilibrium, the gas phase in each flask was kept small, and the solutions were shaken vigorously. The sample for PAS measurement was taken from the gas phase.

Plotting calculated concentration vs. measured concentration was linear (Fig. 20) so this technique can be used as an easy method for measuring ozone in any solution, and with a sensitivity 0.3 times the detection limit of PAS of ozone in the gas phase for distilled water.

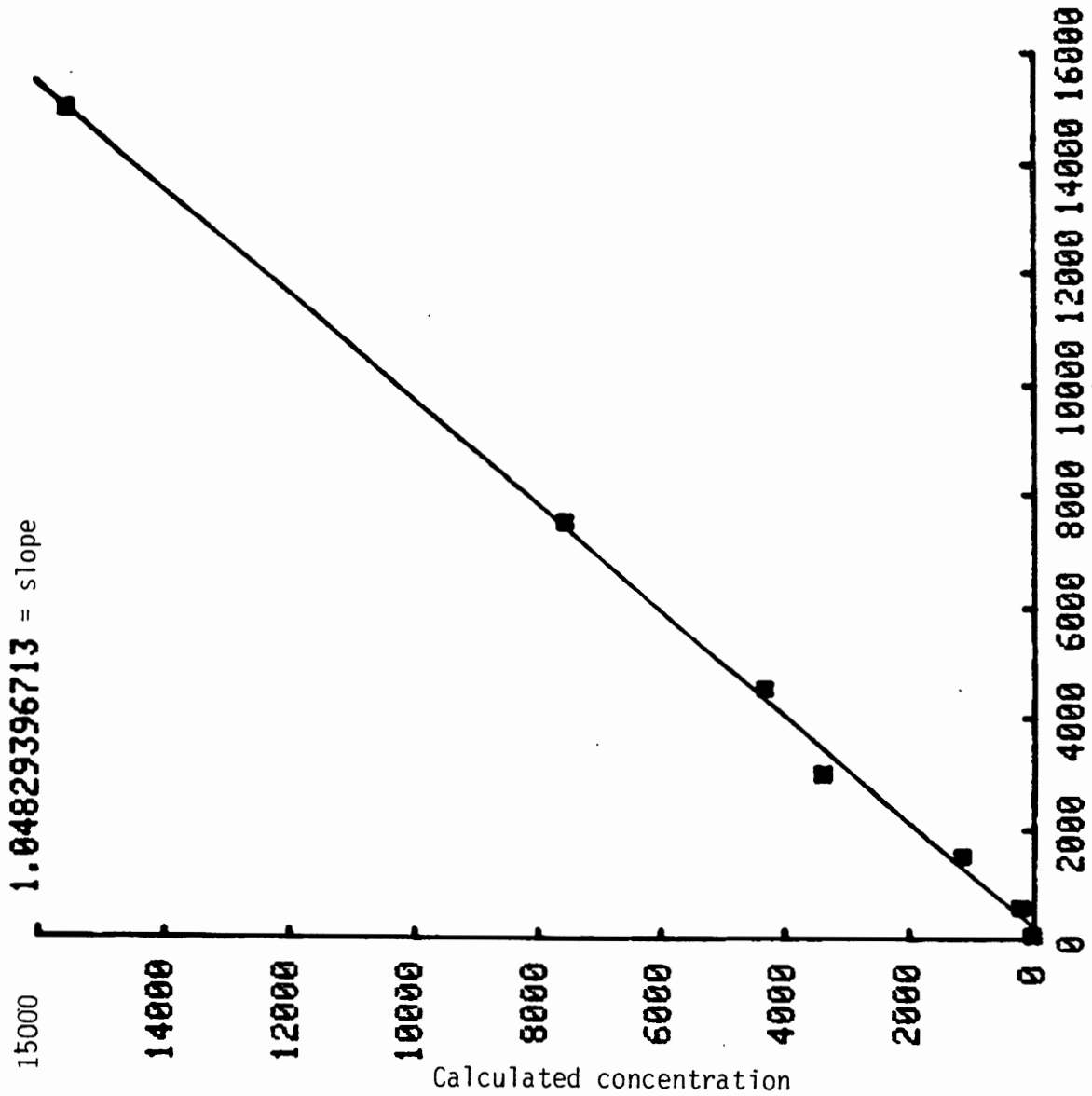

Figure 9 . Calculated ozone concentration and PAS measurement.

Effect of Light on the Decomposition of Ozone. For the study of the effect of light on the decomposition of ozone, the reactor tank was covered with a black plastic sheet. Then the experiments for measuring K_d and also for measuring the decomposition constant of ozone in solution was repeated. The K_d was the same. The decomposition constants for both light and darkness are shown in Table XVI. and Figures 71-74). Results showed that room light had no significant effect on the decomposition constant of ozone in water.

Deposition Velocity of CO. Liss (18) in his study assumed all the sparingly soluble and non-reactive gases have a deposition velocity of .0056 cm/sec. Although he did not consider the case for ozone, the situation should be almost the same because of low solubility and reactivity. Results of this research showed ozone has a $k_d = 3.37 \times 10^{-3}$ cm/sec for distilled water and 5.54×10^{-3} cm/sec for ocean water. In the case of ocean water, the k_d value is very similar to Liss' k_d value, but the k_d value is a function of the mixing (stirring). Thus comparison is not applicable, so to get a comparable k_d value for sparingly soluble and low reactive gases, the experiment which was done for measurement of ozone was repeated for CO (which was reported by Liss). For detection CO was separated by gas chromatography, reduced to CH_4 and measured with a flame ionization detector. Results showed that the deposition velocity of CO in distilled water is about 1.5×10^{-3} (Fig. 10, 11). The k_d value for CO was about half of the k_d for ozone measured under identical conditions with the same stirring rate.

TABLE XVI

DECOMPOSITION RATE CONSTANT OF OZONE WITH ROOM LIGHT AND DARKNESS IN DISTILLED WATER

Status	Trial 1	Trial 2	Average	Ref. Fig.
Decomposition rate in room light (sec^{-1})*	4×10^{-5}	5.5×10^{-5}	$4.8 \pm 1.0 \times 10^{-5}$	71, 72
Decomposition rate in darkness (sec^{-1})*	4×10^{-5}	7.5×10^{-5}	$5.75 \pm 2.5 \times 10^{-5}$	73, 74

Gas phase volume = 70 cm^3

Liquid phase volume = 5000 cm^3

* Solutions stirred

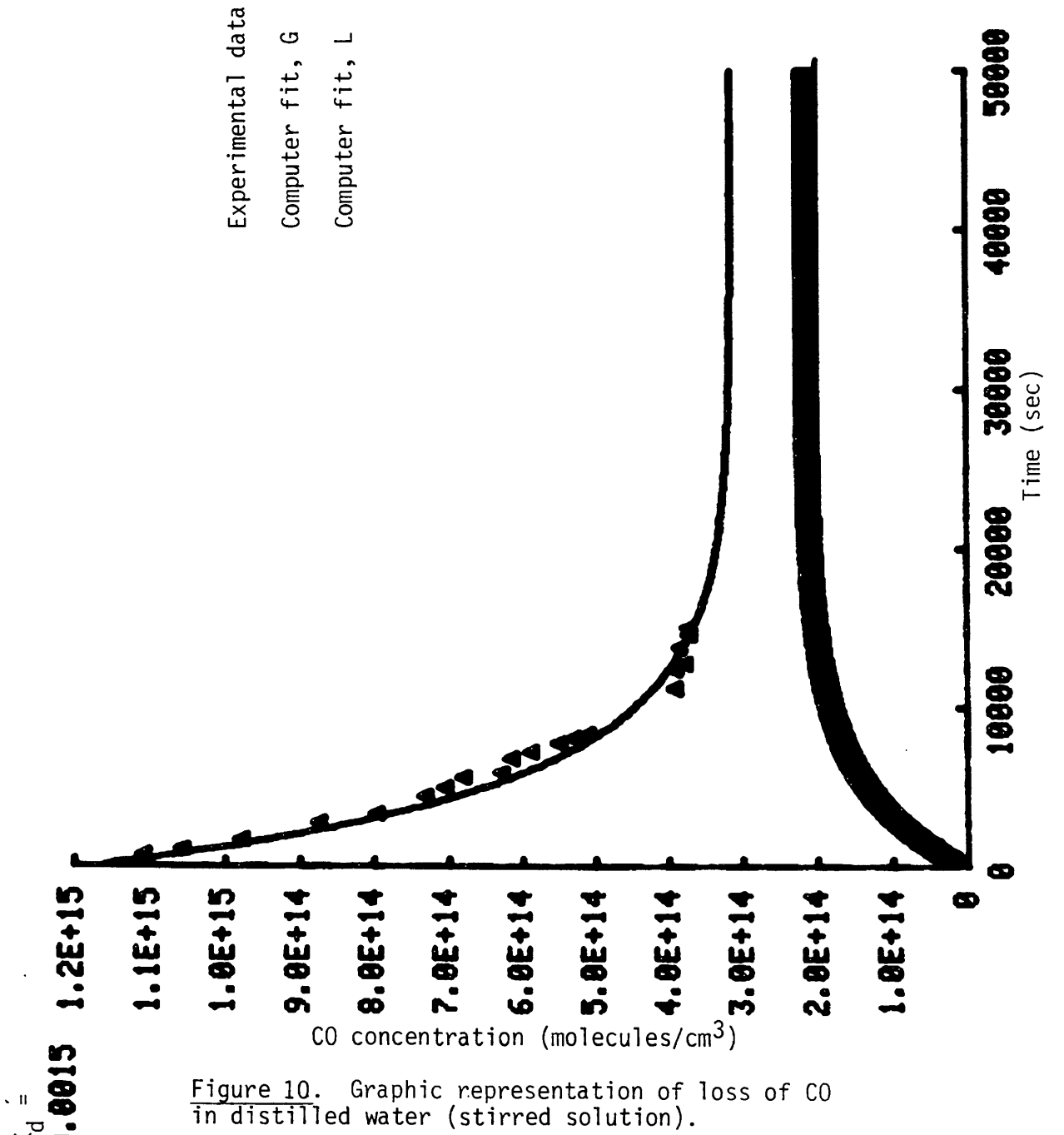

Figure 10. Graphic representation of loss of CO in distilled water (stirred solution).

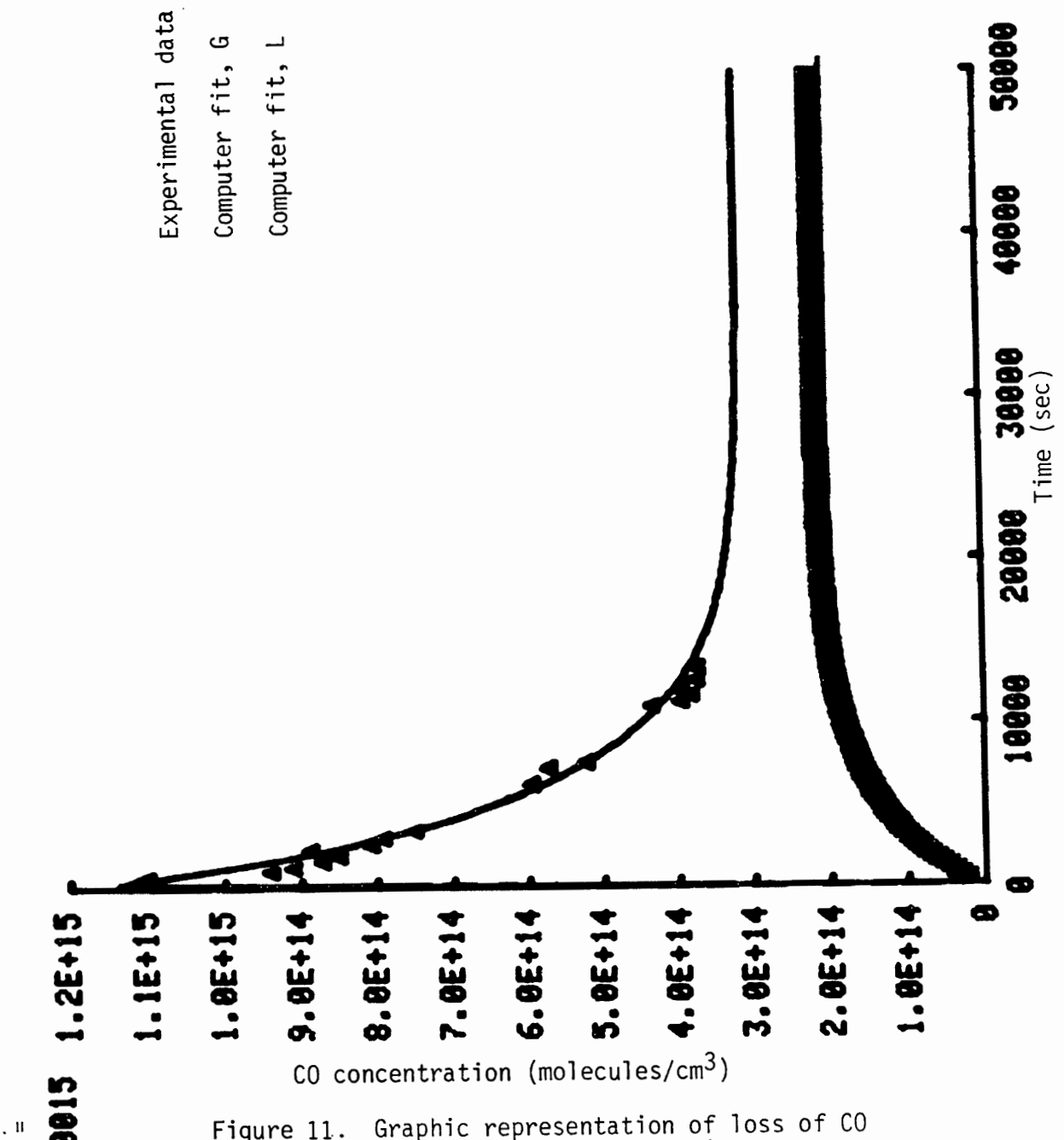

Figure 11. Graphic representation of loss of CO in distilled water (stirred solution).

CHAPTER IV

CONCLUSIONS

In all previous studies of ozone loss through liquid surfaces, it was assumed that ozone would be destroyed upon surface contact. No investigators considered any diffusion of ozone into the water and the decomposition in water. But O_3 is soluble in water (Henry's Law coefficient of O_3 is 3.3 for distilled water at 25°C). Thus ozone will dissolve in water and it is likely that dissolved ozone is destroyed by chemical reaction with water. In this research that possibility was considered. Experimental results showed that loss of ozone was due to chemical reaction in solution. Deposition velocity (transport rate) and decomposition rate of O_3 in solution were functions of solution pH. Increasing the pH value lead to larger values for decomposition rate and deposition velocity, which makes decomposition more significant in sea versus fresh water, because the ocean water is slightly basic (pH = 8.5).

Most current tropospheric models assume the earth's surface is the main sink for stratosphere-borne ozone. Ocean surfaces cover 70% of the earth. Thus uncertainty in the value of the global sink of ozone is significant. These results showed deposition velocity in ocean water to be about two times larger than in distilled water, but decomposition rate constant of ocean water is larger than distilled

water by a factor of 10. So that shows that the decomposition rate is more highly dependent on the pH of the solution than the deposition velocity. Values for the flux rate determined in this study are 10 to 100 times lower than measured previously.

Theoretically, the flux (F) of ozone through water can be calculated as a function of mixing depth for the model of Figure 1. The flux of ozone into water is

$$F = \frac{k_\ell}{H} (G - HL) \tag{30}$$

The rate of loss of ozone through water is

$$\frac{dL}{dT} = \frac{k_\ell}{H_d} (G - HL) - k_5 L \tag{43}$$

(See theory)

$d = h_\ell$ = mixing depth

Assuming steady state,

$$\frac{dL}{dT} = \frac{k_\ell}{H_d} (G - HL) - k_5 L = 0 \tag{46}$$

$$\frac{k_\ell}{d} L + k_5 L = \frac{k_\ell}{H_d} G$$

$$L = \frac{\frac{k_\ell}{Hd} G}{\frac{k_\ell}{d} + k_5} = \frac{G}{H + \frac{k_5 x H x d}{k_\ell}} \tag{47}$$

Eliminating L between equations (47) and (30) gives

$$F = \frac{k_\ell}{H} \left(G - \frac{G}{1 + \frac{k_5 x d}{k_\ell}}\right)$$

$$F = \frac{k_\ell \times G}{H} \left(1 - \frac{1}{1 + \frac{k_5 x d}{k_\ell}}\right) \tag{48}$$

Now we can define a Flux Effectiveness ratio = $\frac{F}{\frac{k_\ell}{H} \times G} = \left(1 - \frac{1}{1 + \frac{k_5 x d}{k_\ell}}\right)$

which describes the fraction of O_3 entering the water which is actually destroyed. This ratio is plotted vs. mixing depth, for both distilled water and ocean water (Fig. 12). For k_5 the experimental value was used. For deposition velocity the value k_ℓ = .0112 cm/sec was used which was two times larger than Liss' number. Our studies showed the deposition velocity for ozone is two times larger than the deposition velocity for CO. Liss calculated the k_ℓ for CO as .0056 cm/sec. In that situation the k_ℓ for ozone must be .0112 cm/sec. For the case of distilled water the values of .0112 was multiplied in ratio of the experimental value of k_ℓ in distilled water over the experimental value of k_ℓ for ocean water.

To show that ozone can diffuse through the water, equation (47) was considered. That equation shows that L is a function of mixing depth. Then L/G was plotted vs. mixing depth (Fig. 13). Figure shows that ozone can exist in significant concentrations at more than one meter depth. Also, results show concentration of ozone in ocean drops faster than in distilled water, which agrees with the increased reactivity of ozone in ocean water (due to the alkalinity of ocean water).

Photoacoustic spectroscopy was used in this study for the detection of O_3 and the loss of O_3 through the liquid surface.

This method had a detection limit of 8 ppm for ozone which can be improved by modification in the electronics (e.g., decrease the noise level.) PAS has the advantage of simplicity compared to other techniques of measurement of ozone (e.g., chemiluminescent)). Also, if the solubility of ozone in solution was known, it is possible to use PAS as

an indirect method for measurement of ozone concentrations in solution, by providing a rapid equilibrium between the liquid and gas phases of the sample solution. Then the gas phase is measured by PAS and by using the solubility of ozone in solution, ozone concentration solution can be calculated.

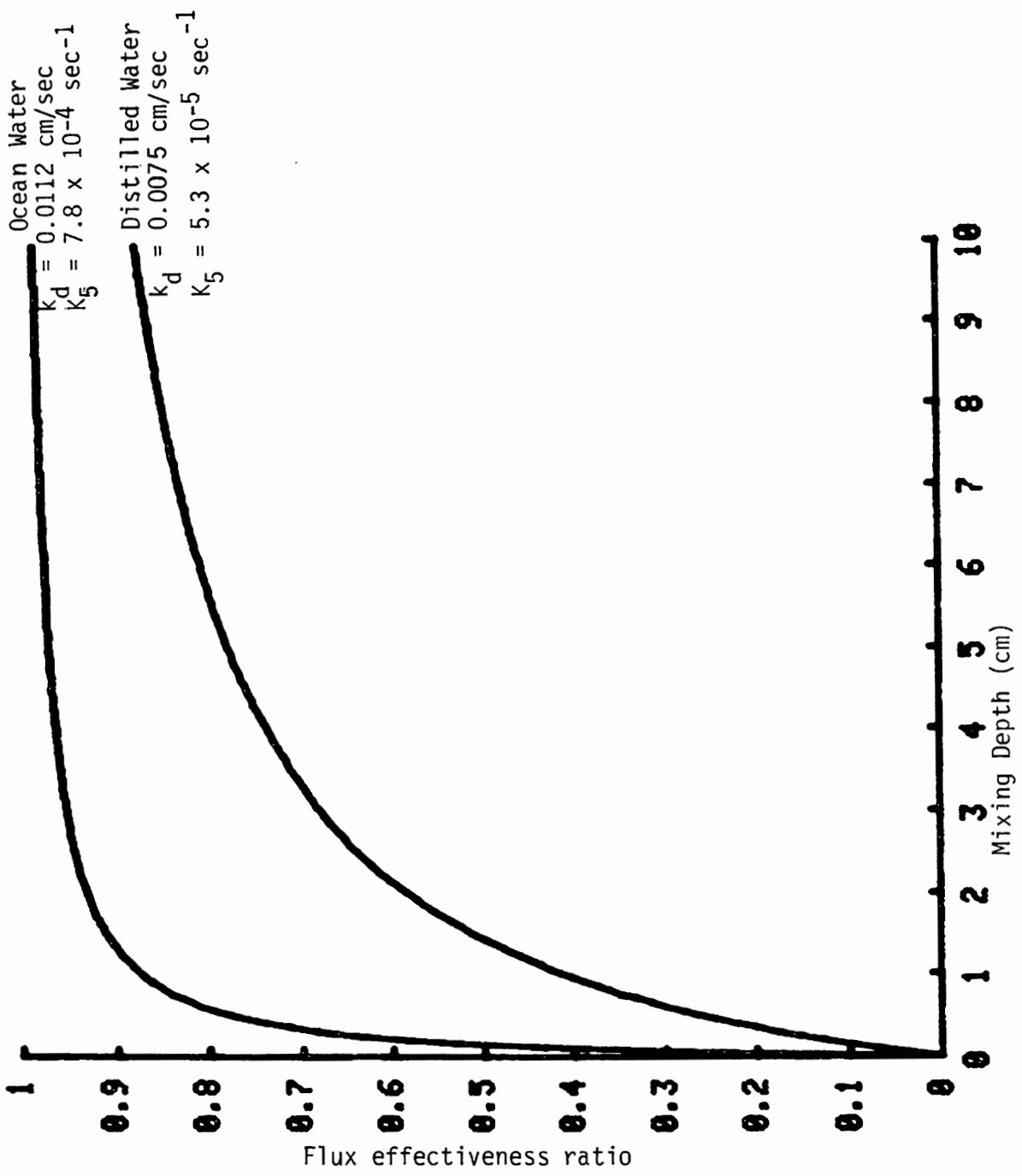

Figure 12. Flux effectiveness ratio as function of mixing depth.

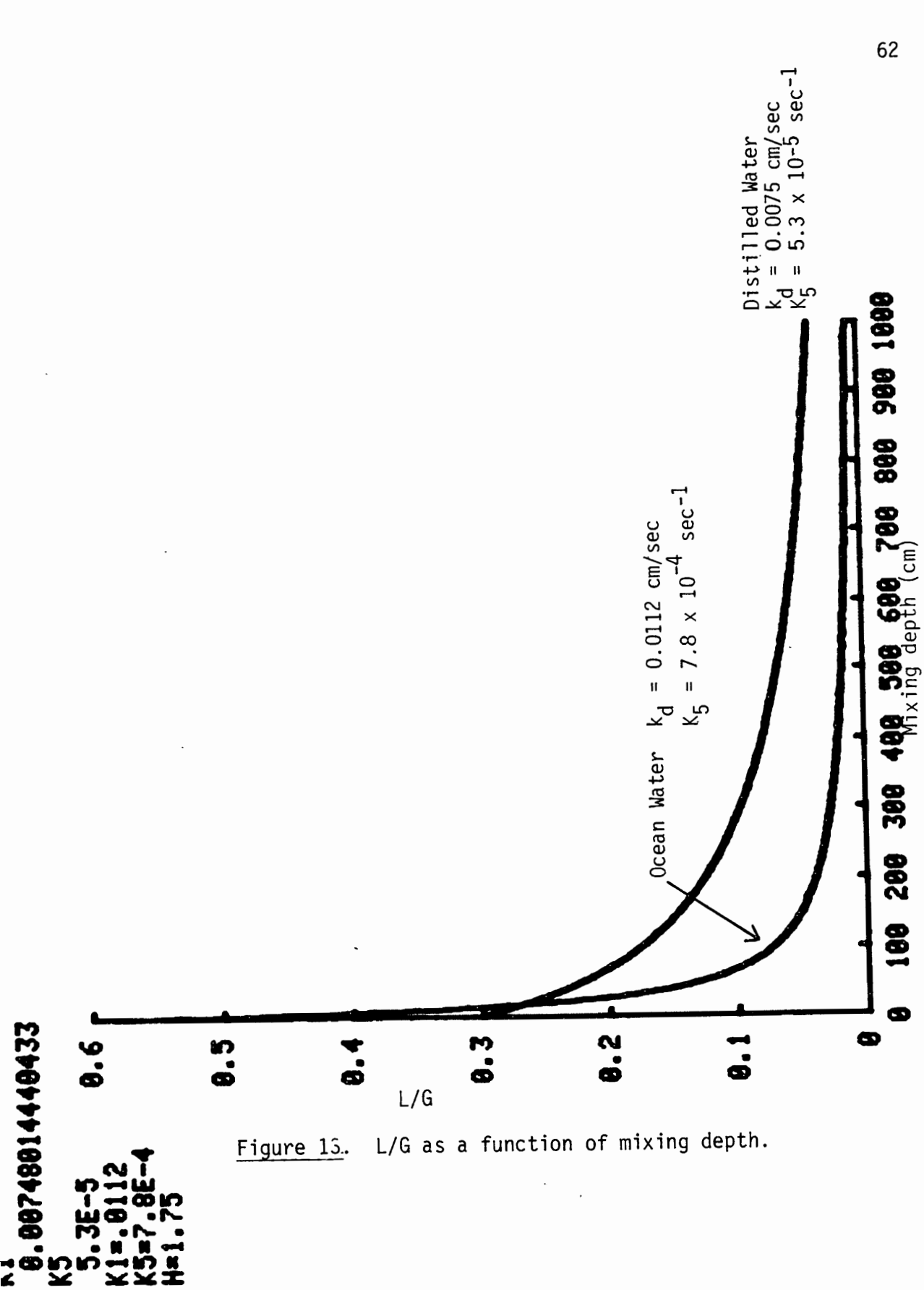

Figure 13. L/G as a function of mixing depth.

REFERENCES

1. Fabian, P. and P.G. Pruchniewize. "Tropospharishes Ozone. Final Report," MPA E-W-100-76-21, Max Planck Institut for Aeronomie, W. Gemrnay, 28 pp.

2. UC Environmental Protection Agency, 1978. "Air Quality Criteria for Ozone and Other Photochemical Oxidants," EPA-600/81/78.

3. Ripperton, L.A. and F.M. Vukovich. "Gas Phase Destruction of Tropospheric Ozone," Journal of Geophysical Research, 76, 7328-38, 1971.

4. Crutzen, P.J. and J. Fishman. "A Numerical Study of Tropospheric Photochemistry: A One Dimensional Model," Journal of Geophysical Research, 82, 5897-5906, 1977.

5. Crutzen, P.J., I.H. Isaksen and J.R. McAfee. "Impact of the Chlorocarbon Industry on the Ozone Layer," Journal of Geophysical Research, 83, 345-363, 1978.

6. Chameides, W.L. and J.G. Walker, "A Photochemical Theory of Tropospheric Ozone," Journal of Geophysical Research, 78, 8700-8751, 1973.

7. Chameides, W.L and D.H. Stedman, "Tropospheric Ozone: Coupling Transport and Photochemistry," Journal of Geophysical Research, 82, 1778-94, 1977.

8. Singh, H.B., F.L. Ludwig and W.B. Johnson, "Tropospheric Ozone: Concentrations and Variabilities in Clean Remote Atmosphere," Atmospheric Environment, 12, 12185-94, 1978.

9. L. Aldaz, "Flux Measurements of Atmospheric Ozone over Land and Water," Journal of Geophysical Research, 71, 6943-6, 1969.

10. Fabian, P. and C.H.R. Junge, "Global Over of Ozone Destruction at the Earth's Surface," Journal Arch. Met. Geoph. Biokl., Series A, 19, 161-172, 1970.

11. Crutzen, P.J. "A Two-Dimensional Photochemical Model of the Atmosphere Below 55 Km: Estimation of Natural and Man-Caused Perturbations due to NO_x," Proceedings of the 4th Conference on the Impact Assessment Program, Editor T.M. Hard, 264-279, 1975.

12. Fishman, J. and P.J. Crutzen, "A Numerical Investigation of Tropospheric Photochemistry Using a One-Dimensional Model," The Non-urban Tropospheric Composition, a Joint Symposium of the American Geophysical Union and the American Meteorological Society, 23-24, 1976.

13. Regener, V.H. and L. Aldaz. "Turbulent Transport Near the Ground as Determined from Measurements of Ozone Flux and Ozone Gradient," J. Geophys. Res., 74, 6935-42, 1969.

14. Regener, V.H. "Measurement of Atmospheric Ozone with the Chemiluminscent Method," J. of Geophys. Res., 69, 3795-3800, 1964.

15. Tiefenau, H. and P. Fabian. "The Specific Ozone Destruction at the Ocean's Surfaces and its Dependence on Horizontal Wind Velocity from Profile Measurement," Arch. Met. Geophys. Biotl. Series A, 21, 399-412, 1972.

16. Tiefenau, H. "The Specific Ozone Destruction Rate of the Ocean Surface and its Dependence on Horizontal Wind Velocity," Par and Applied Geophysics, vol. 106-108 (1116-23), 1973.

17. Regener, V.H. "Destruction of Atmospheric Ozone of the Ocean Surface," Arch. Met. Geophys., Series A, 23, 131-135, 1974.

18. Liss, P.S. and P.G. Slater. "Flux of Gases Across the Air-Sea Interface," Nature, 247, 181-184, 1974.

19. Briner, E. and E. Perrottet. "Determination des Solubilites de l'ozone dans l'eau et dans une solution aquease de chloure de sodium, calcul des solubilites de ozone atmospher ique dans les eaux," Helv. Chim. Acta., 22, 397-404, 1939.

20. Wilhem, E., R. Battino and R.J. Wilcock. "Low-Pressure Solubility of Gases in Liquid Water," Chem. Reviews, 77, 219-262, 1977.

21. Junge, C. "The Role of the Oceans as a Sink for Chlorofluormethanes and Similar Compounds," Z. Naturforsch. 31a, 182-187, 1976.

22. Broecker, W.S. and T.H. Peny. Tellus, 26, 21, 1974.

23. Chameides, W.L. and J.C. Walker, "A Time Dependent Photochemical Model for Ozone Near the Ground," J. Geophys. Res., 81, 413-420, 1976.

24. Weiss, J. "Investigation on the Radical HO_2 in Solution," Trans. Faraday Soc., 31, 668 (1935).

25. Alder, M.G. and G.R. Hill. "The Kinetics and Mechanism of Hydroxide-Ion Catalyzed Ozone Decomposition in Aqueous Solution, J. Am. Chem. Soc., 72, 1884-86, 1950.

26. Kilpatrick, M.L., C. Herr and C.K. and M. Kilpatrick, "The Decomposition of Ozone in Aqueous Solution," J. Am. Chem. Soc., 78, 1784-89, 1956.

27. Danckwerts, P.V. Gas-liquid Reaction (London: McGraw-Hill, 1970).

28. Kreuzer, L.B. "The Physical Signal of Generation and Detection," Opto Acoustic Spectroscopy and Detection, ed. by Y. Han Pao. (New York: Academic Press, 1977).

29. Cary, R.A. "Determination of Mercury by Photoacoustic Spectroscopy," Master's Thesis, Portland State University, 1977.

30. Ternus, L. M. "Photolysis of Ozone and Chlorine Mixtures," Master's Thesis, Portland State University, 1978.

31. DeMore, W.B. and M. Patapoff. "Comparison of Ozone Determination by Ultraviolet Photometry and Gas Phase Titration," Environmental Science and Technology, 10, 897-99, 1976.

32. Fabjan, C. "Die Kahodisce Reduktion von Ozon in Sauren Elektrolyten," Electrochim. Acta., 20, 863, 1975.

33. Fabjan, C. and R. Movahdi, "Die Katodische Reduktion von Ozon an Iridium in Sauren Elektrolyten," Electrochim. Acta., 22, 185-189, 1977.

34. Johnson, D.C., D.T. Napp and Stanley Bruckenstein, "Electrochemical Reduction of Ozone in Acid Media," Anal. Chem., 40, 482-8, 1968.

35. Smart, R.B., R.D. Herrera and K.H. Nancy, "In Situ Voltammetric Membrane Ozone Electrode," Anal. Chem., 51, 2315-19, 1979.

APPENDIX A

FIGURES 12 THROUGH 77

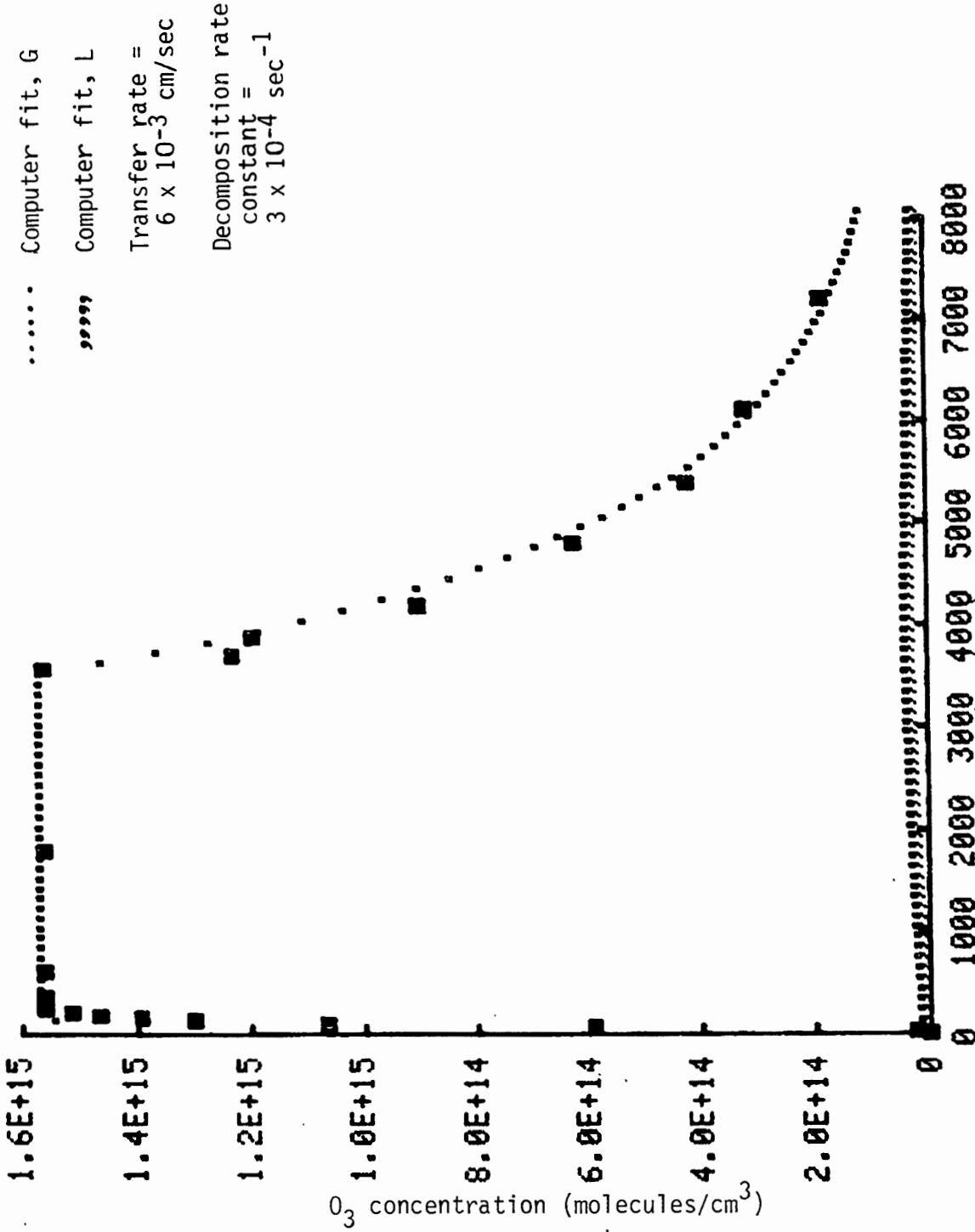

Figure 14. Loss of ozone through distilled water (continuous method).

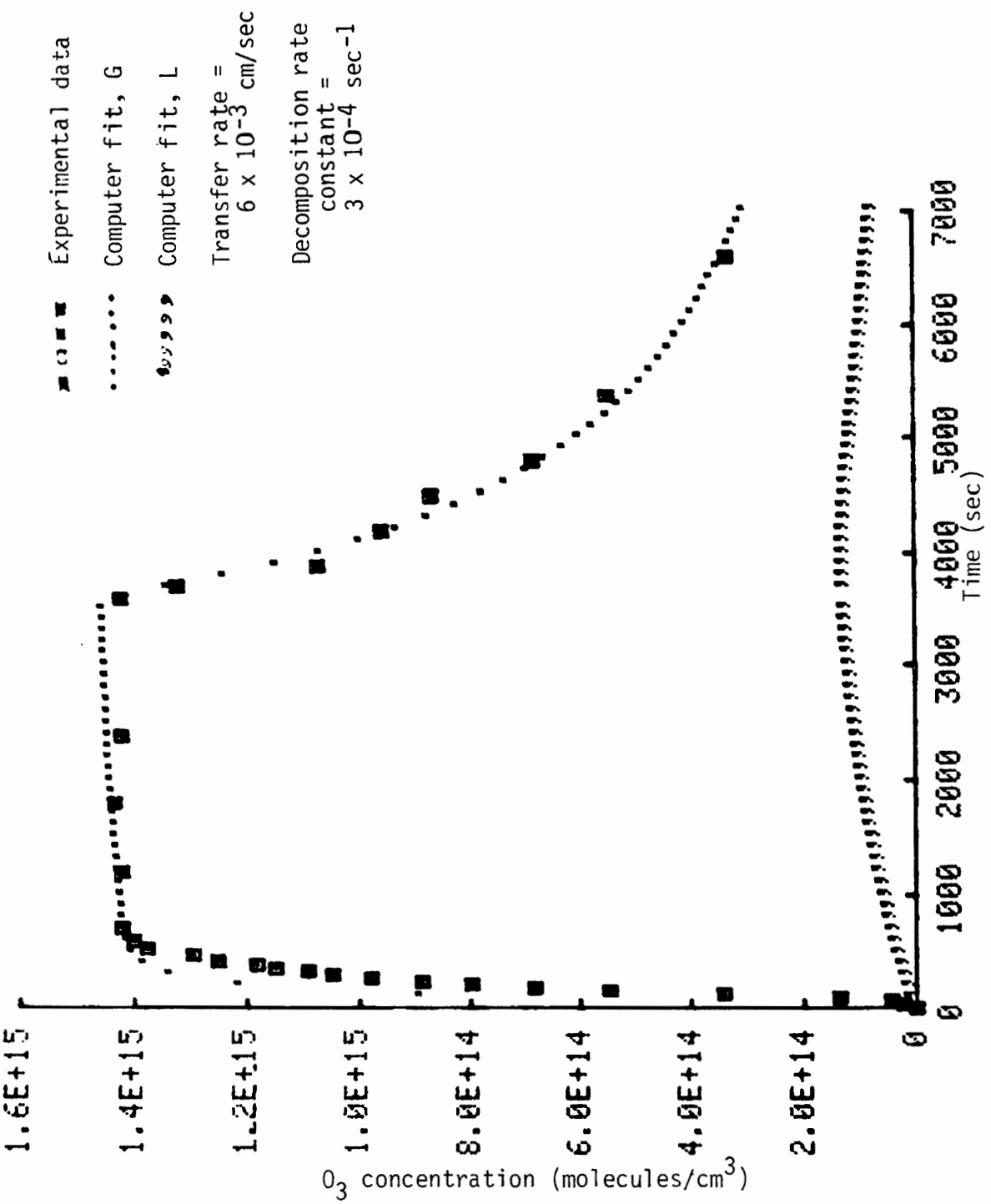

Figure 15. Loss of ozone through distilled water (continuous method).

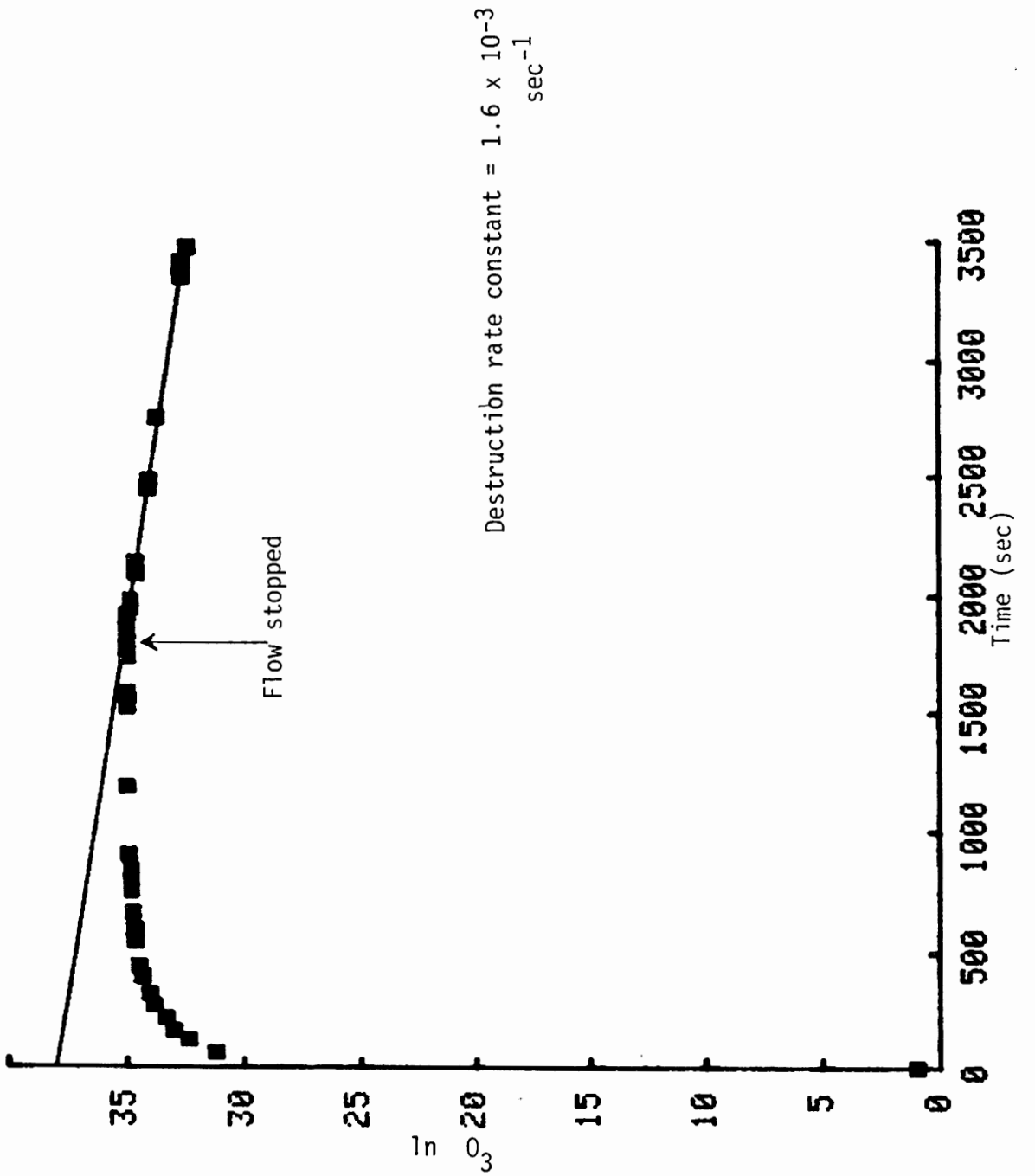

Figure 16. Graphic presentation of Rate Constant of Destruction of ozone in 250-ml beaker (with teflon cover).

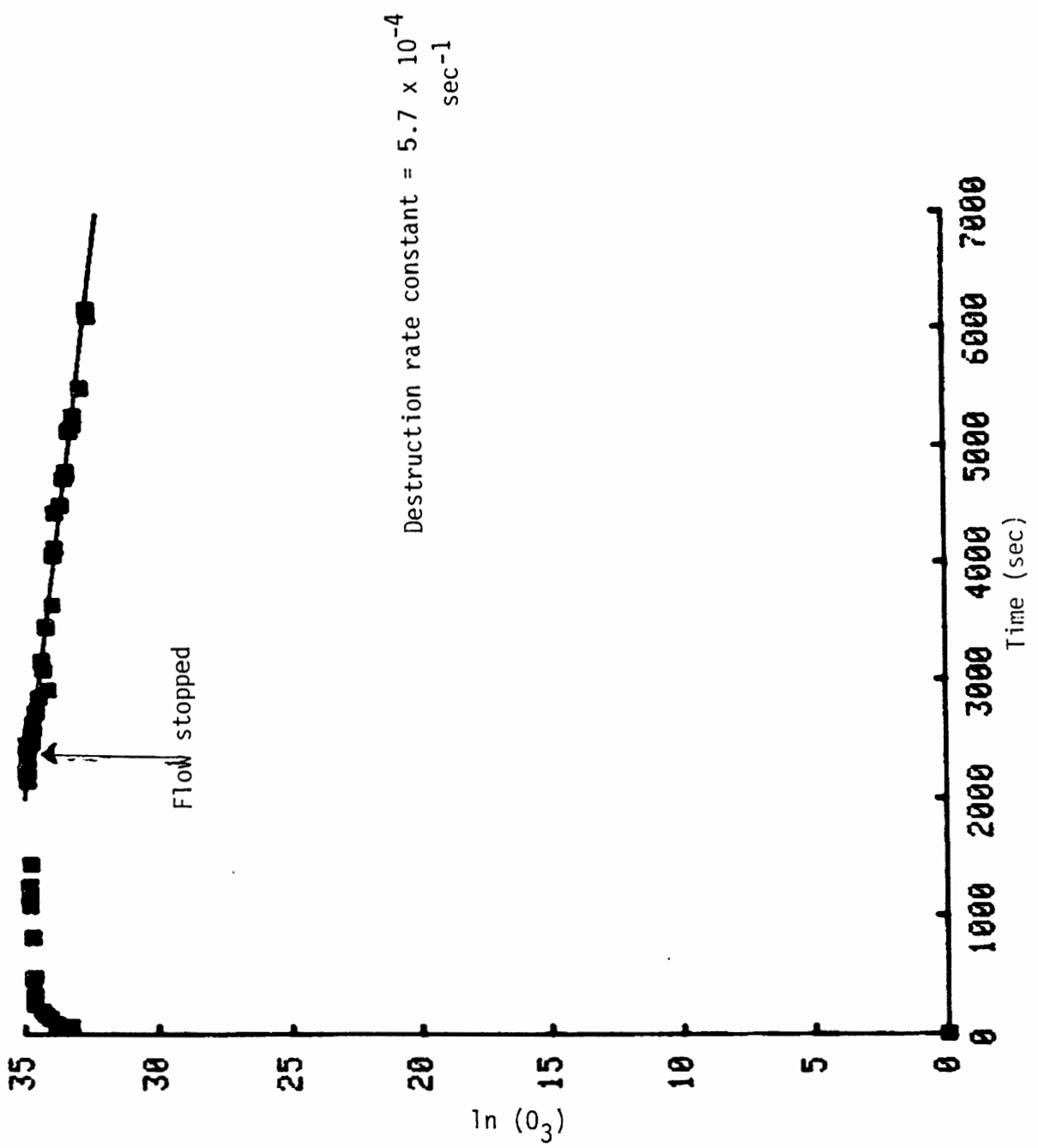

Figure 17. Graphic presentation of rate constant of destruction of ozone in 400-ml beaker (with teflon cover).

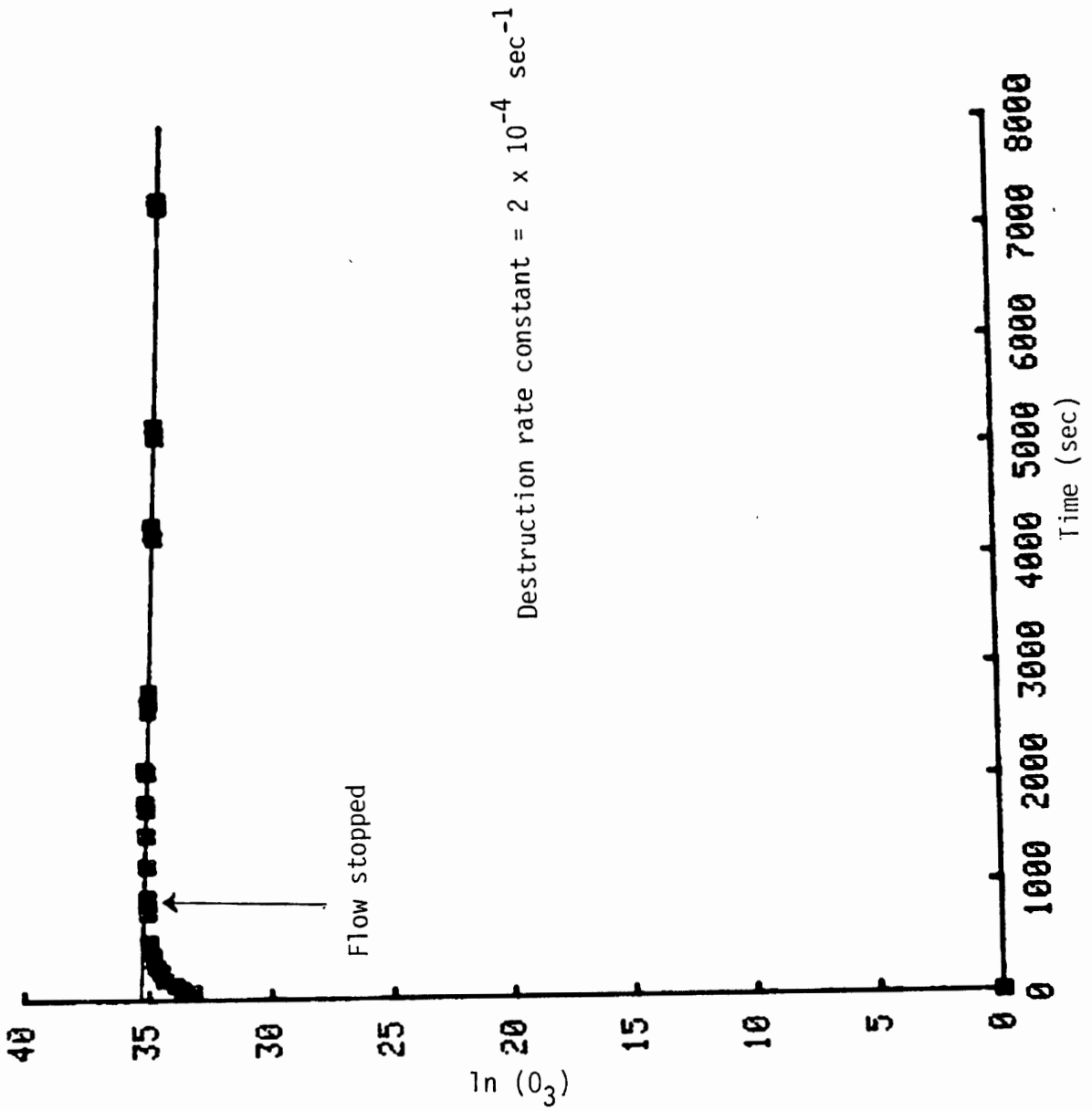

Figure 18. Graphic presentation of rate constant of destruction of ozone in 250-ml beaker (with mylar cover).

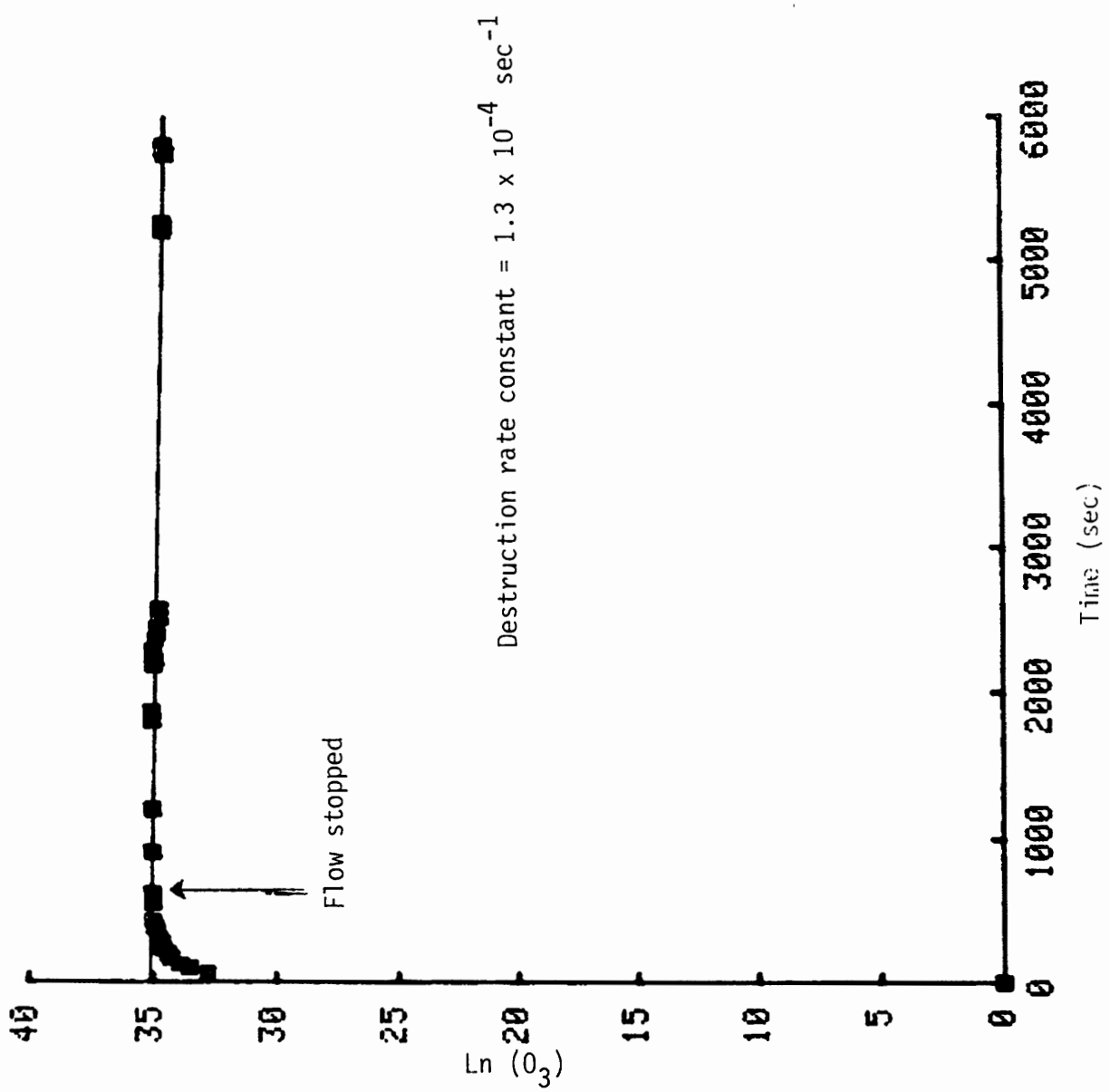

Figure 19. Graphic presentation of rate constant of destruction of ozone in a 40-ml beaker (with mylar cover).

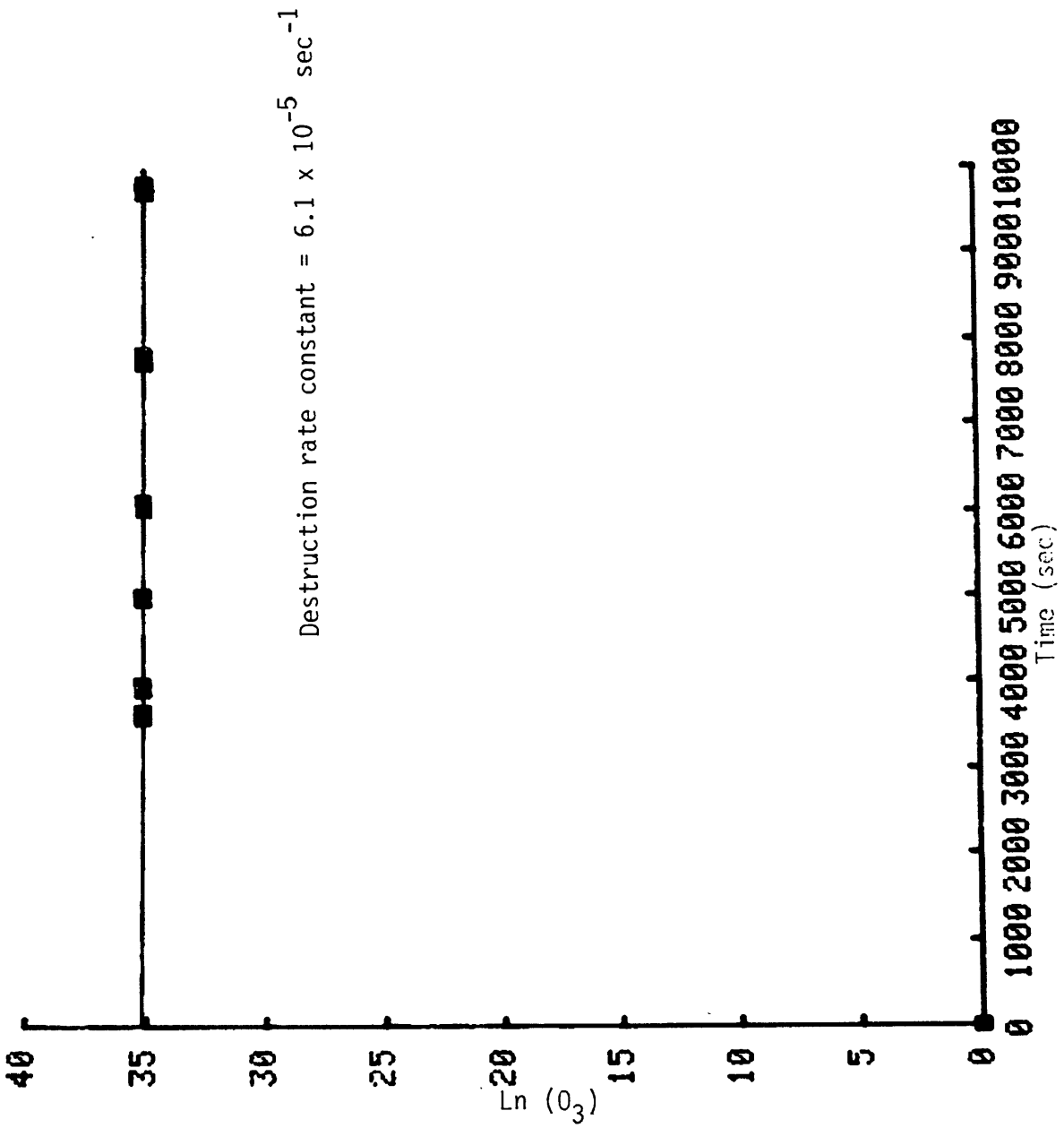

Figure 20. Graphic presentation of rate constant of destruction of ozone on 500-ml glass bottle (with mylar cover).

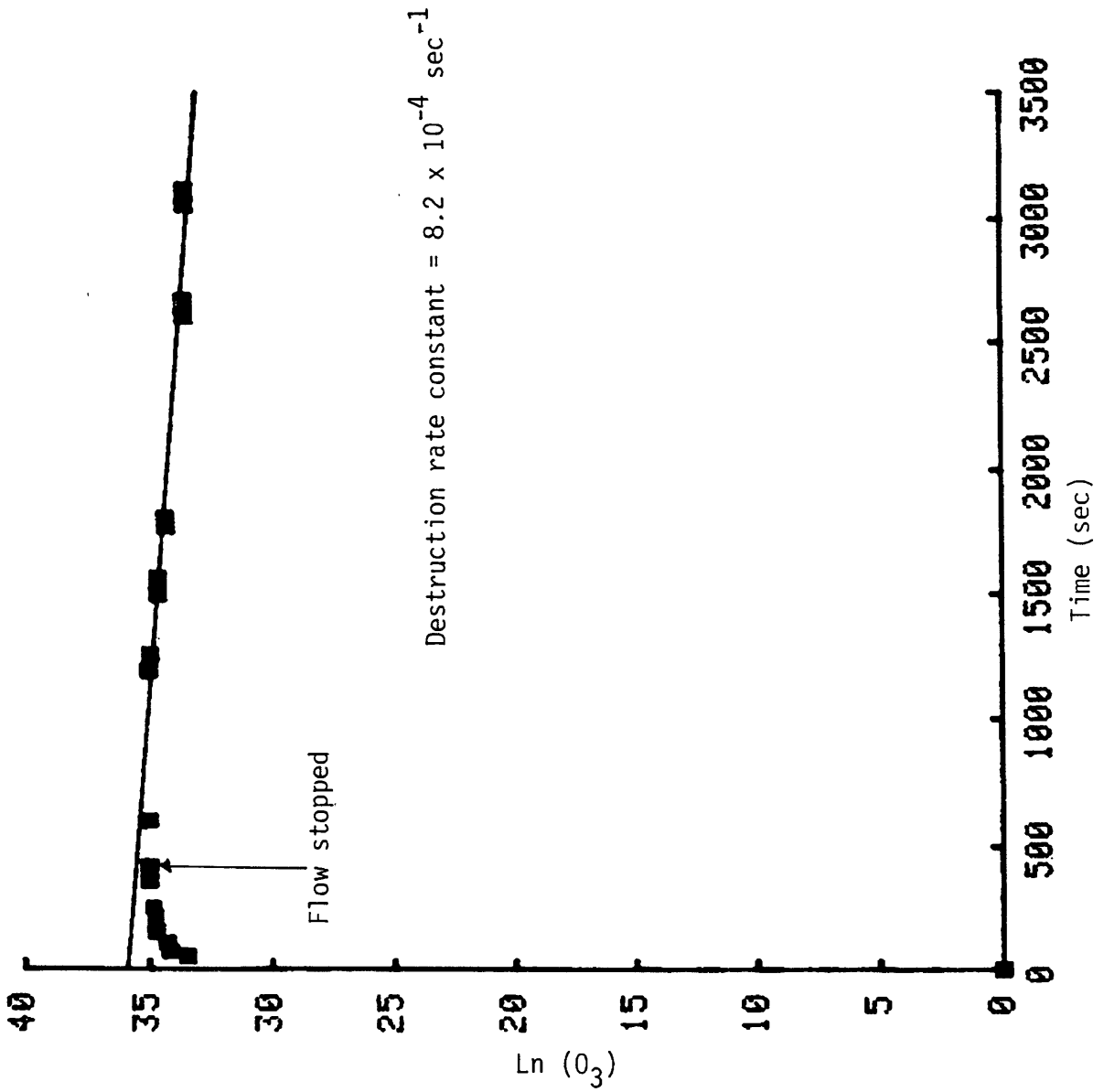

Figure 21. Graphic presentation of rate constant of destruction of ozone on 50-ml beaker (with mylar cover).

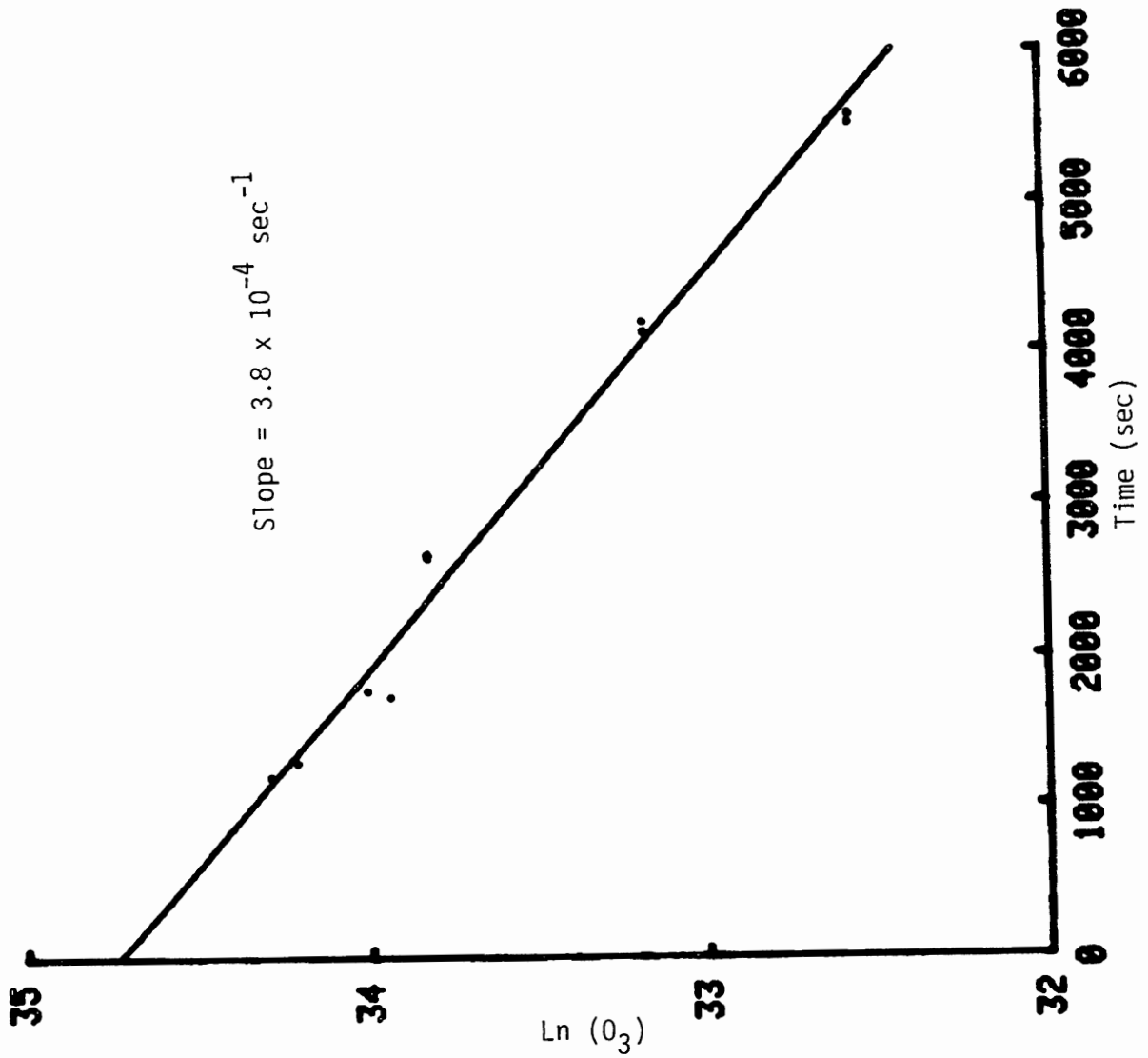

Figure 22. Graphic presentation of O_3 destruction on pH = 1.3 solution.

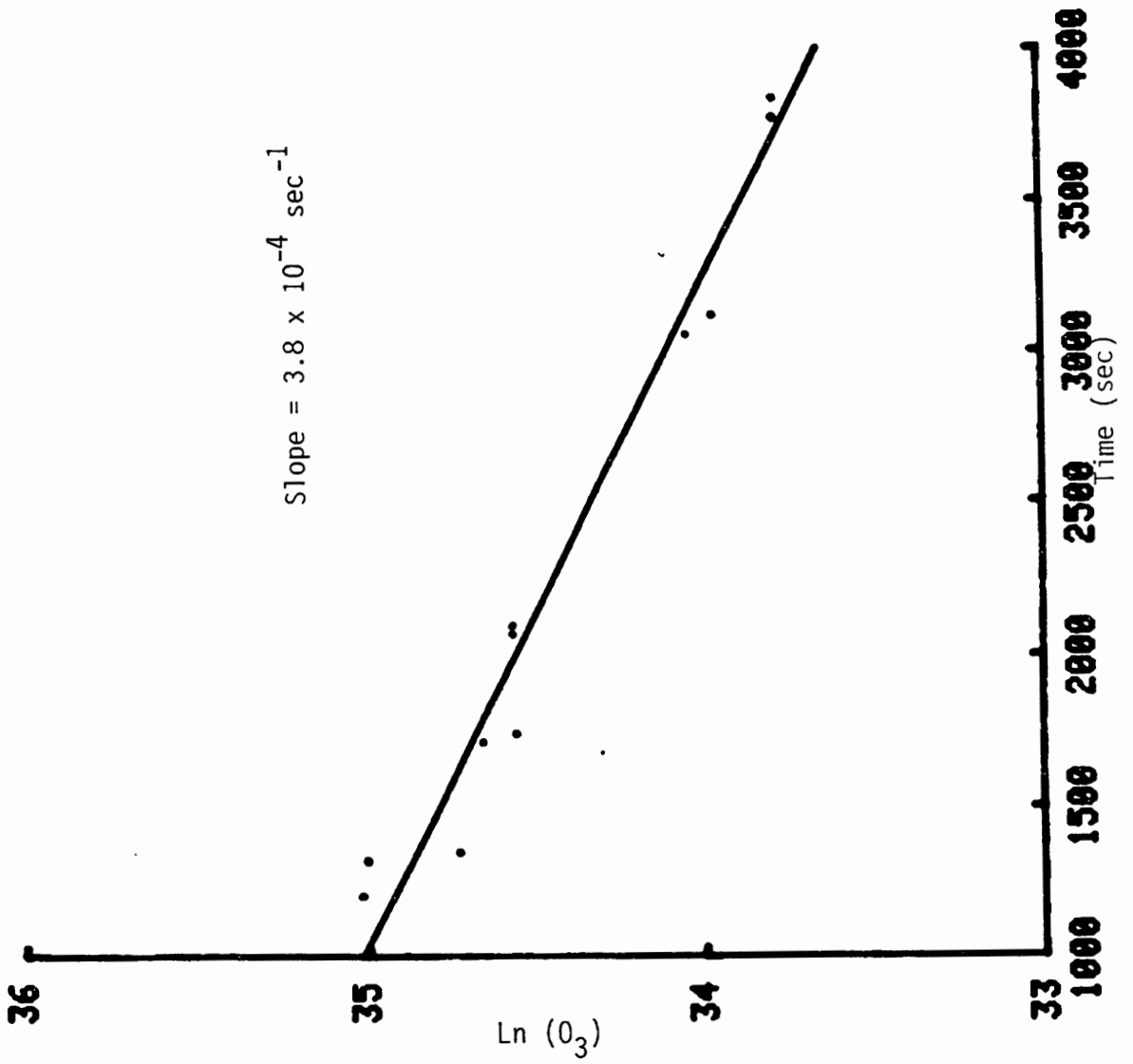

Figure 23. Graphic presentation of O_3 destruction on pH = 1.3 solution.

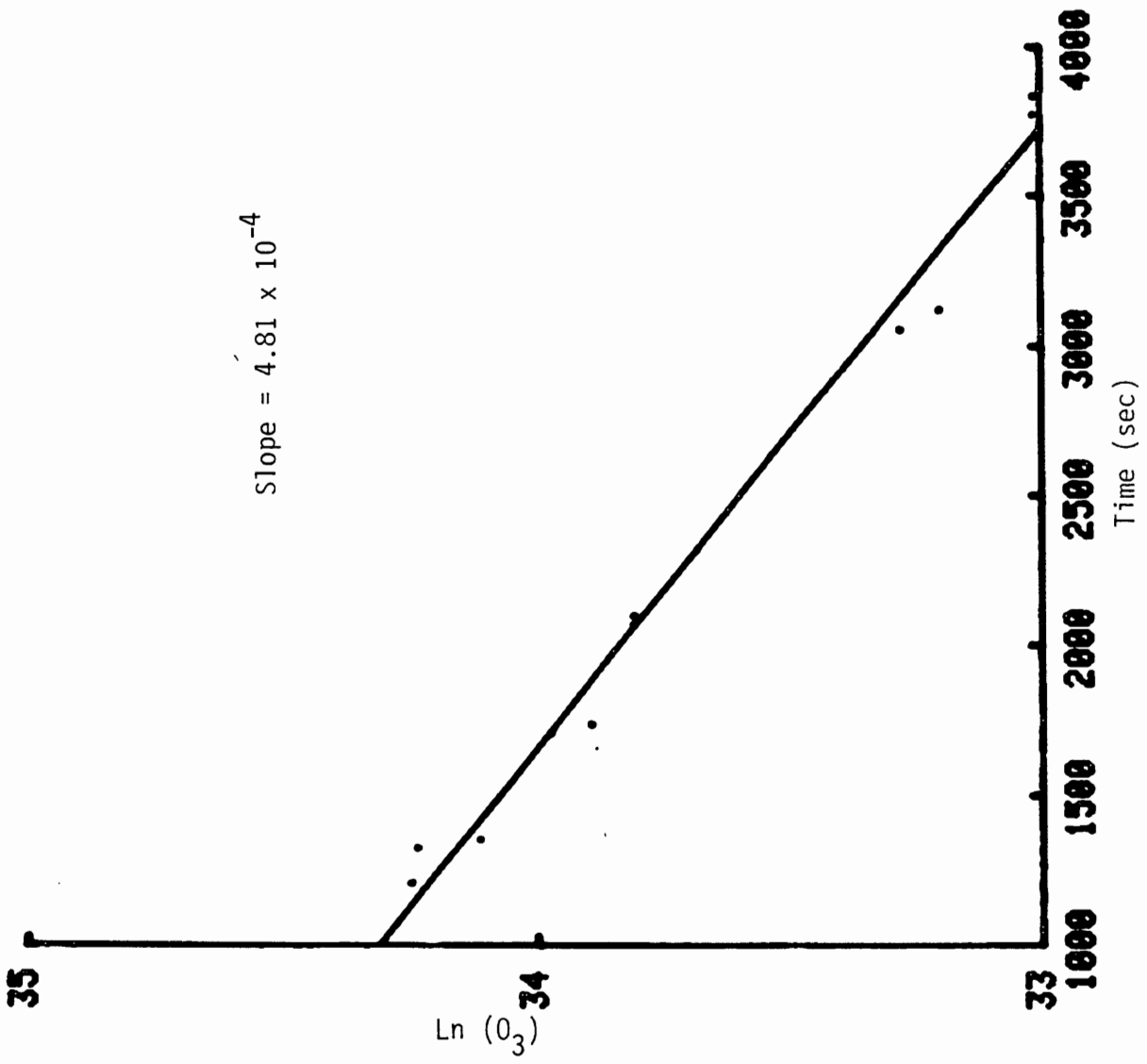

Figure 24. Graphic presentation of O_3 destruction on pH = 5.5 solution.

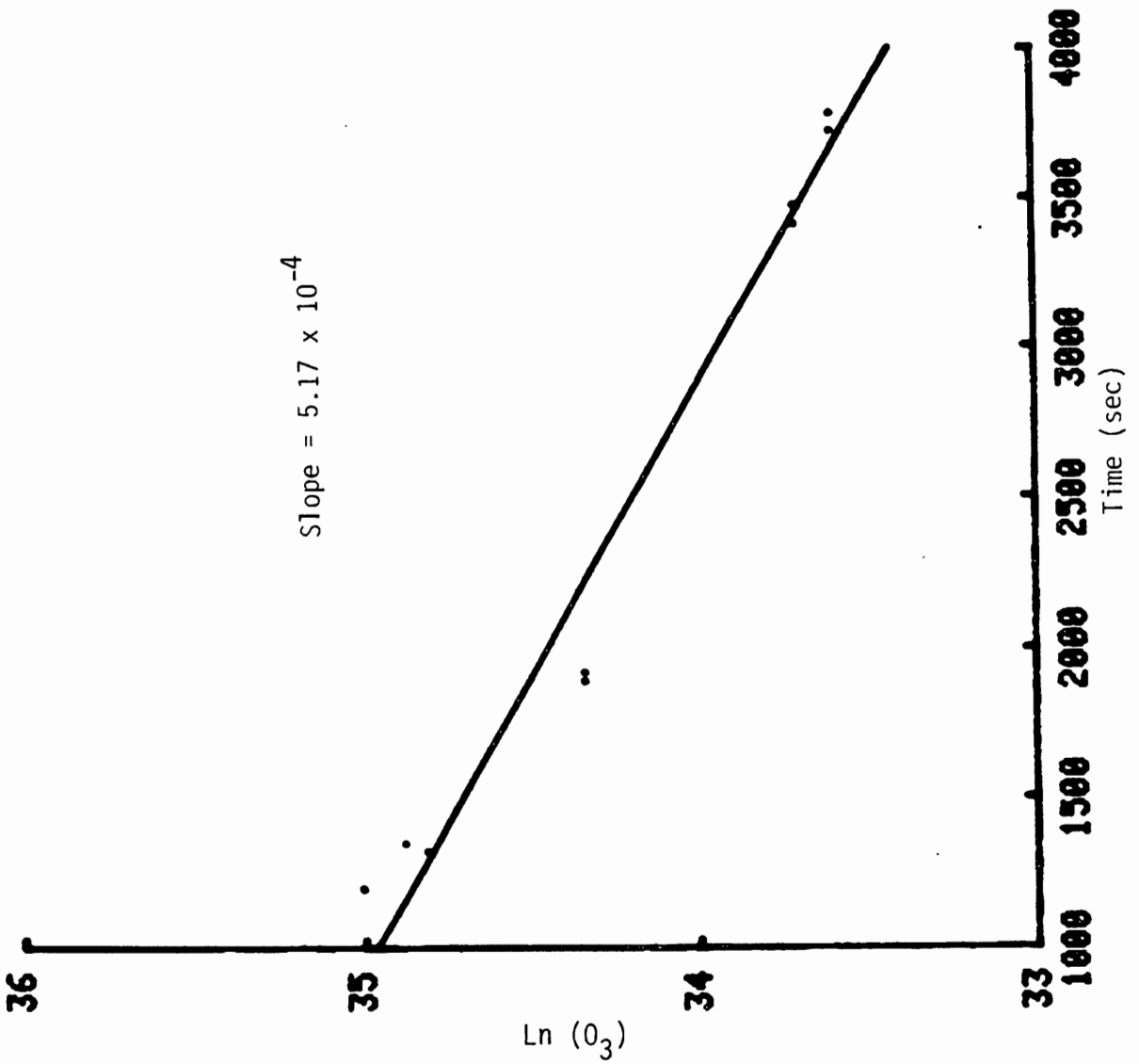

Figure 25. Graphic presentation of O_3 destruction on pH = 5.5 solution.

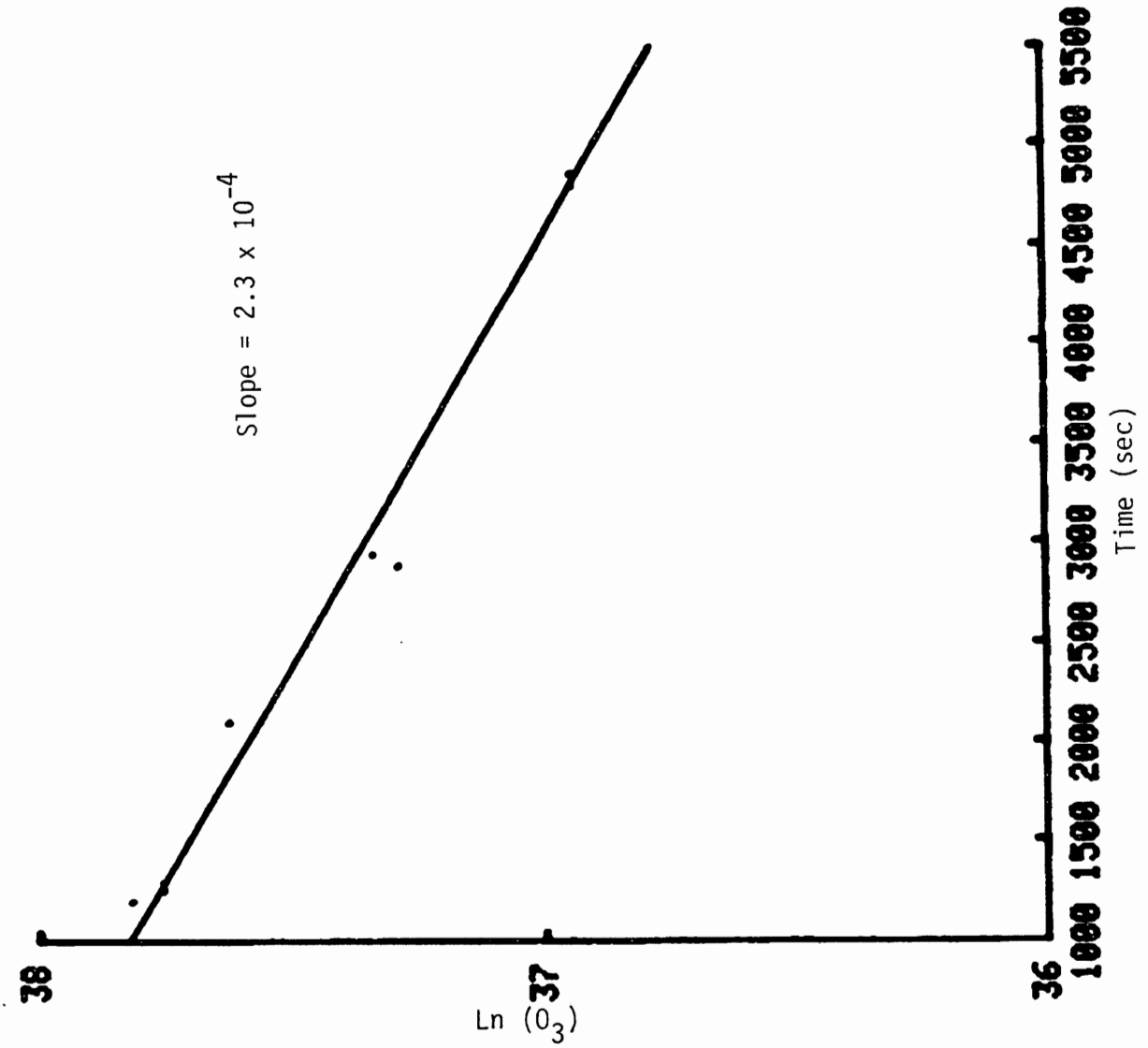

Figure 26. Graphic presentation of O_3 destruction on pH = 9 solution.

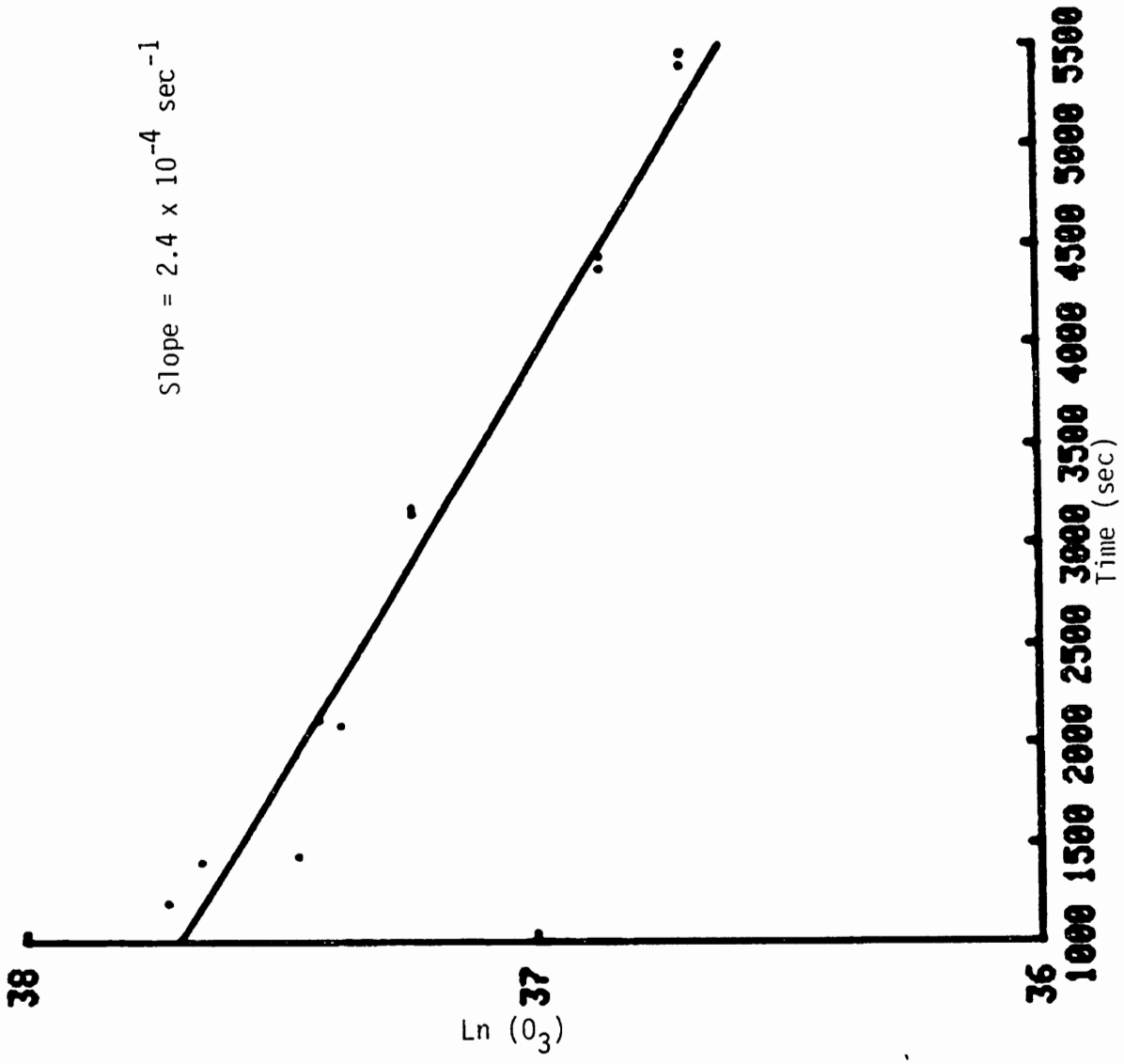

Figure 27. Graphic presentation of O_3 destruction on pH = 9 solution.

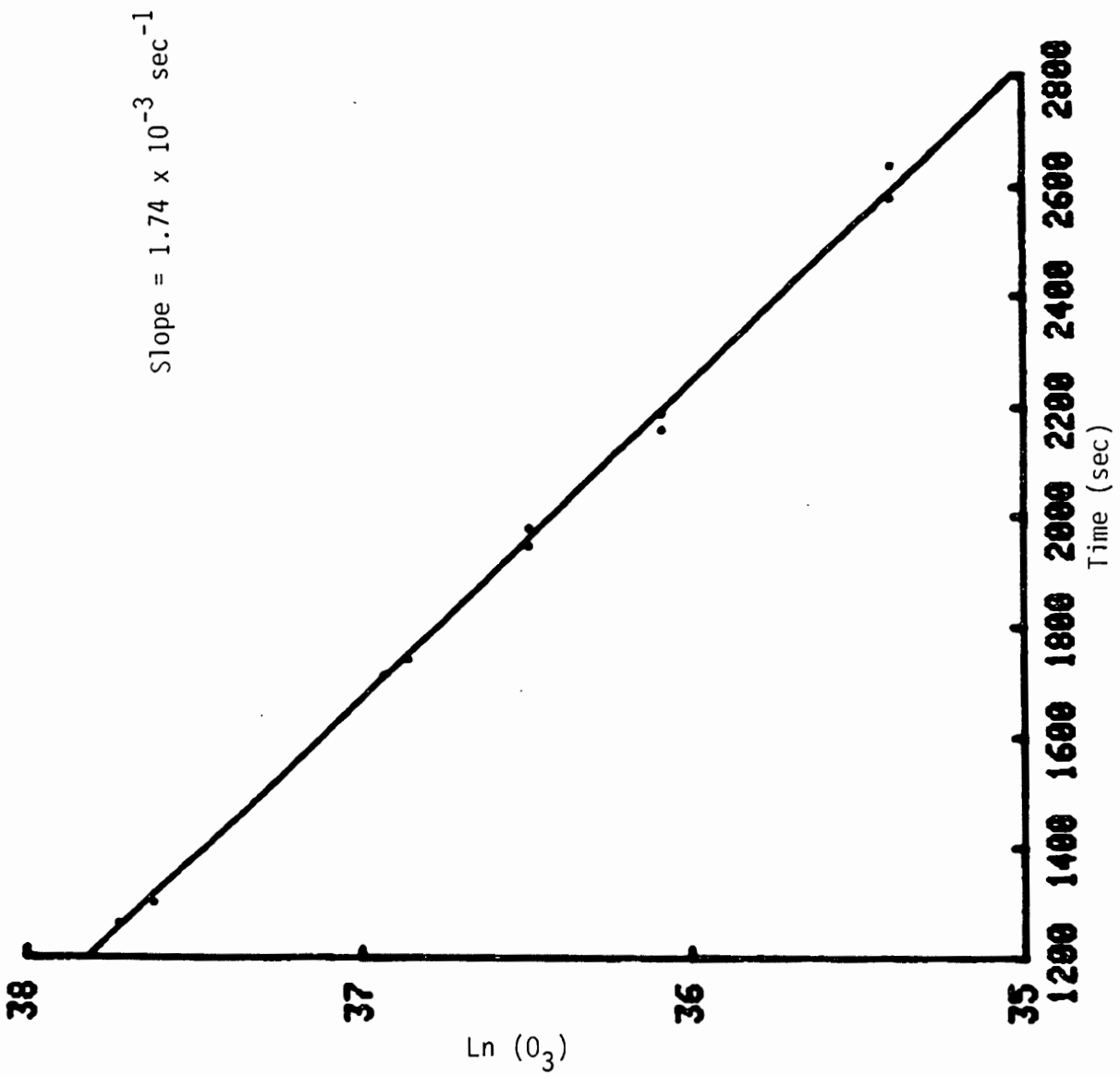

Figure 28. Graphic presentation of ozone destruction on pH = 13 solution.

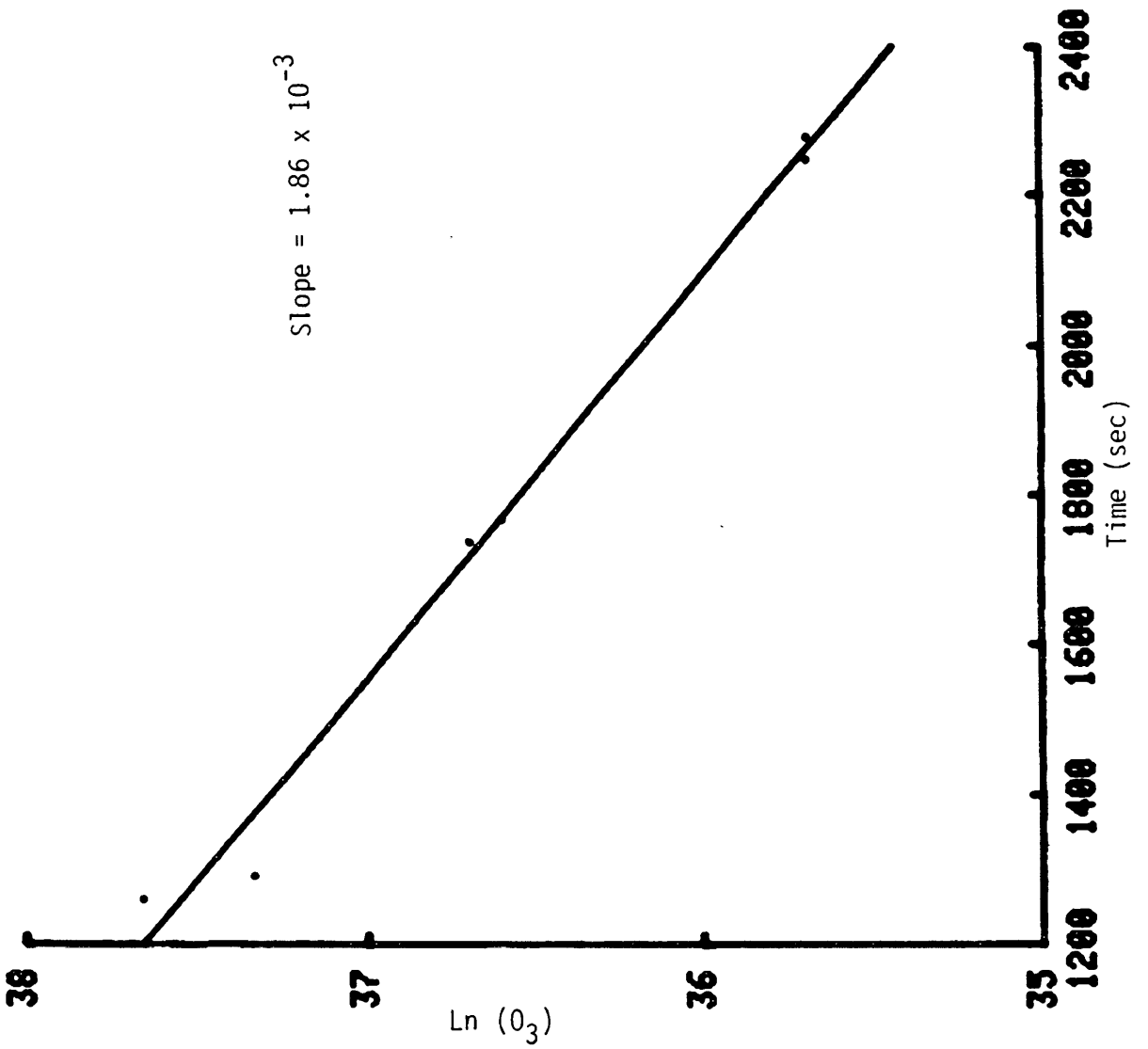

Figure 29. Graphic presentation of ozone destruction on pH = 13 solution.

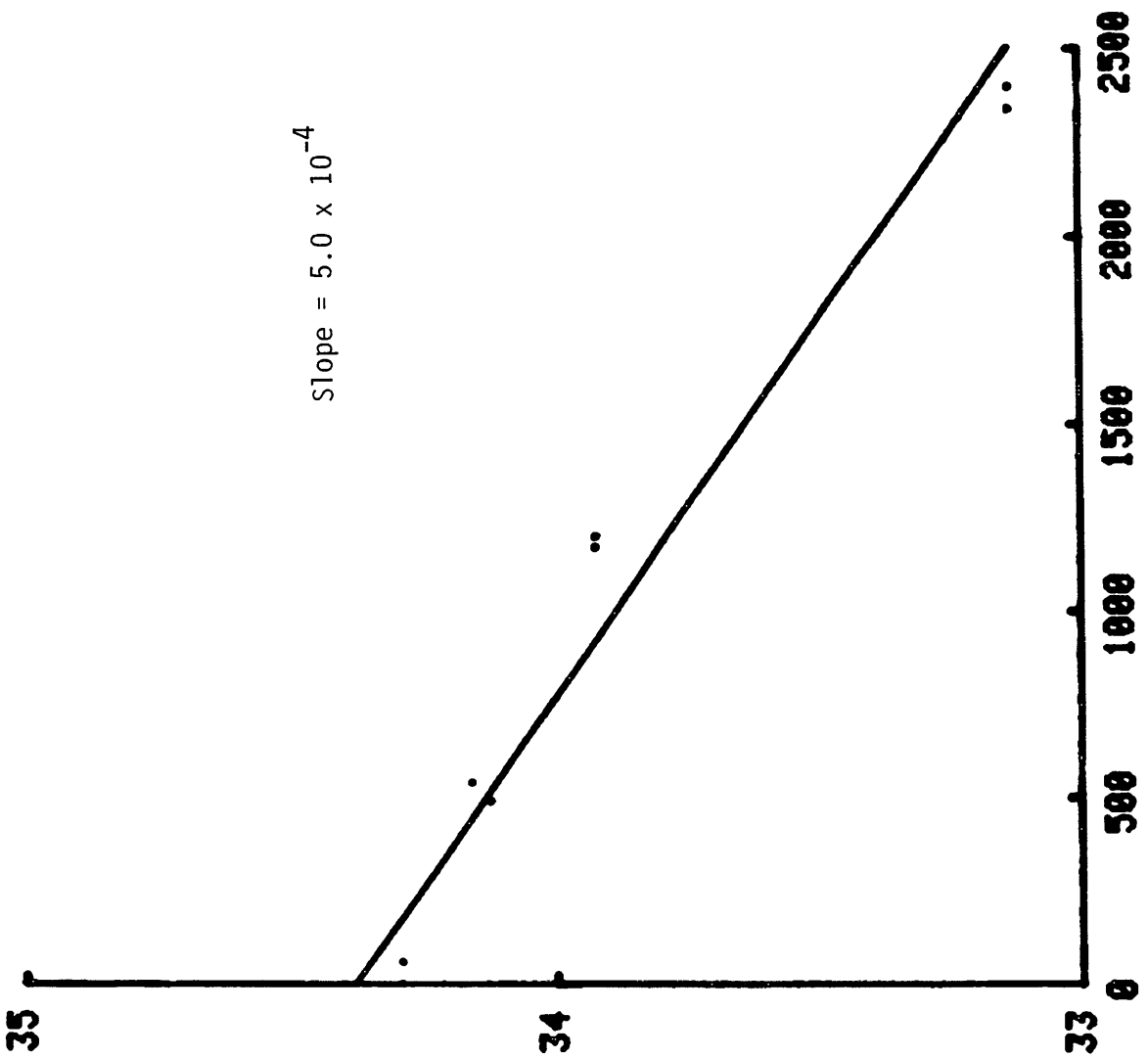

Figure 30. Graphic presentation of destruction of ozone on glass (using hemisphere).

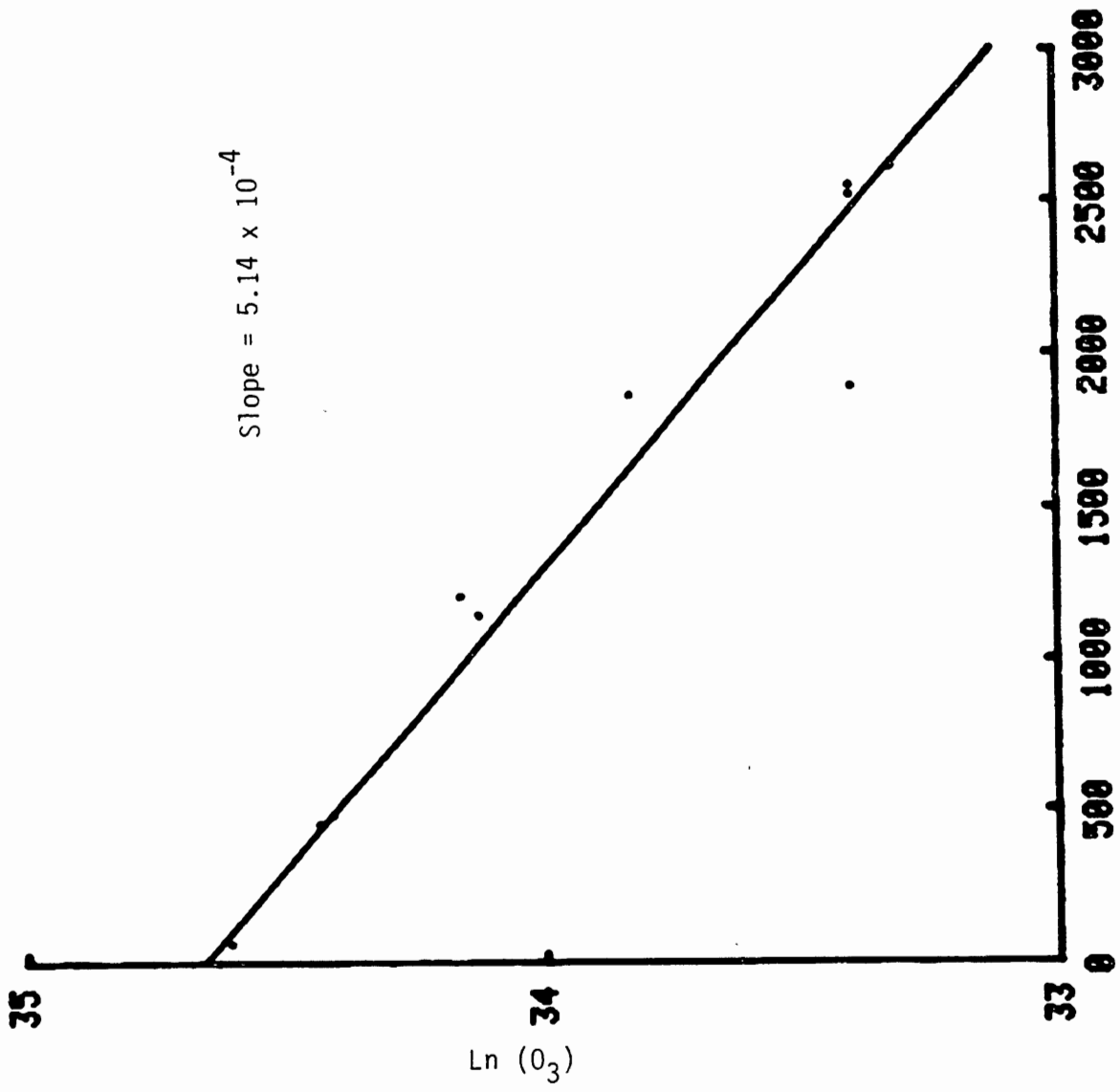

Figure 31. Graphic presentation of transfer rate constant of O_3 on pH = 1.3 solution (using hemisphere).

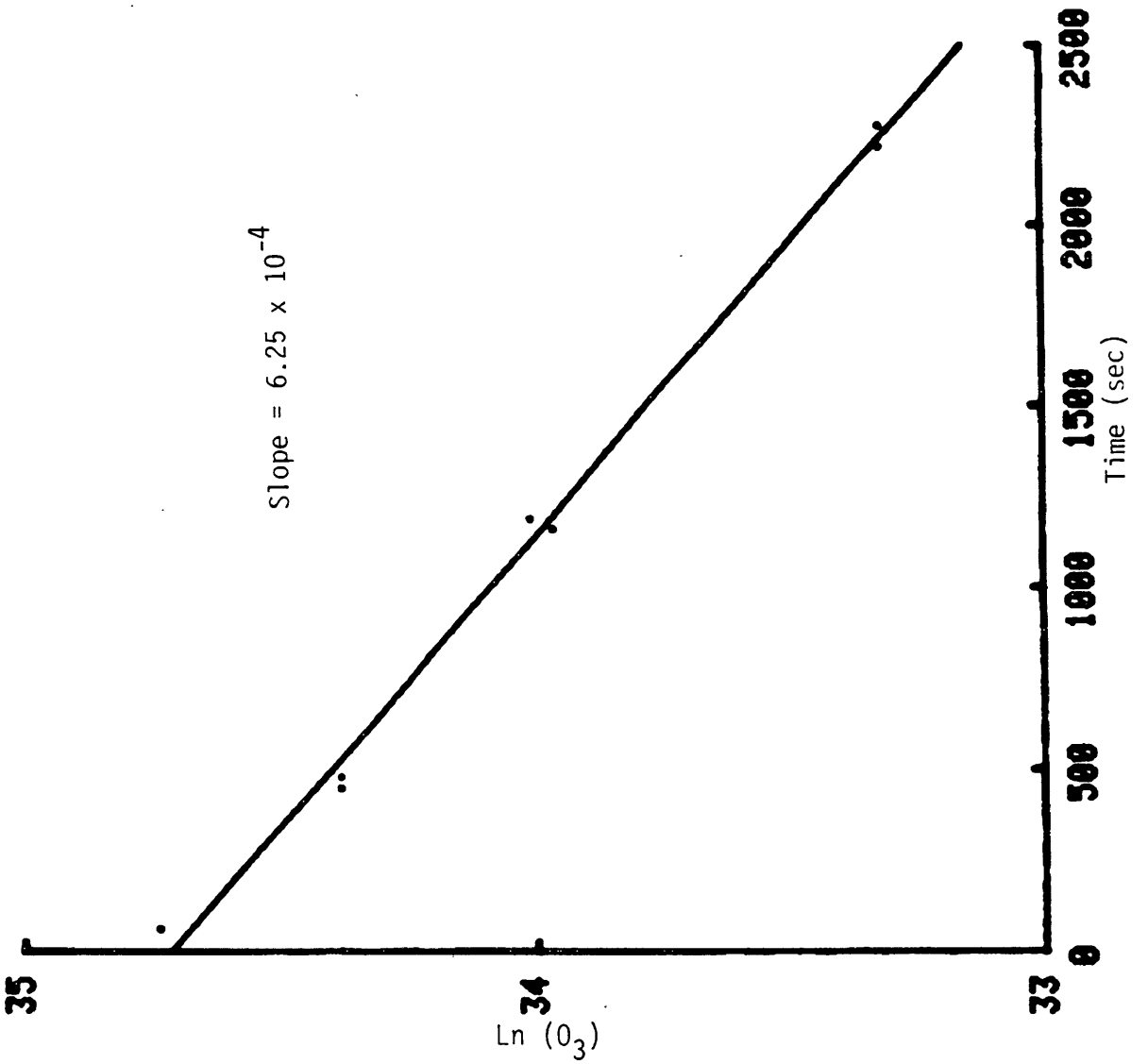

Figure 32. Graphic presentation of transfer rate constant of O_3 in a pH = 5.5 solution (using hemisphere).

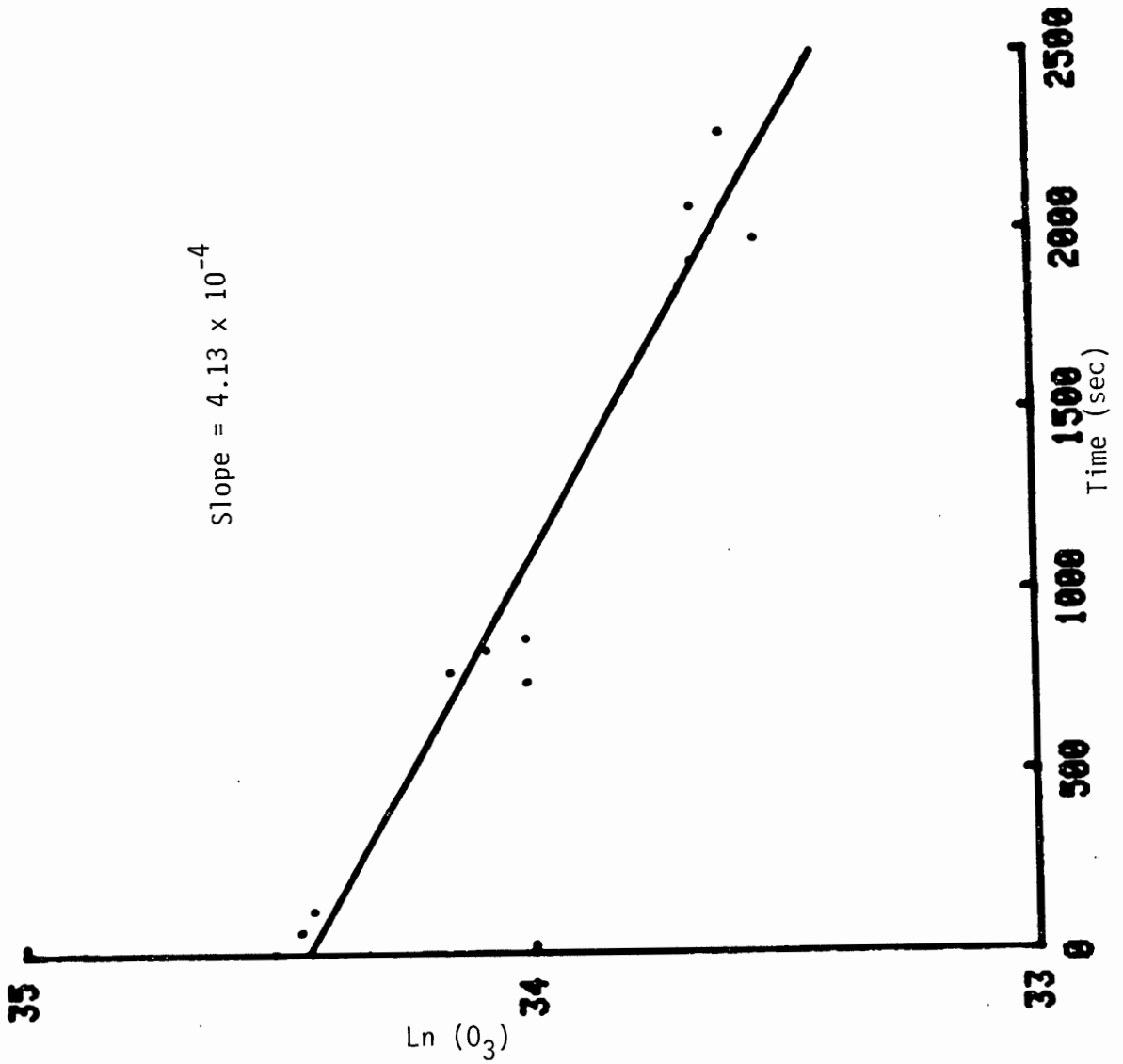

Figure 33. Graphic presentation of transfer rate constant of O_3 in a pH = 9 solution (using hemisphere).

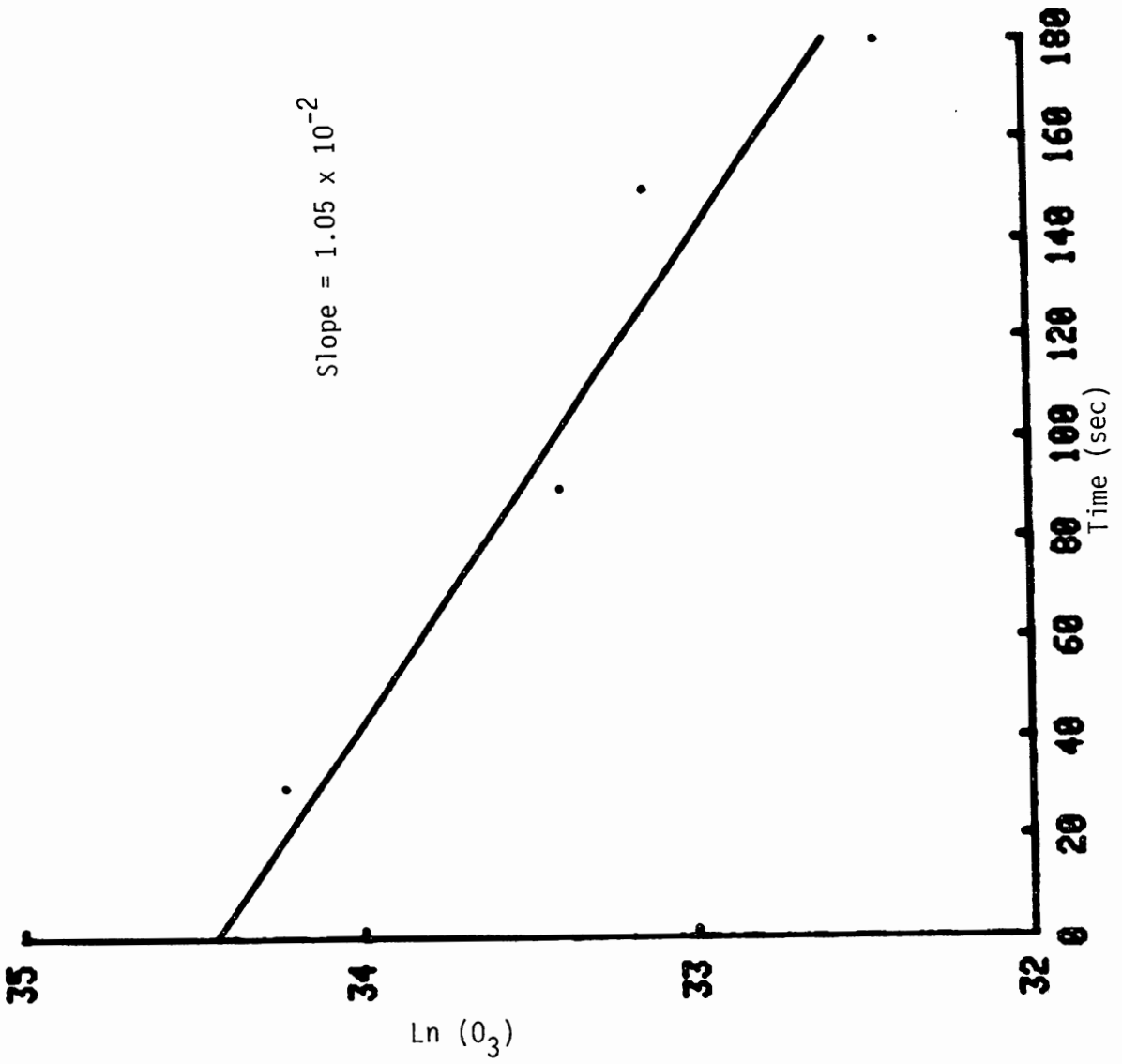

Figure 34. Graphic presentation of transfer rate constant of O_3 on pH = 13 solution (using hemisphere).

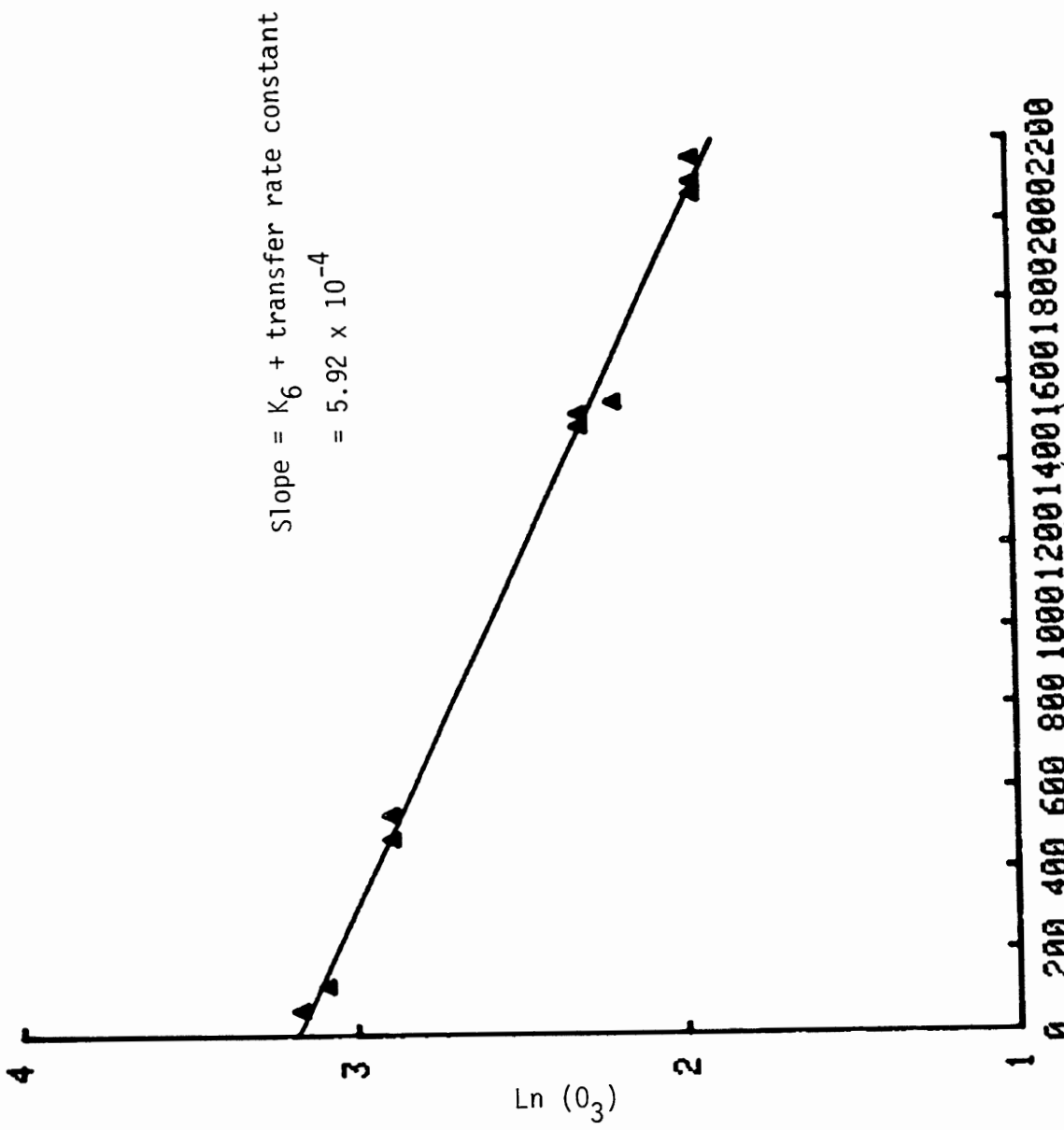

Figure 35. Graphic presentation of the transfer rate constant for O_3 in a pH = 5.5 solution.

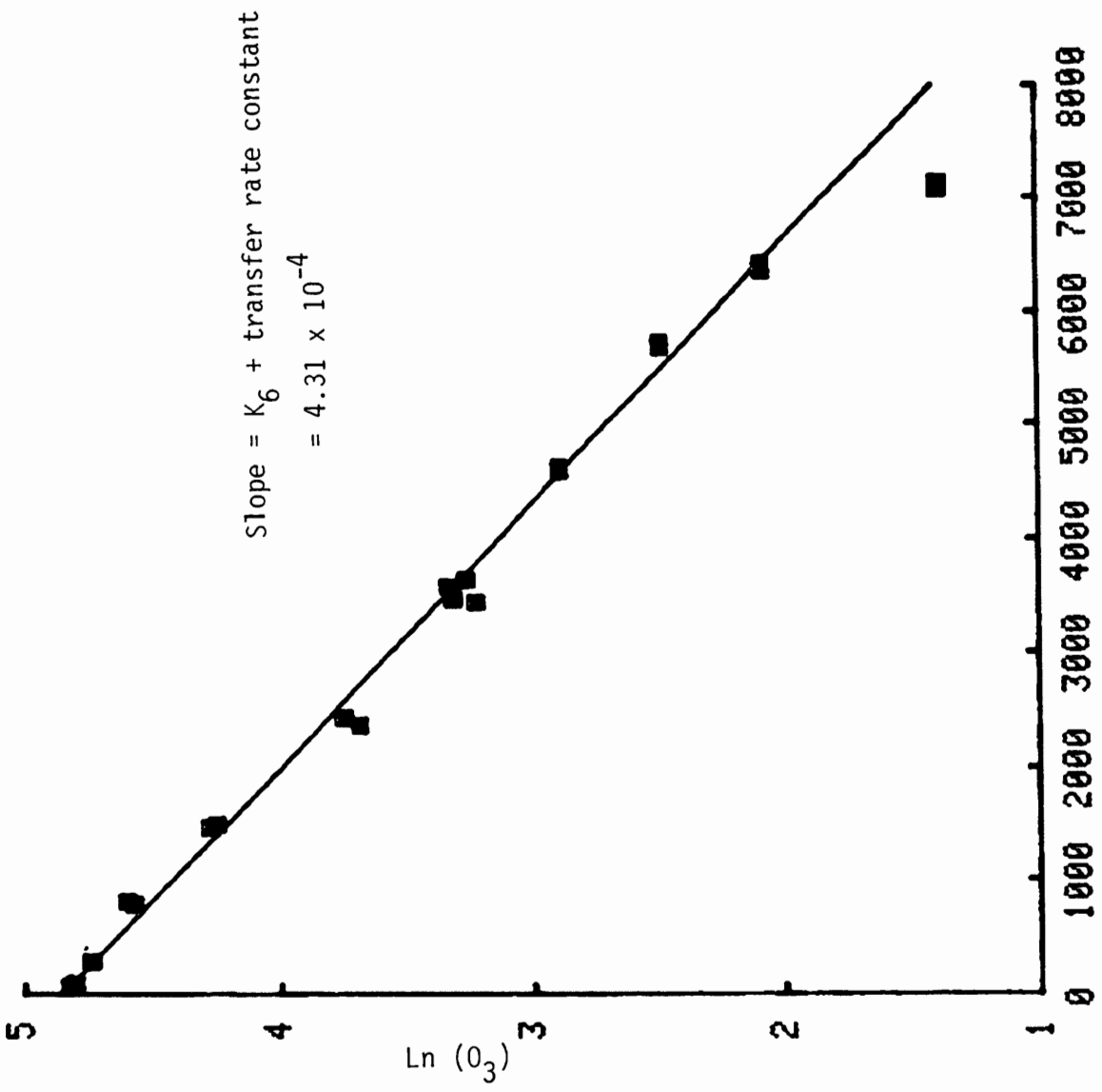

Figure 36. Graphic presentation of the transfer rate constant of O_3 for a pH = 5.5 solution.

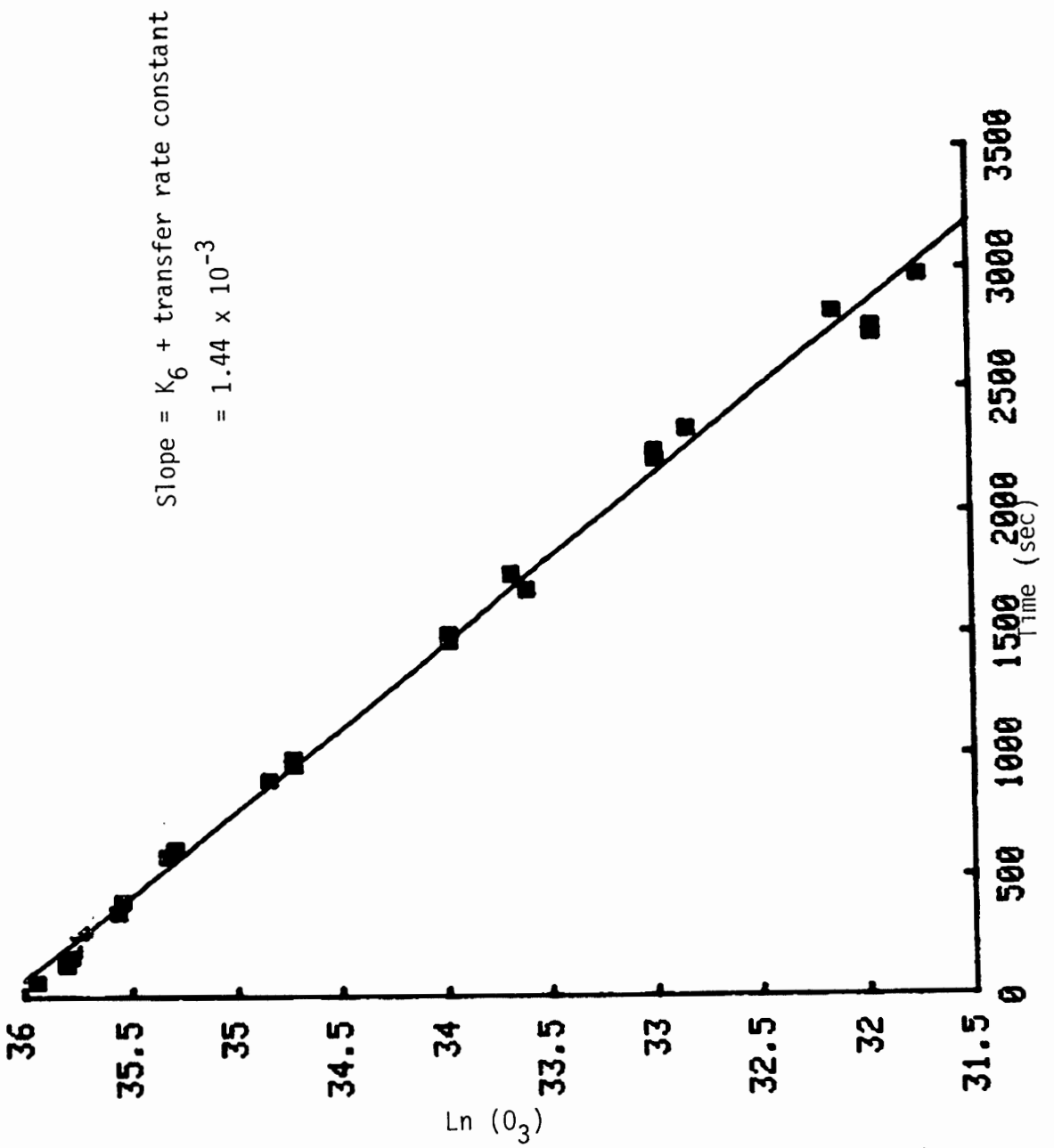

Figure 37. Graphic presentation of transfer rate constant of O_3 in a pH = 8.5 solution.

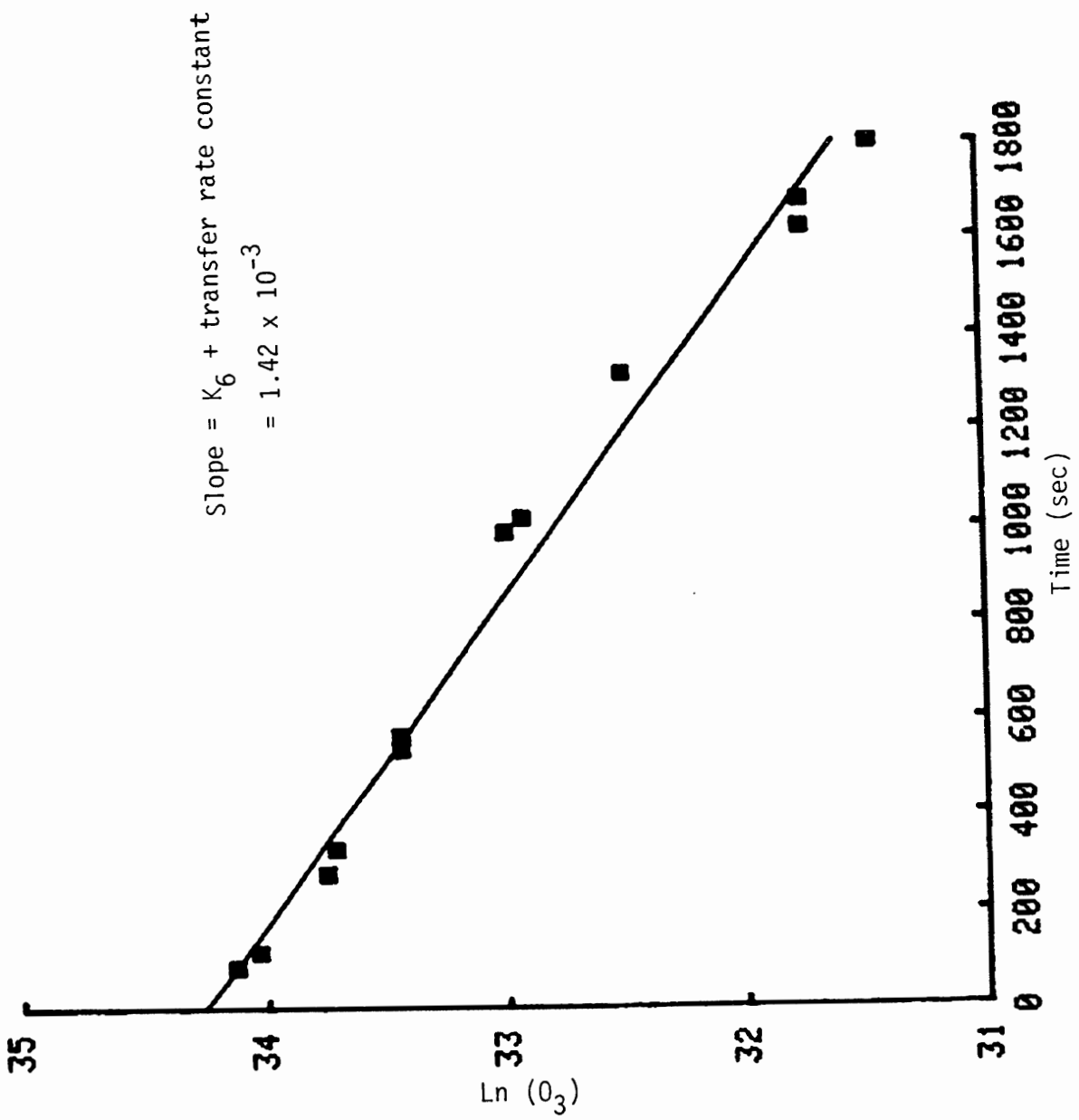

Figure 38. Graphic presentation of the transfer rate constant of O_3 on a pH = 8.5 solution.

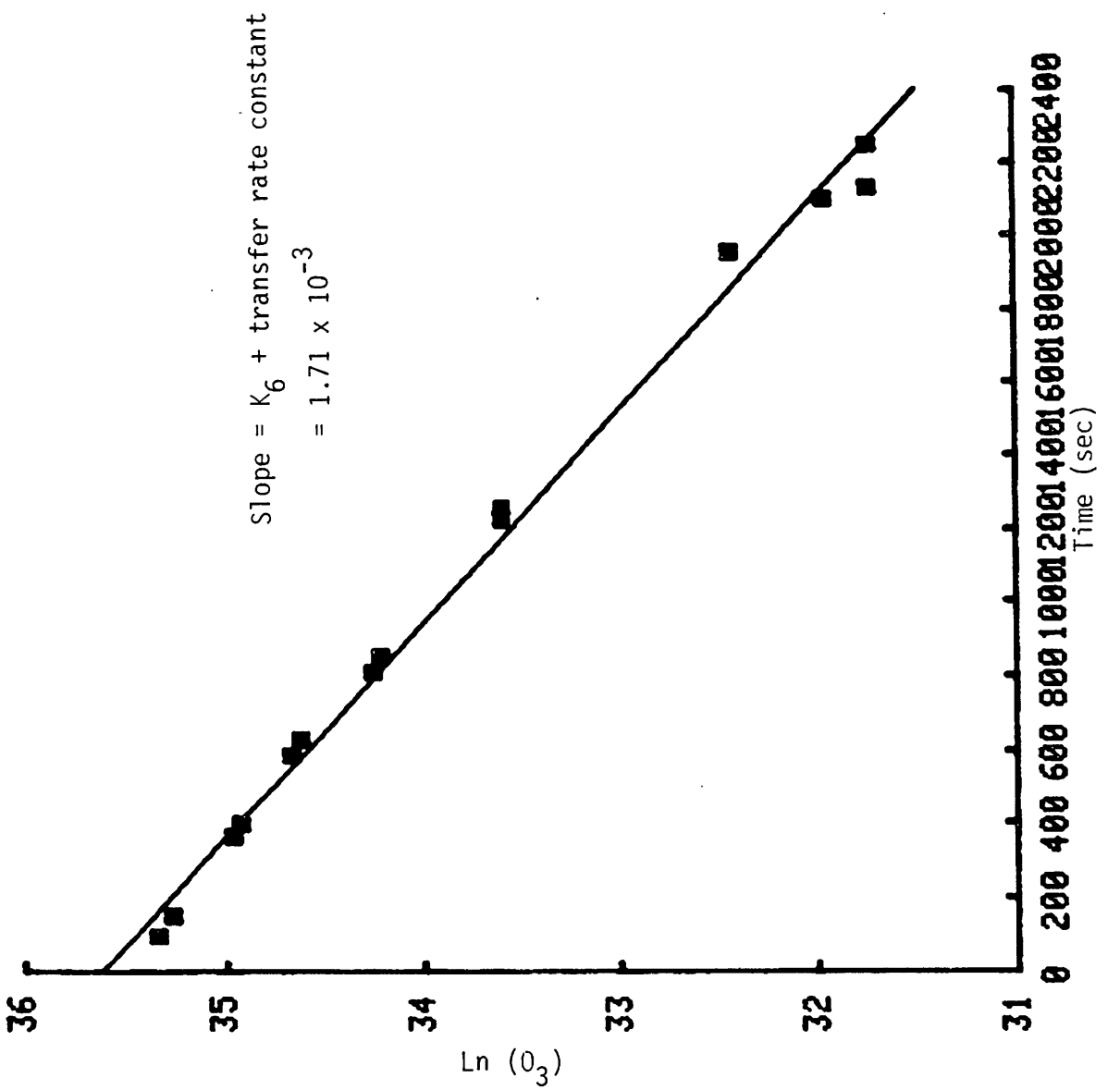

Figure 39. Graphic presentation of the transfer rate constant of O_3 on a pH = 11.5 solution.

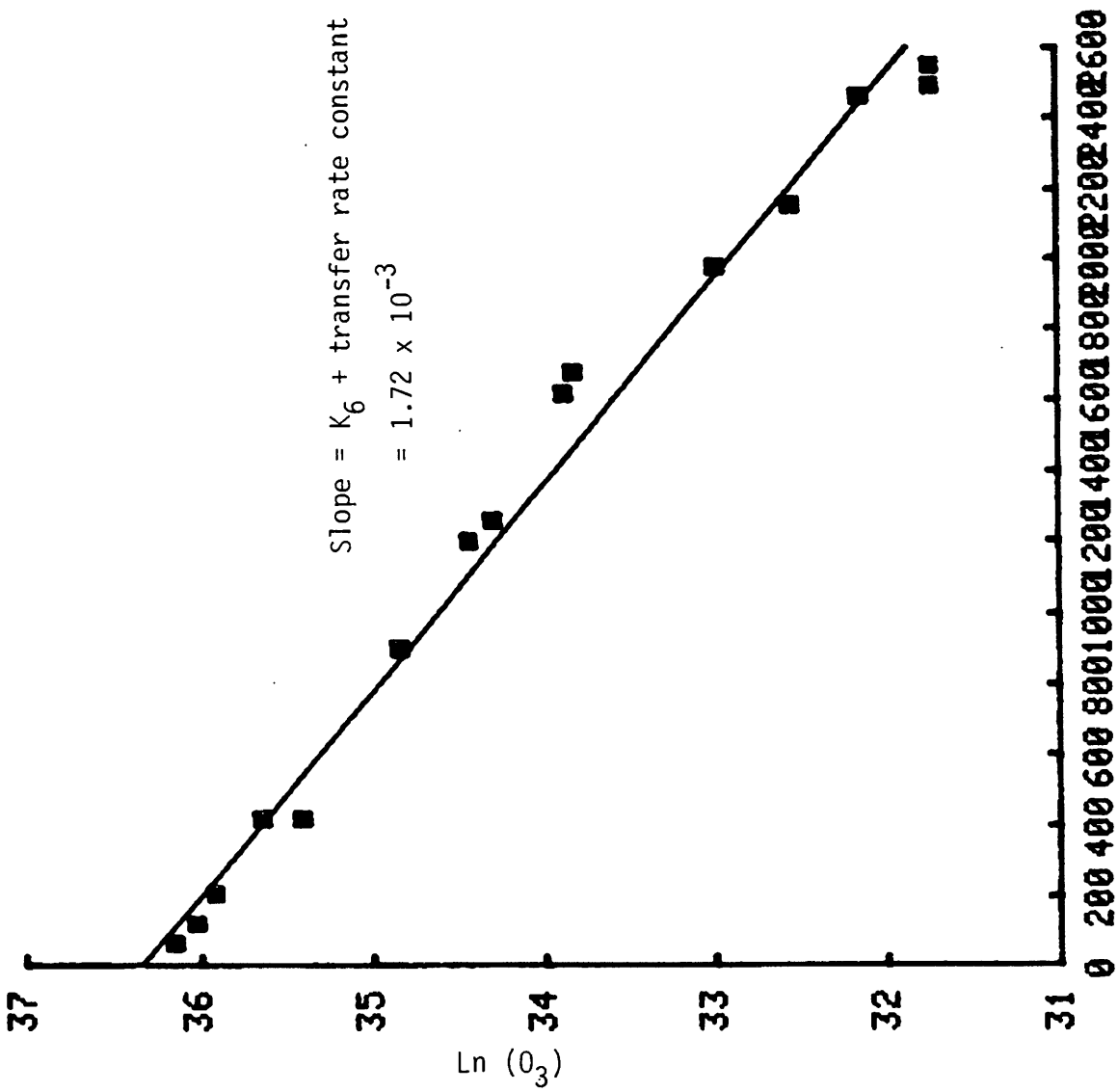

Figure 40. Graphic presentation of transfer rate of O_3 in a pH = 11. 5 solution.

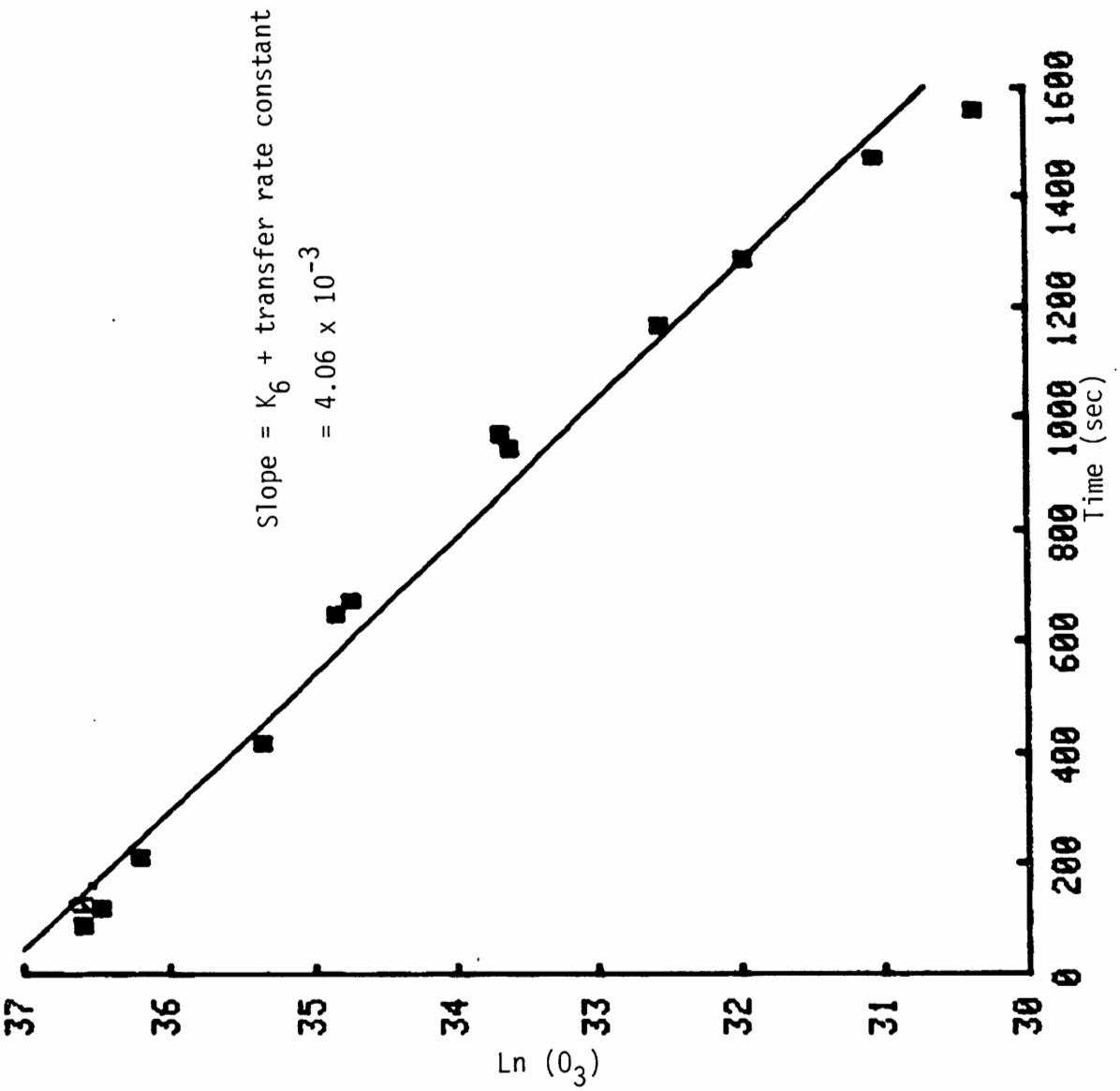

Figure 41. Graphic presentation of the transfer rate constant of ozone in a pH = 14 solution.

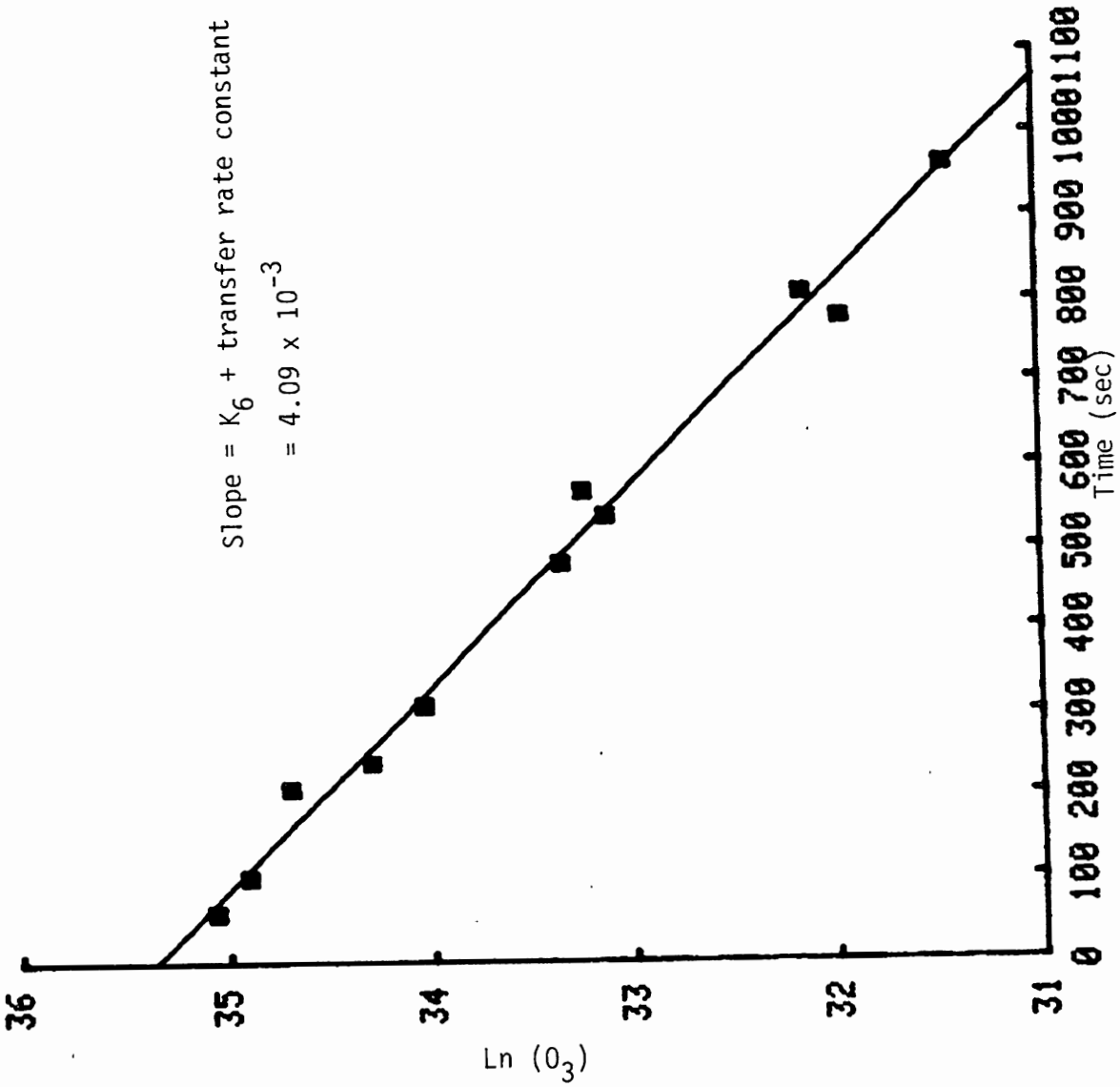

Figure 42. Graphic presentation of transfer rate constant of O_3 in a pH = 14 solution.

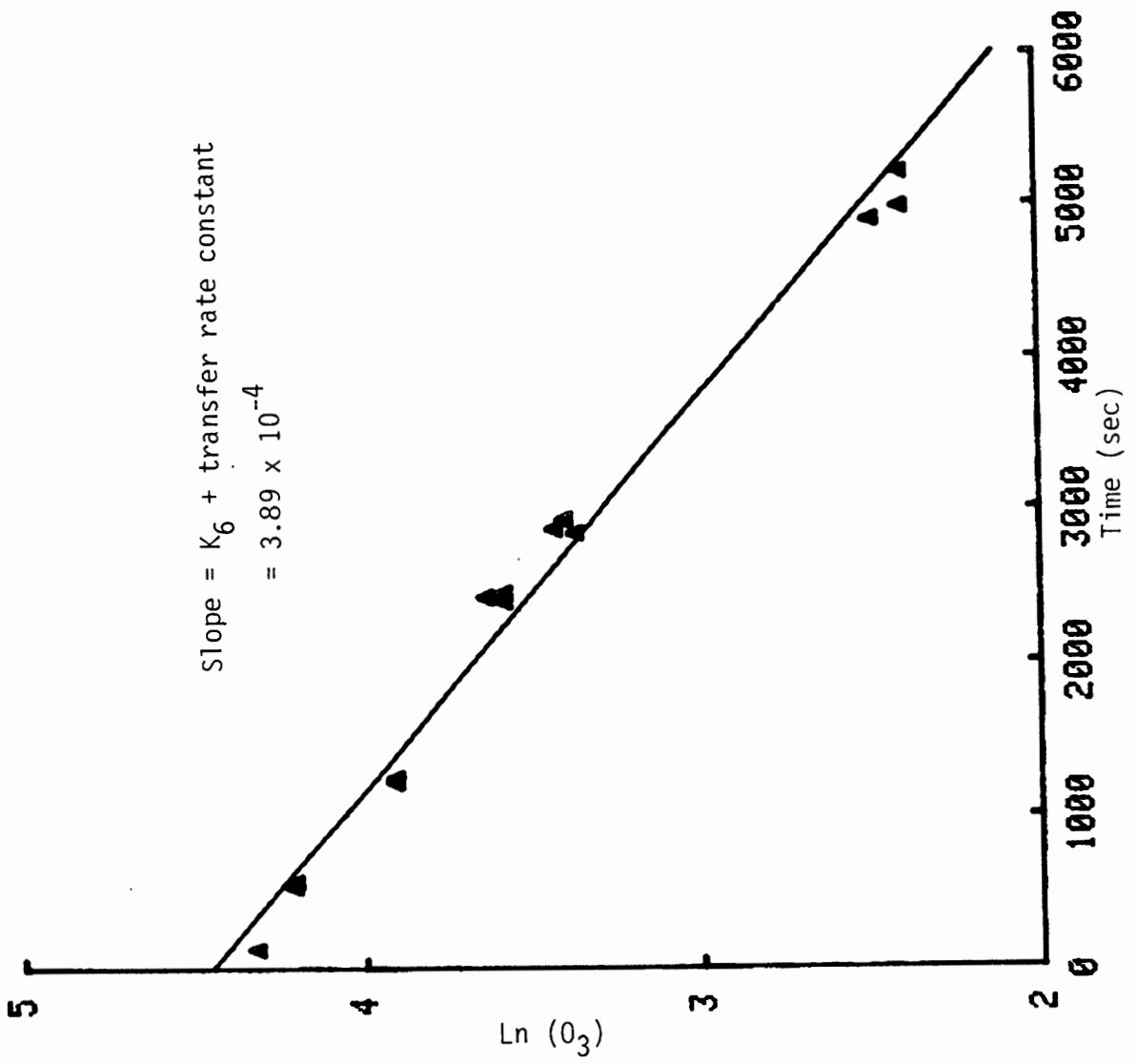

Figure 43. Graphic presentation of transfer rate constant of O_3 in distilled water.

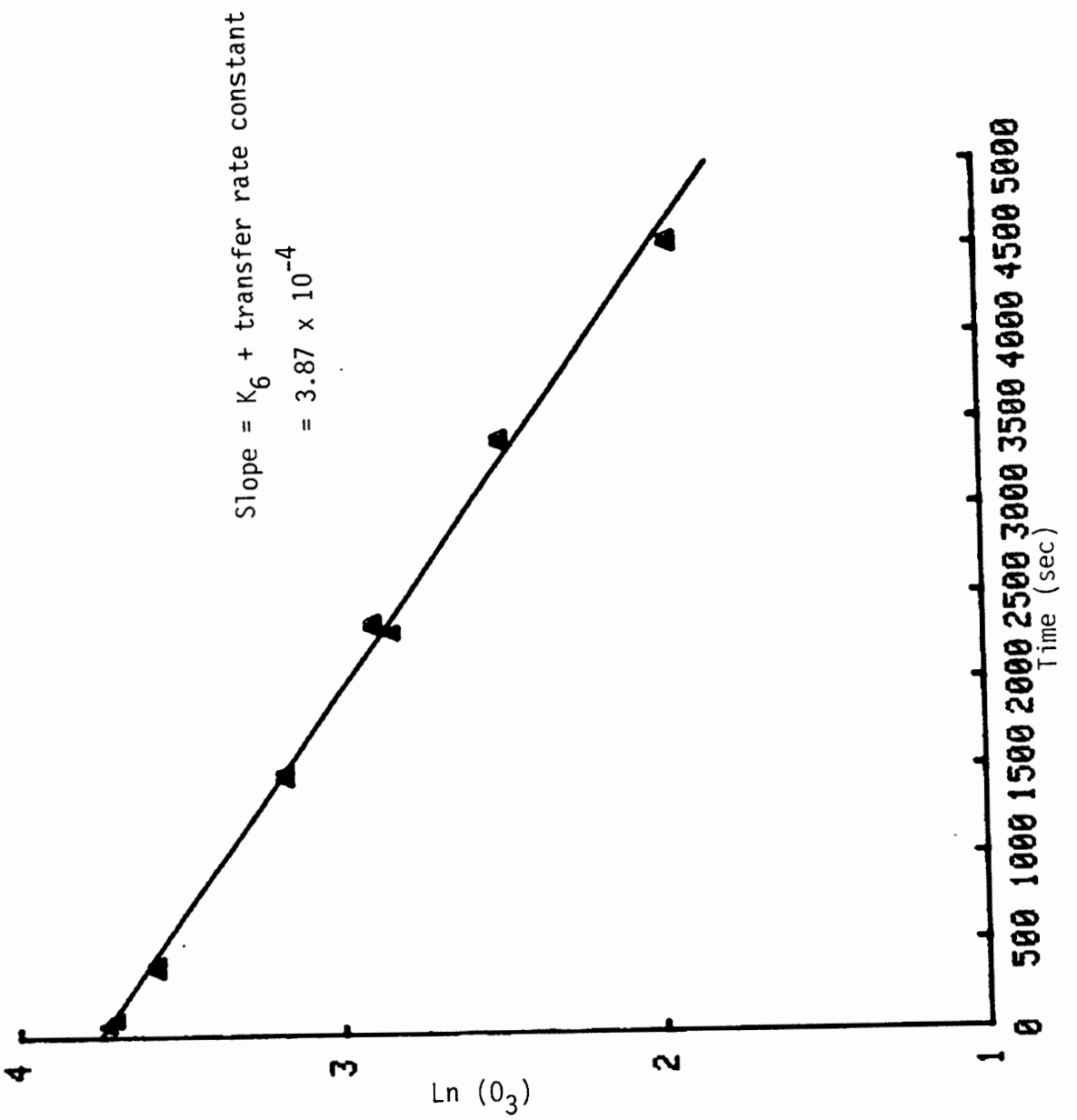

Figure 44. Graphic presentation of transfer rate constant of O_3 in distilled water.

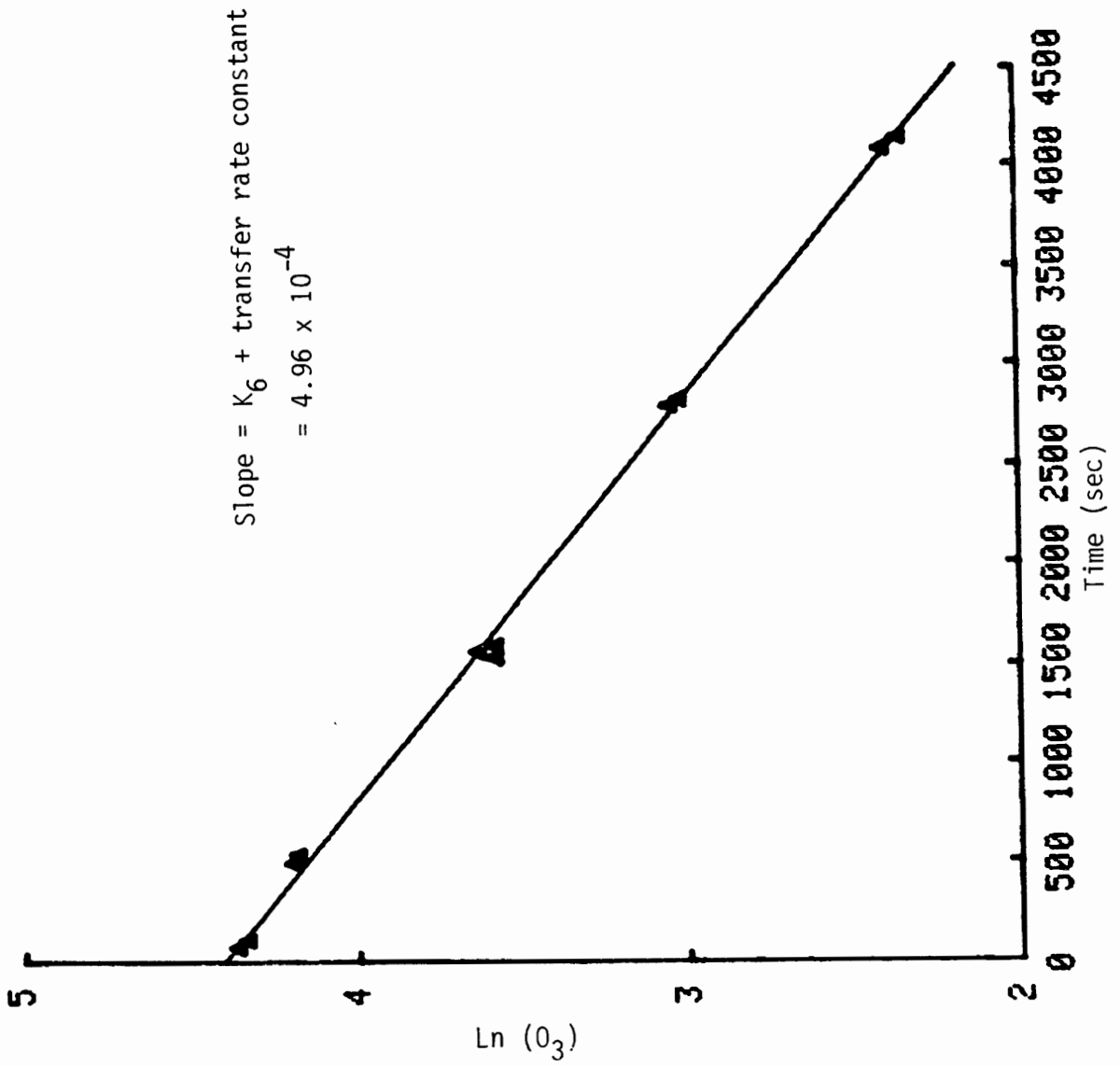

Figure 45. Graphic presentation of transfer rate constant of ozone in distilled water.

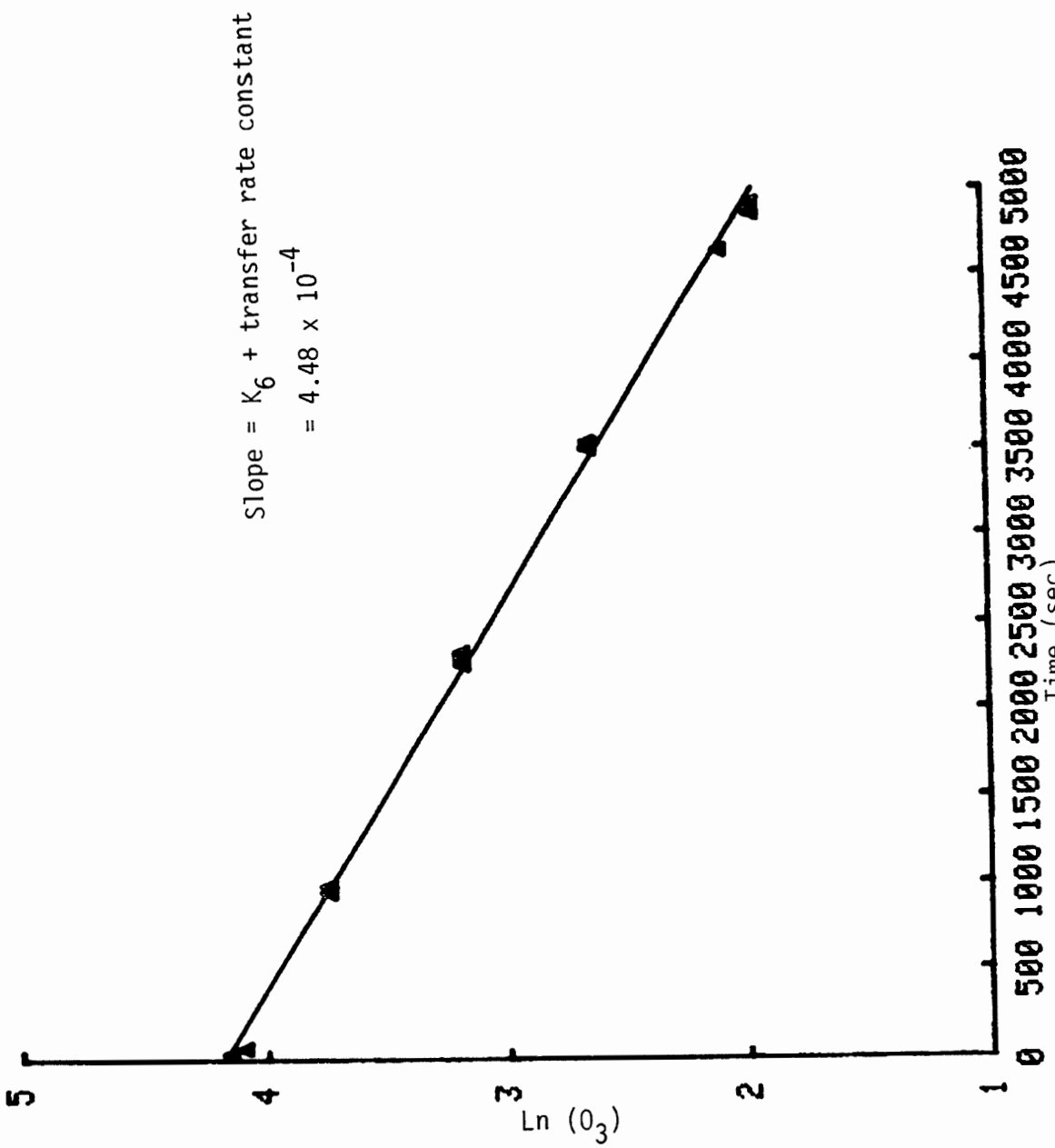

Figure 46. Graphic presentation of transfer rate constant of ozone in distilled water.

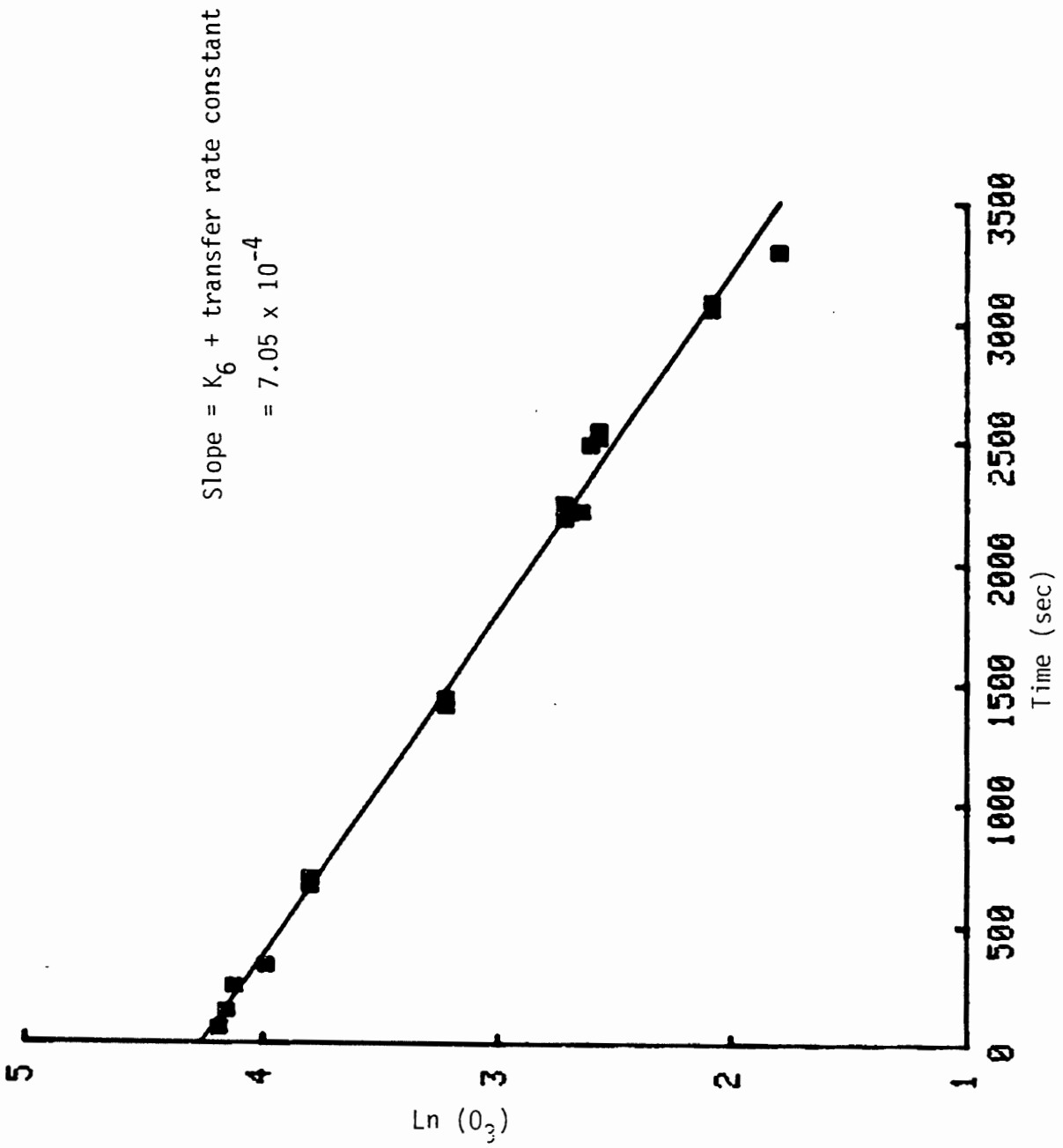

Figure 47. Graphic presentation of rate constant of ozone in ocean water.

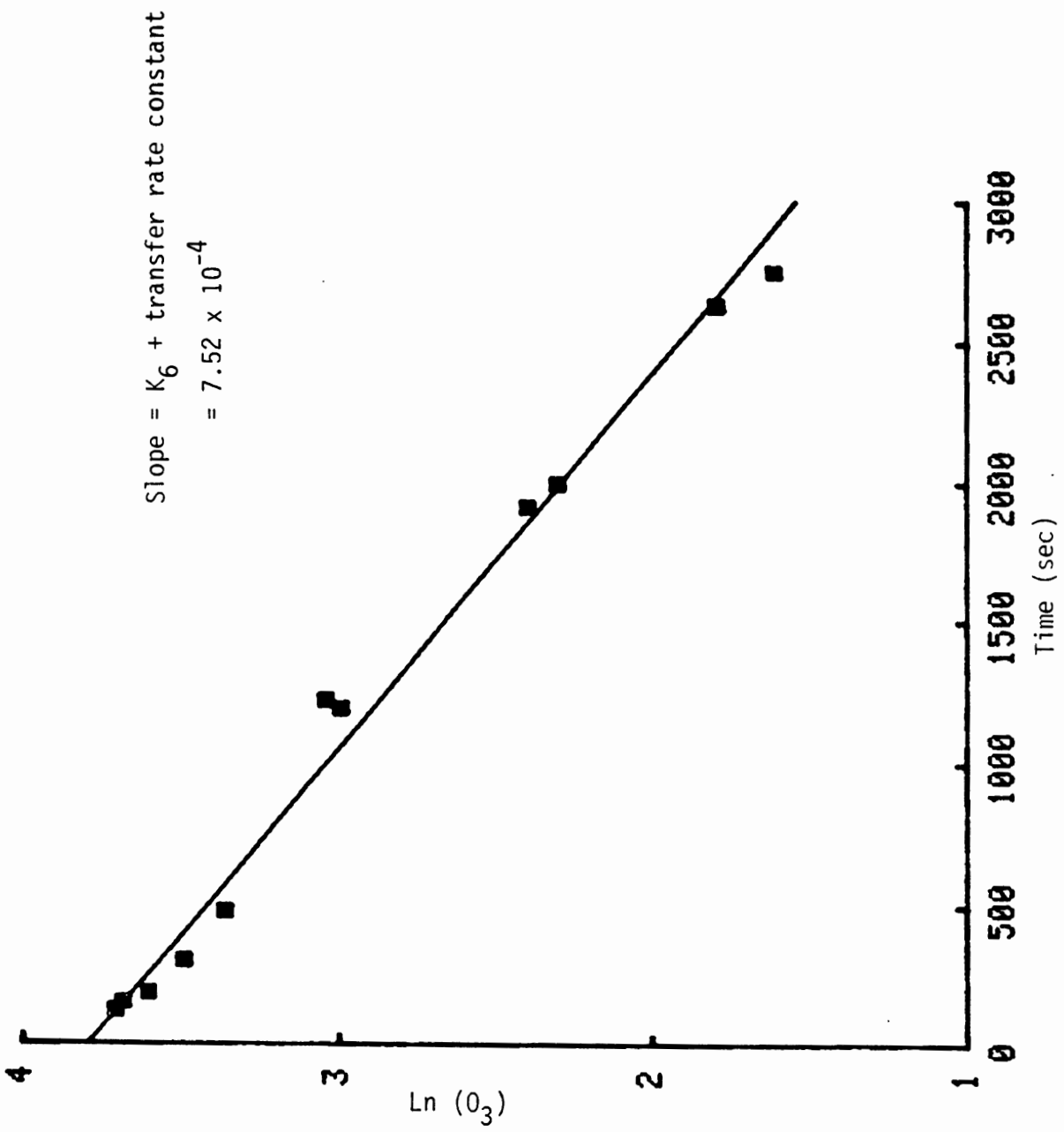

Figure 48. Graphic presentation of rate constant of ozone in ocean water.

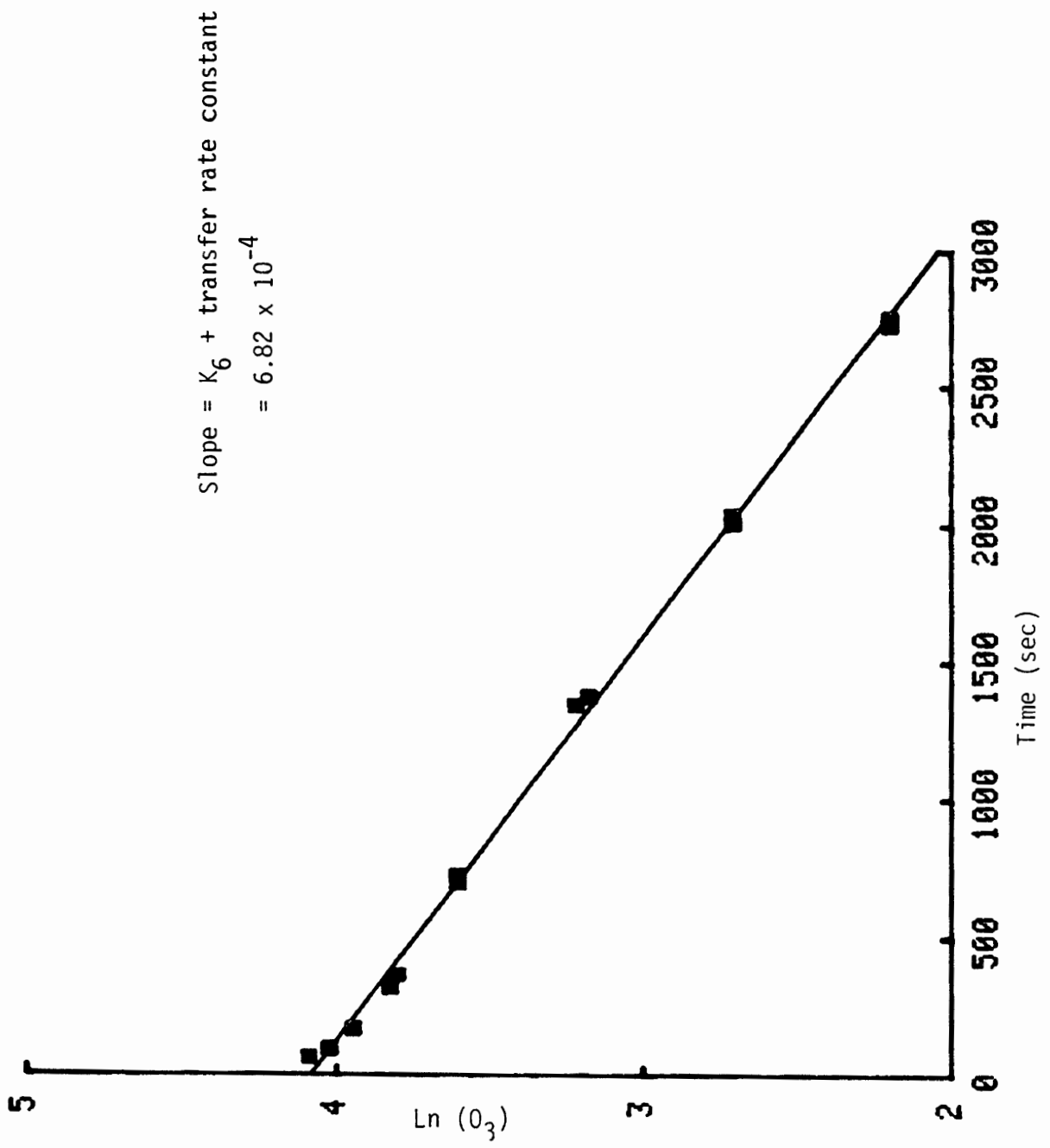

Figure 49. Graphic presentation of rate constant of ozone in ocean water.

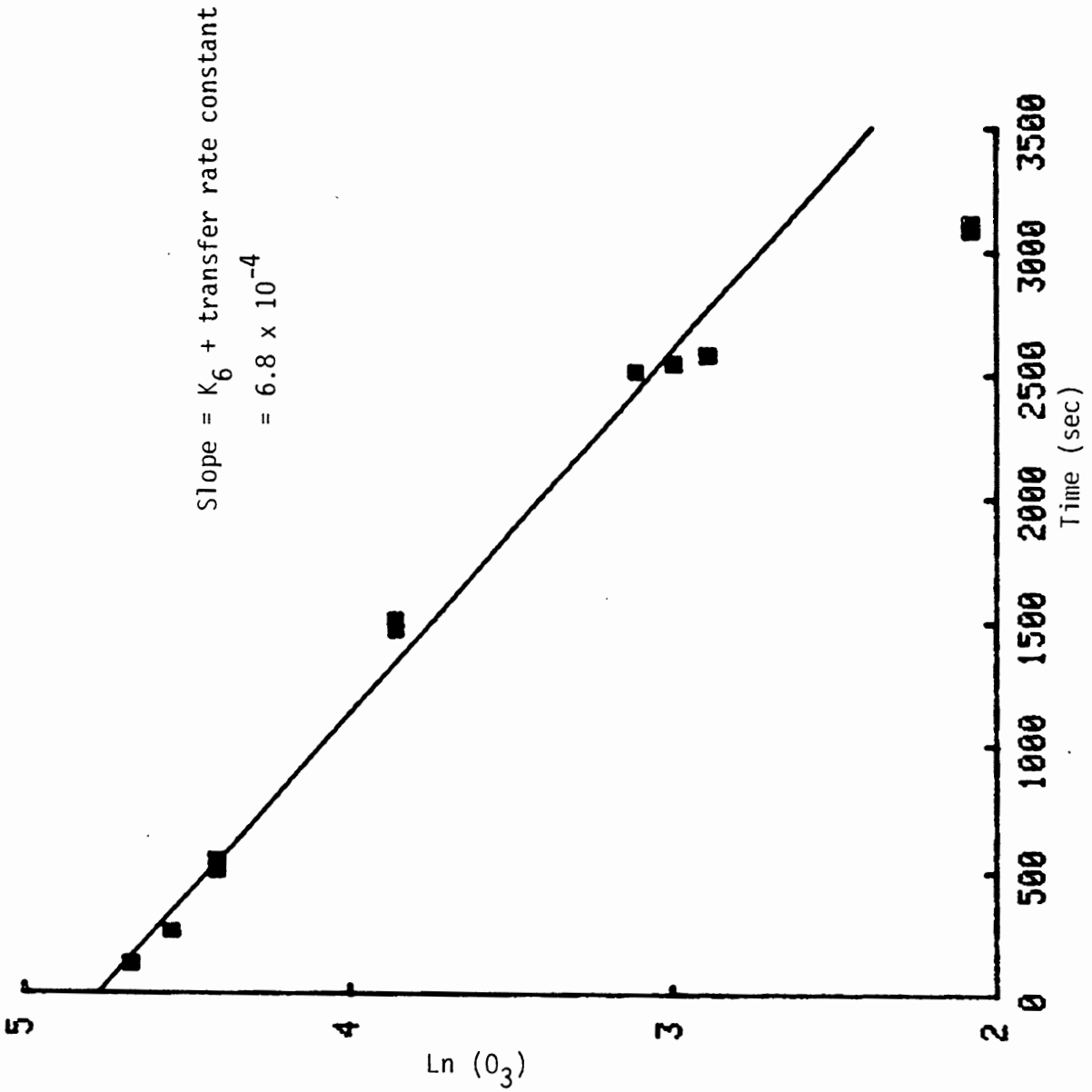

Figure 50. Graphic presentation of rate constant of ozone in ocean water.

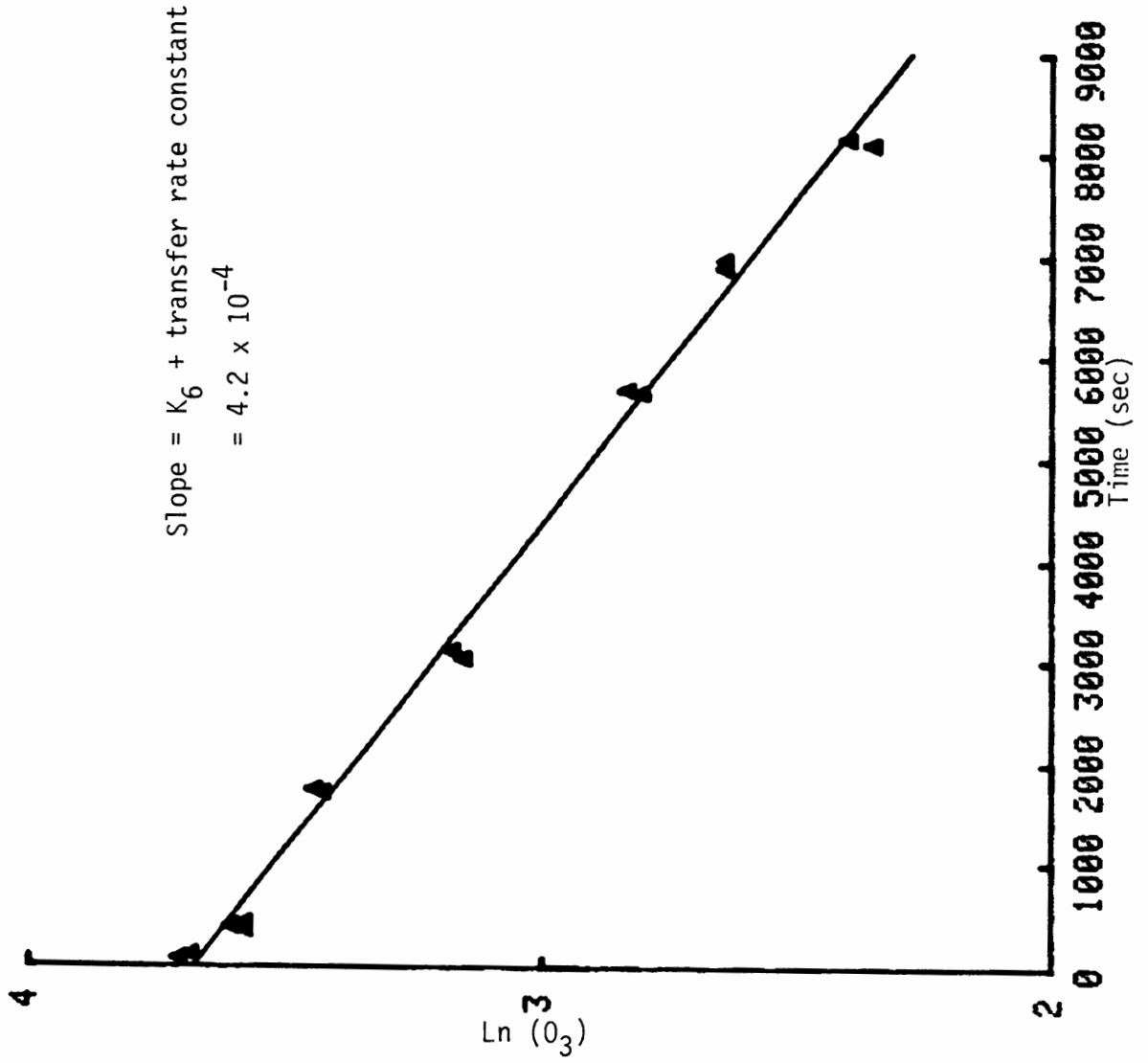

Figure 51. Graphic presentation of transfer rate constant of ozone on distilled water (without stirring).

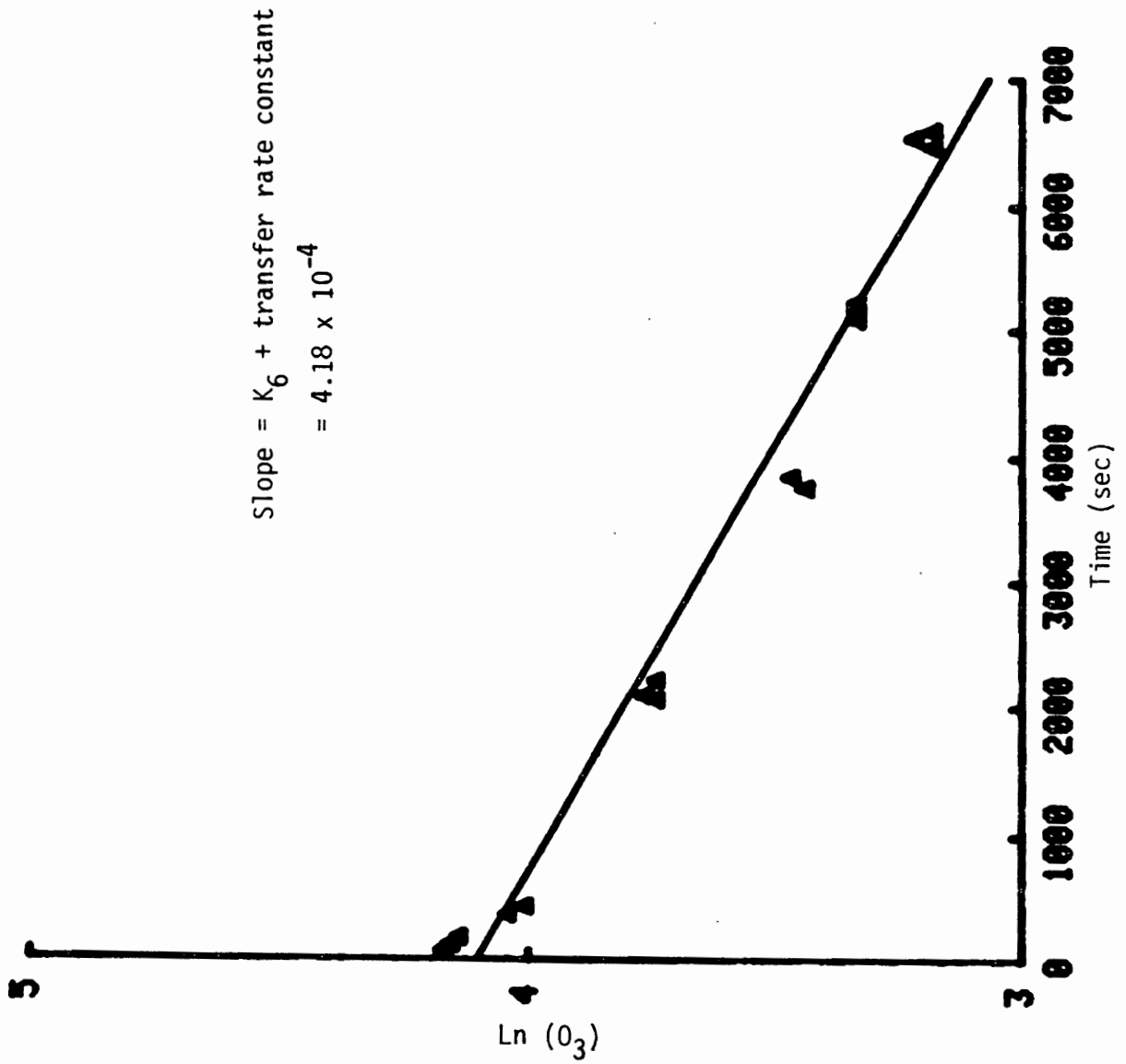

Figure 52. Graphic presentation of transfer rate constant of ozone on distilled water (without stirring).

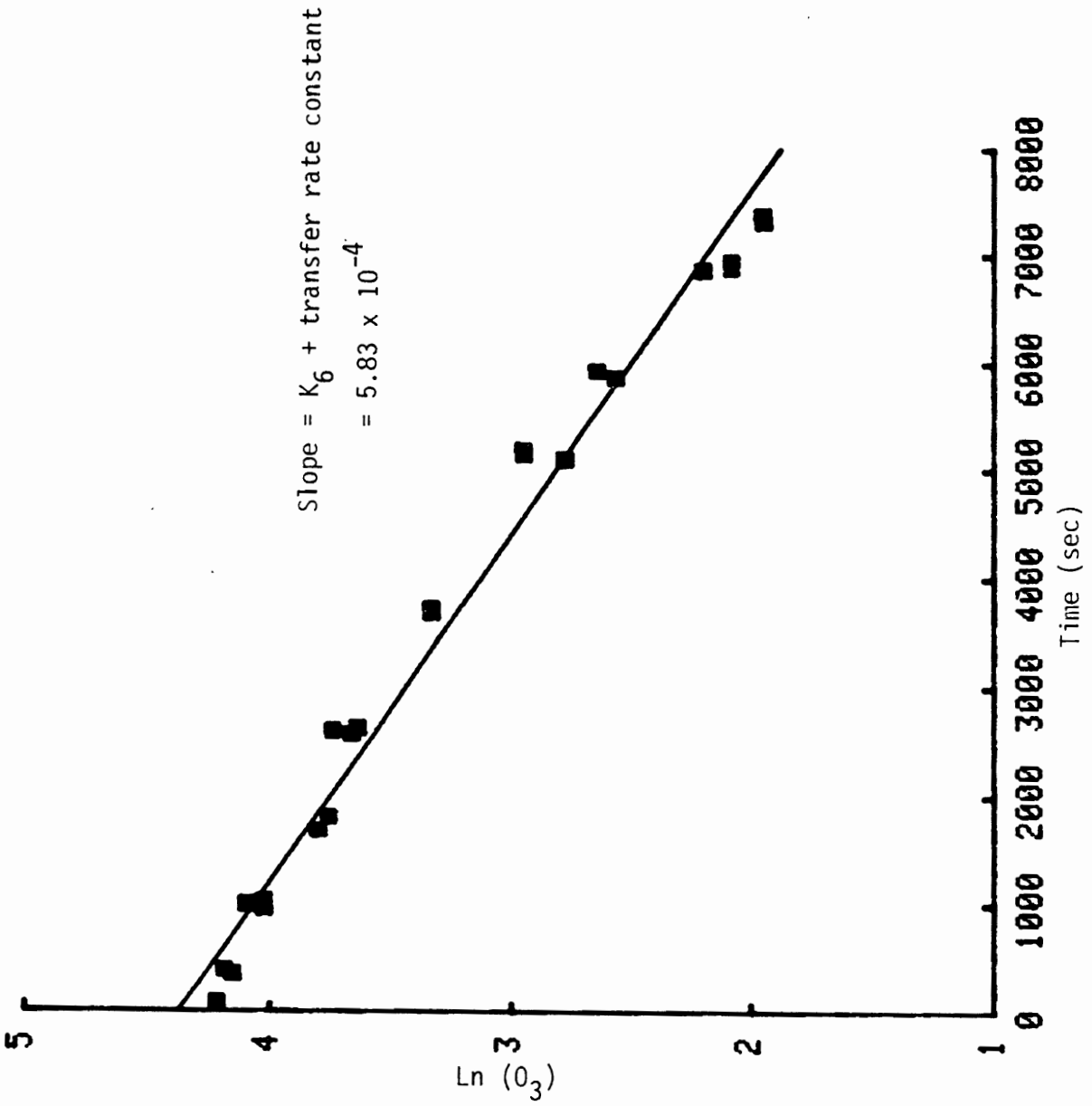

Figure 53. Graphic presentation of transfer rate constant of ozone on ocean water.

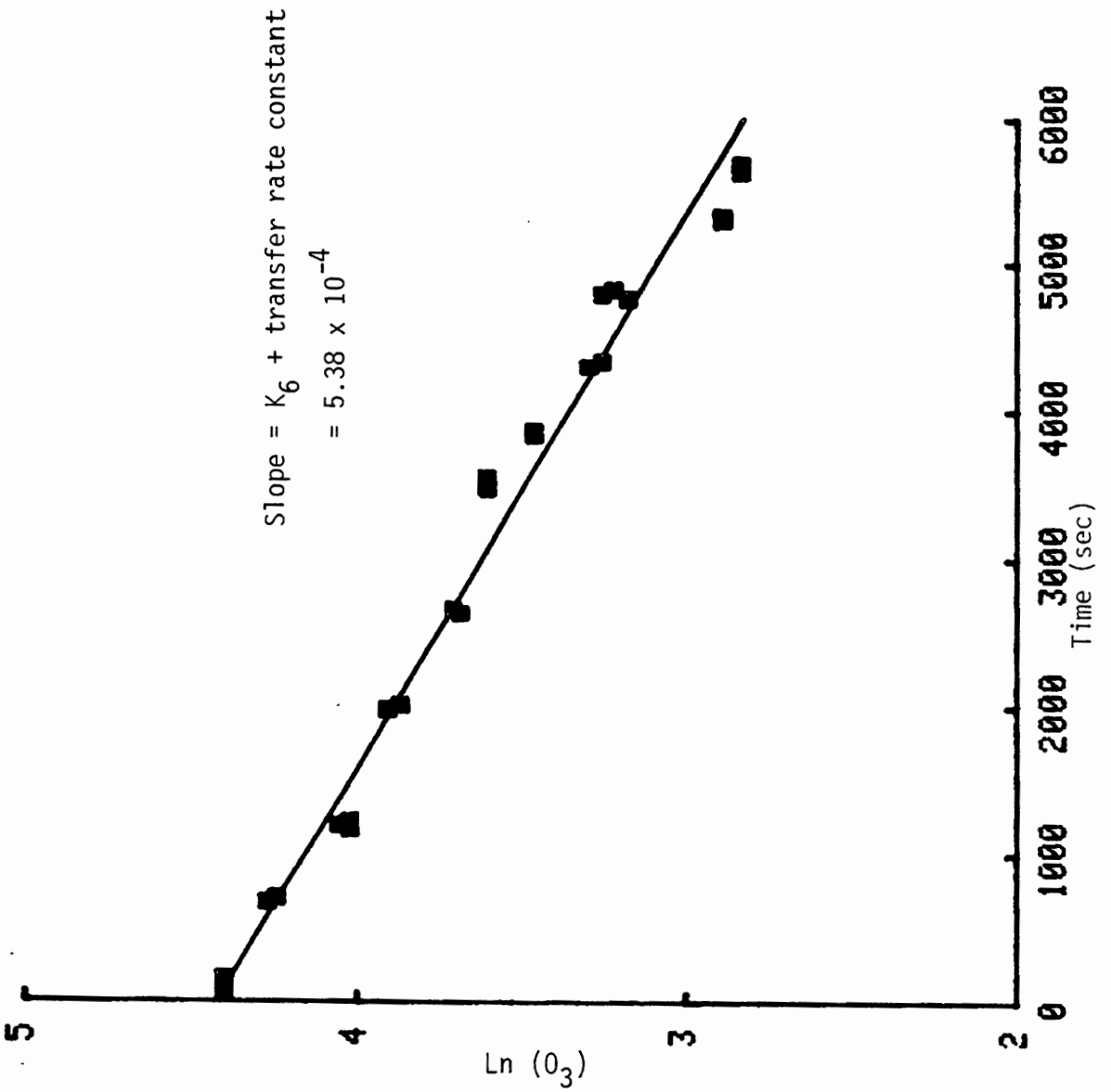

Figure 54. Graphic presentation of transfer rate constant of ozone on ocean water.

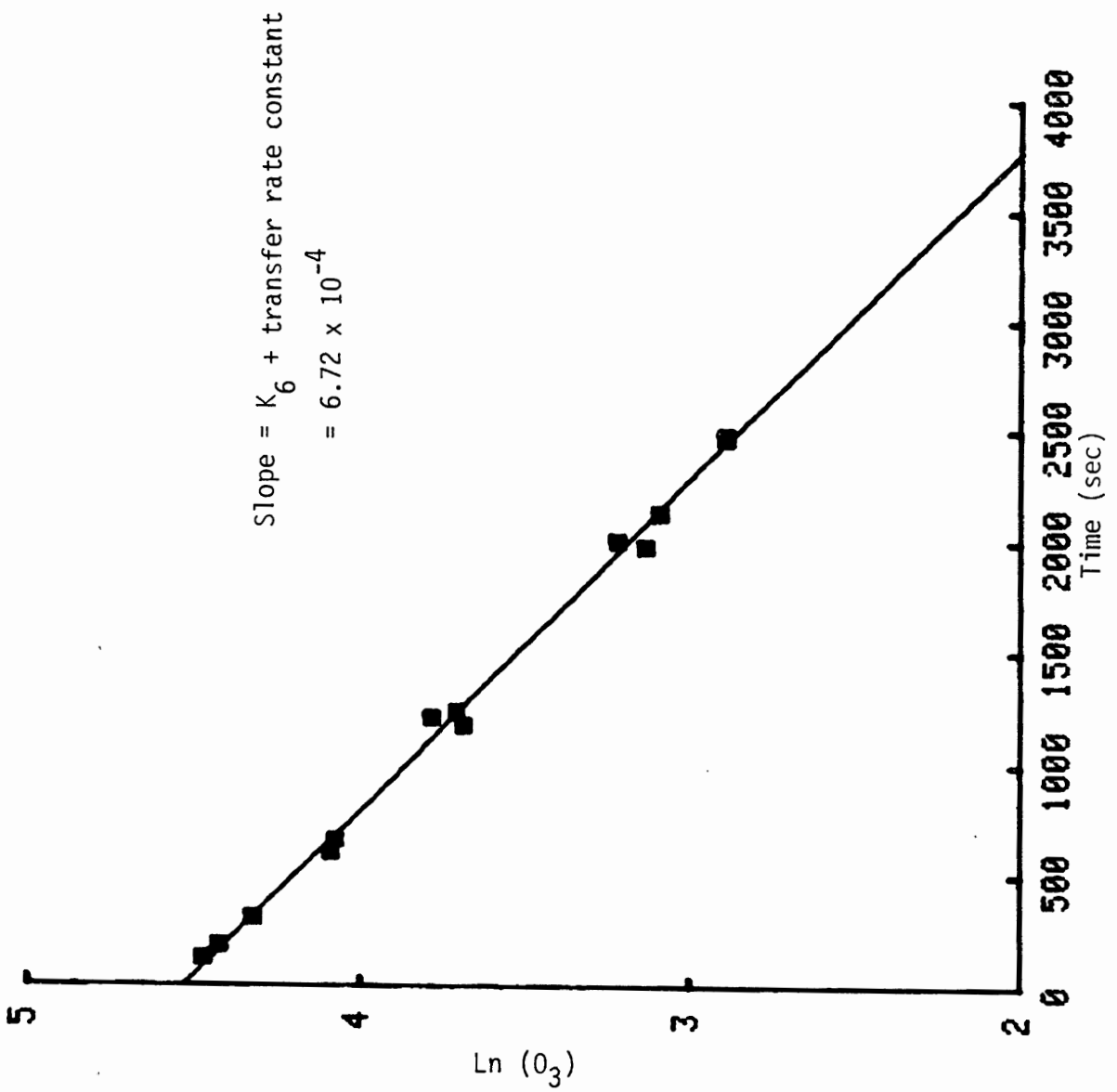

Figure 55. Graphic presentation of transfer rate constant of ozone in distilled water (2100 cm^3 liquid phase volume, with stirring of liquid phase)

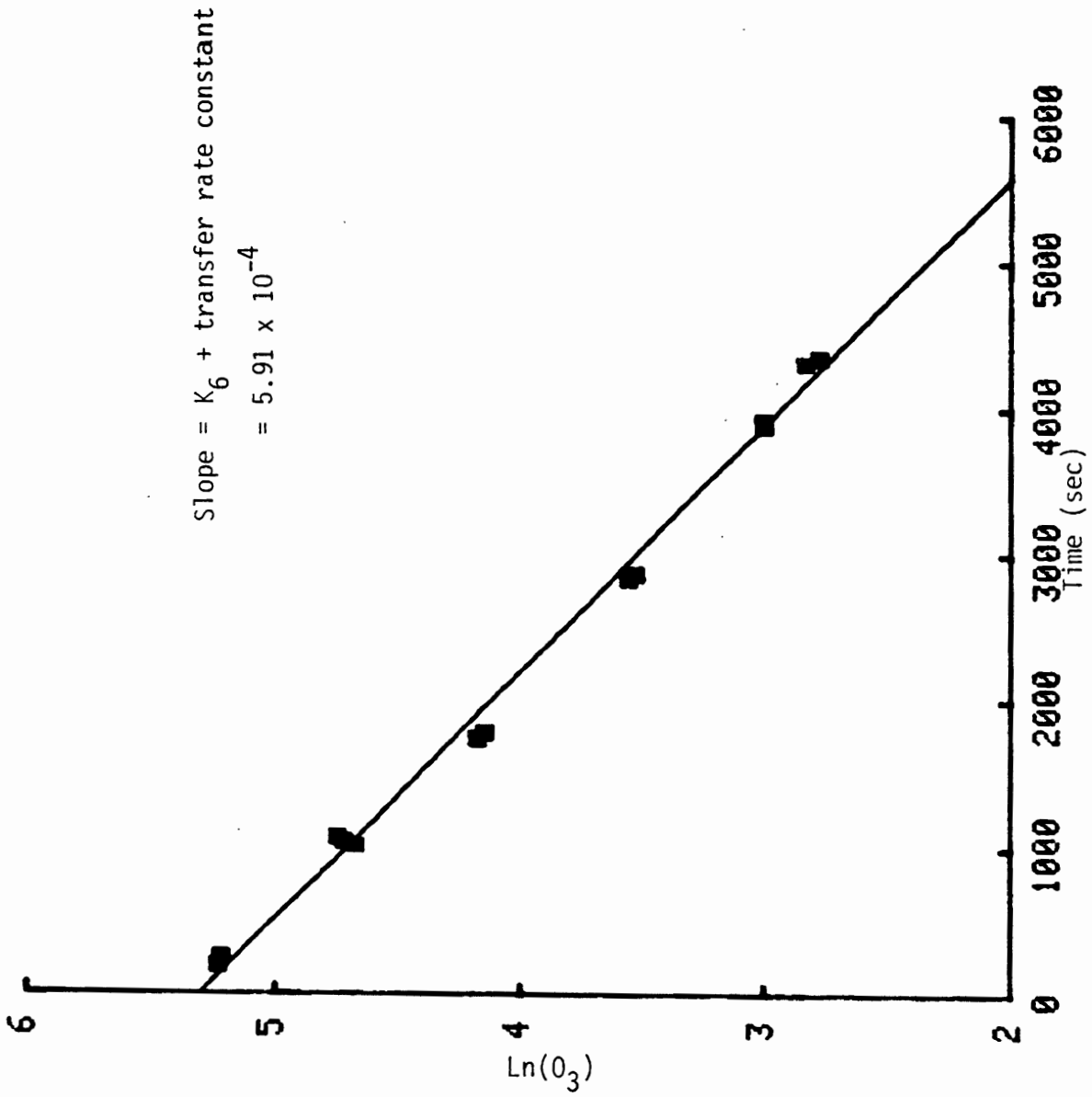

Figure 56. Graphic presentation of transfer rate constant of ozone in distilled water (2100 cm^3 liquid phase volume with stirring liquid phase).

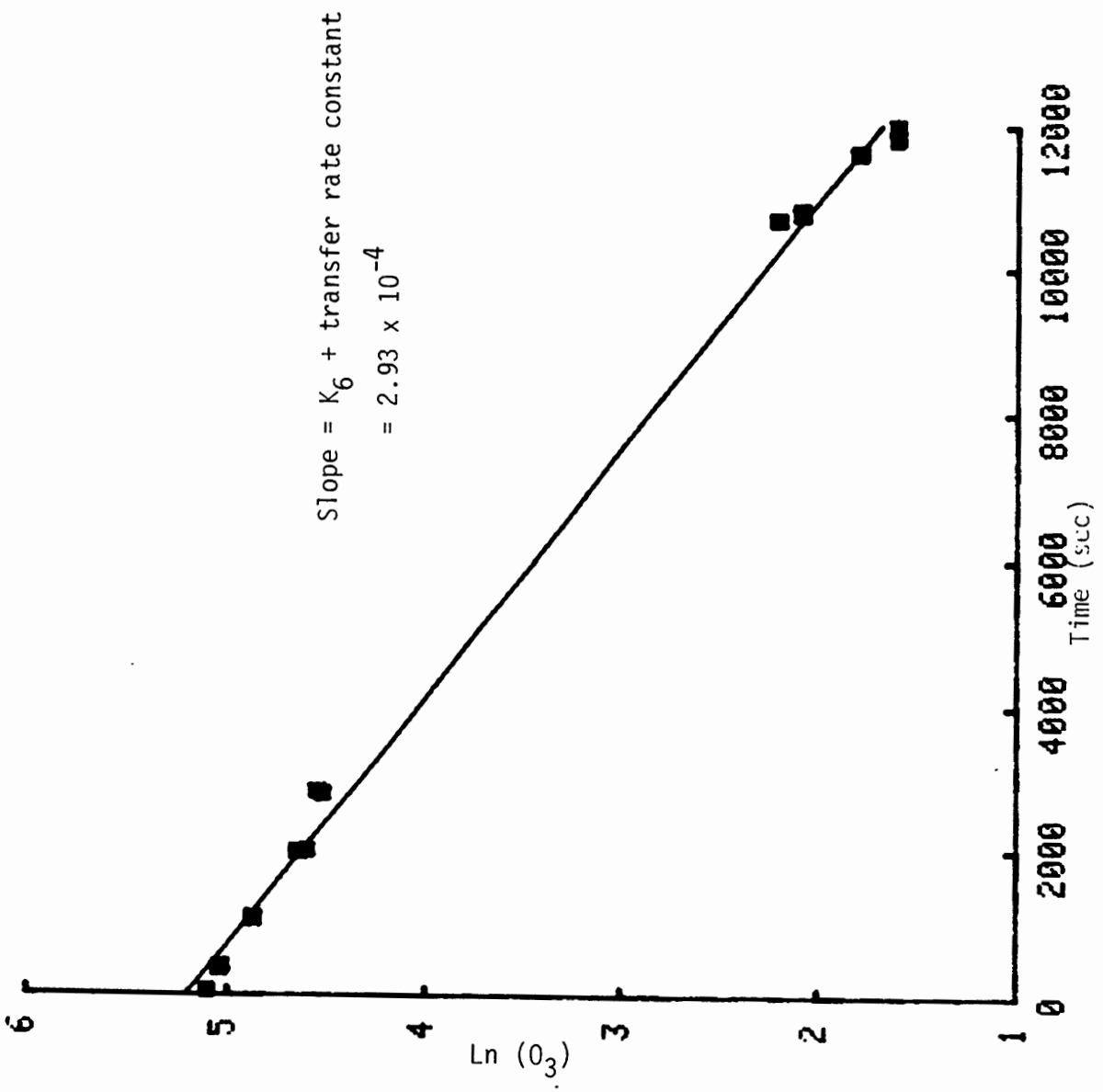

Figure 57. Graphic presentation of transfer rate constant of ozone in distilled water (2100 cm^3 liquid phase volume, no stirring).

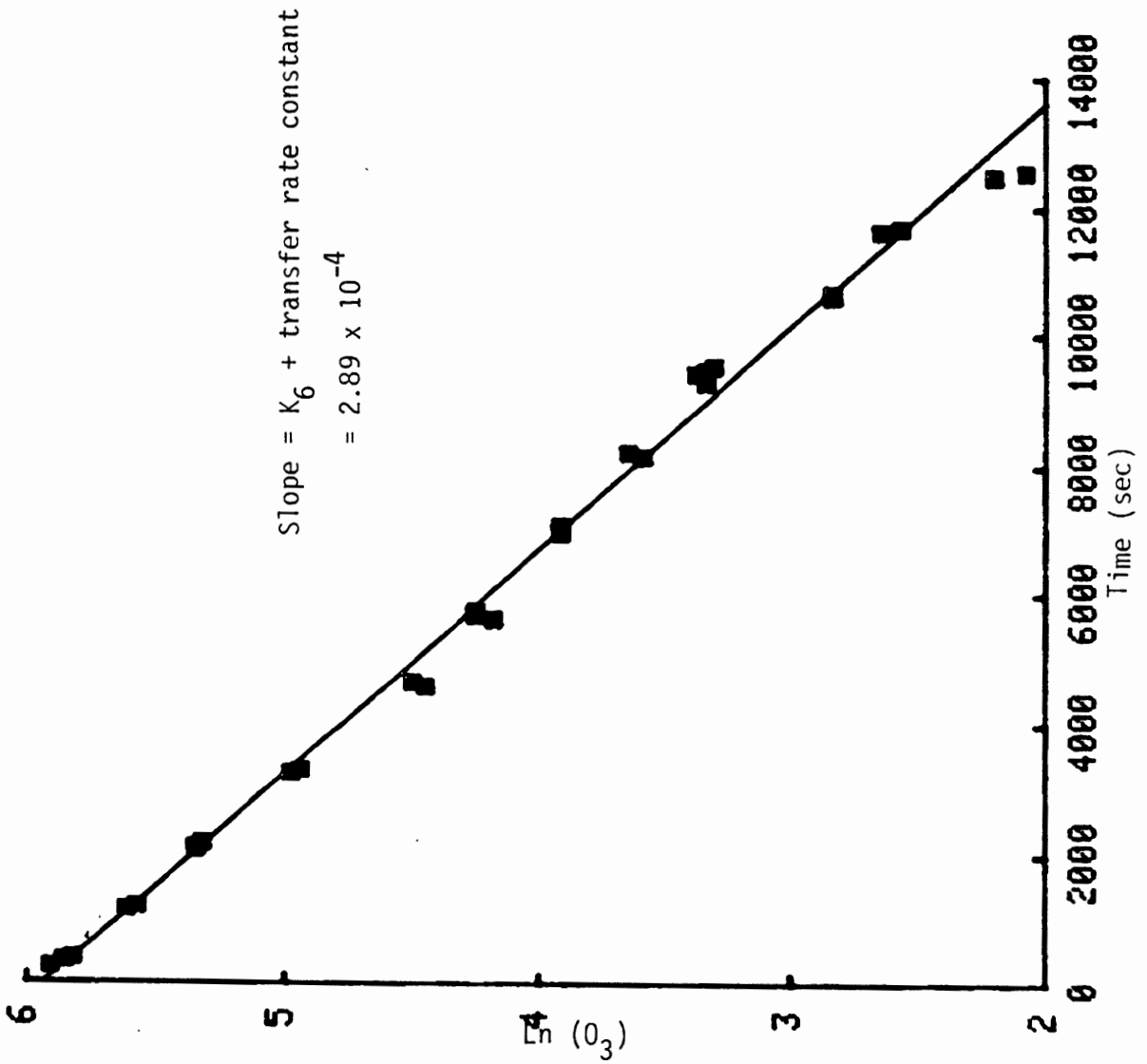

Figure 58. Graphic presentation of transfer rate constant of ozone in distilled water (2100 cm^3 liquid phase volume, no stirring).

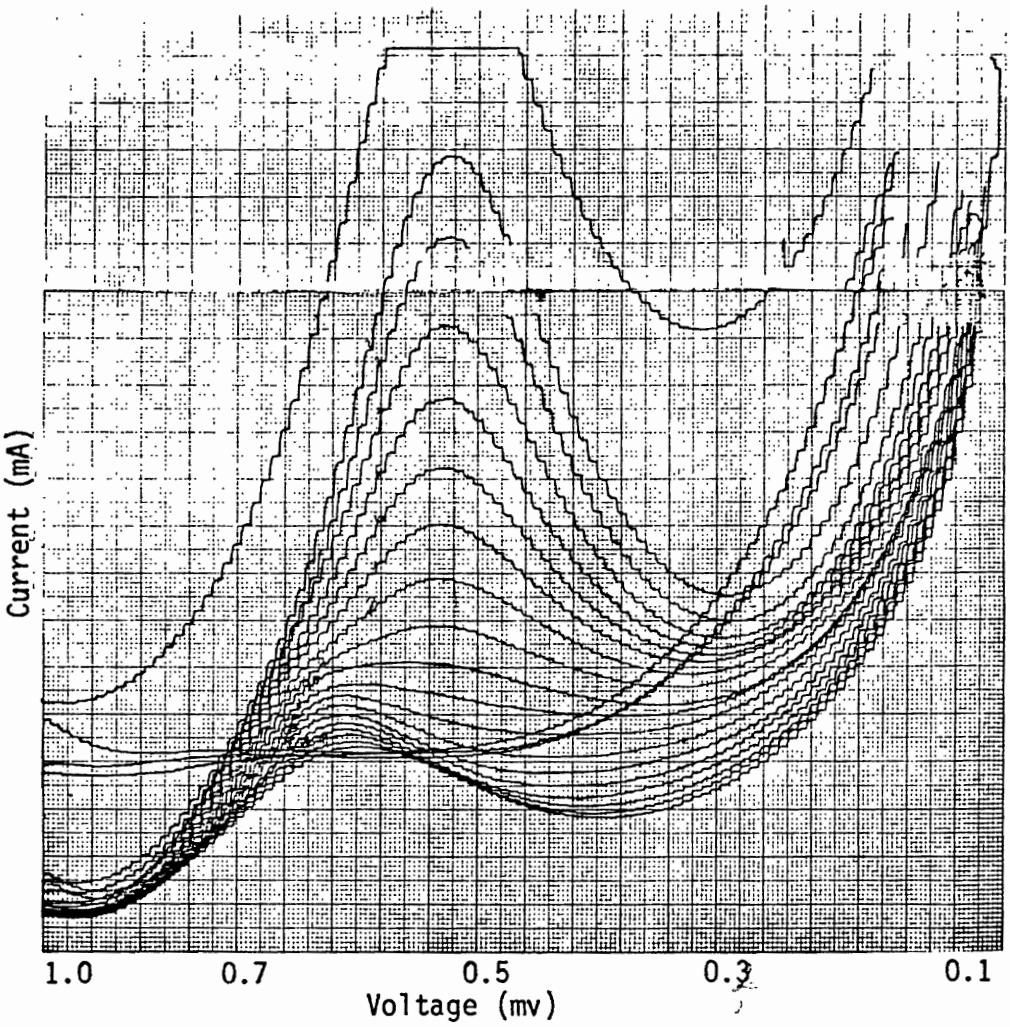

Figure 59. Polarograms for destruction of ozone in 1 M NaCl solution.

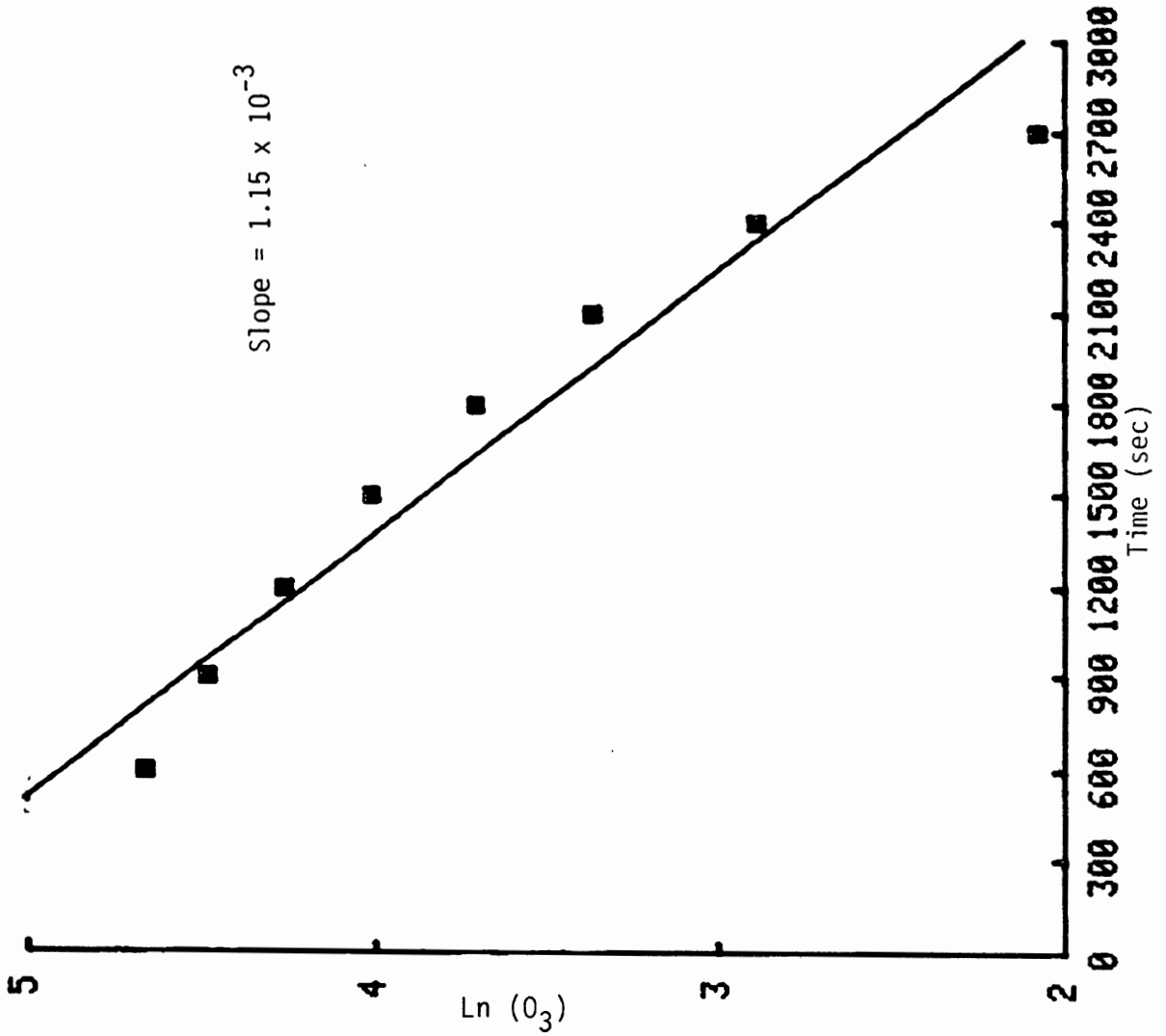

Figure 60. Graphic presentation of decomposition rate of ozone in a 1 M KCl solution using voltammetry.

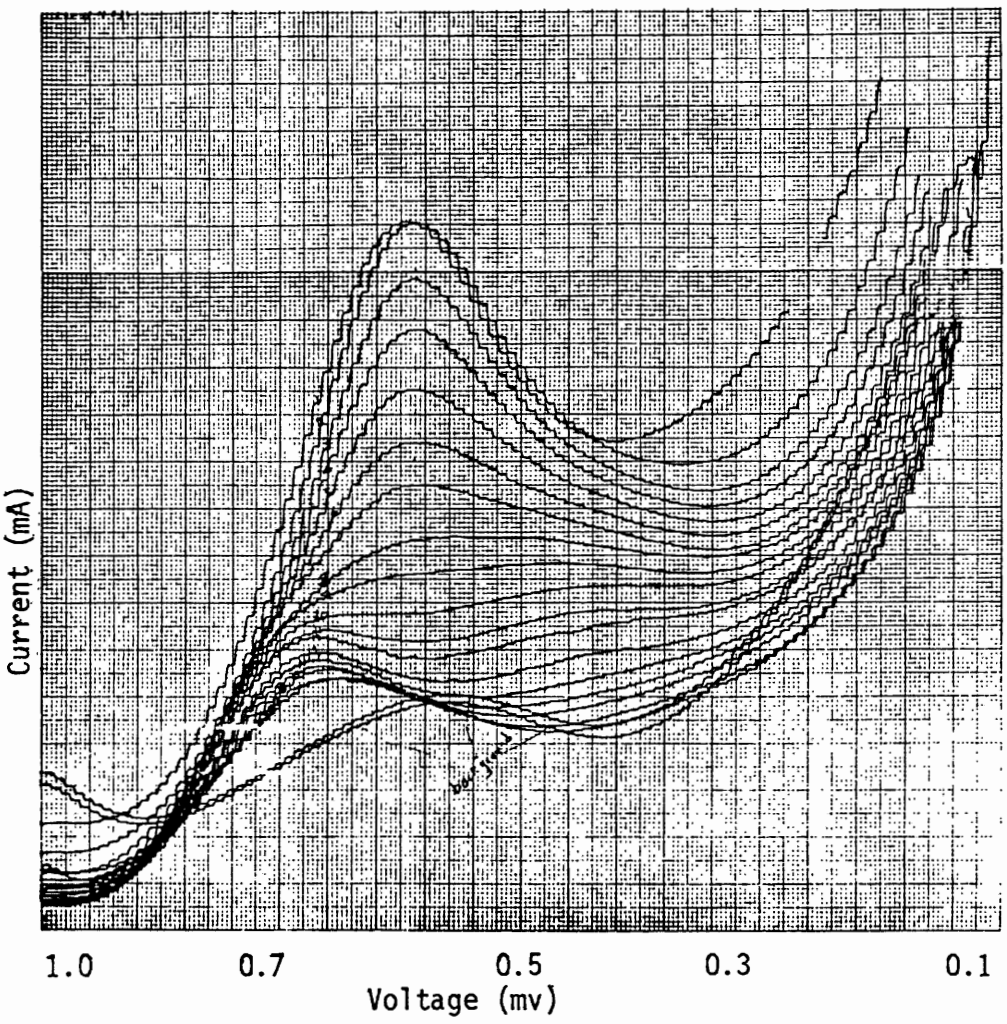

Figure 61. Polarograms for destruction of ozone in 1 M NaCl solution.

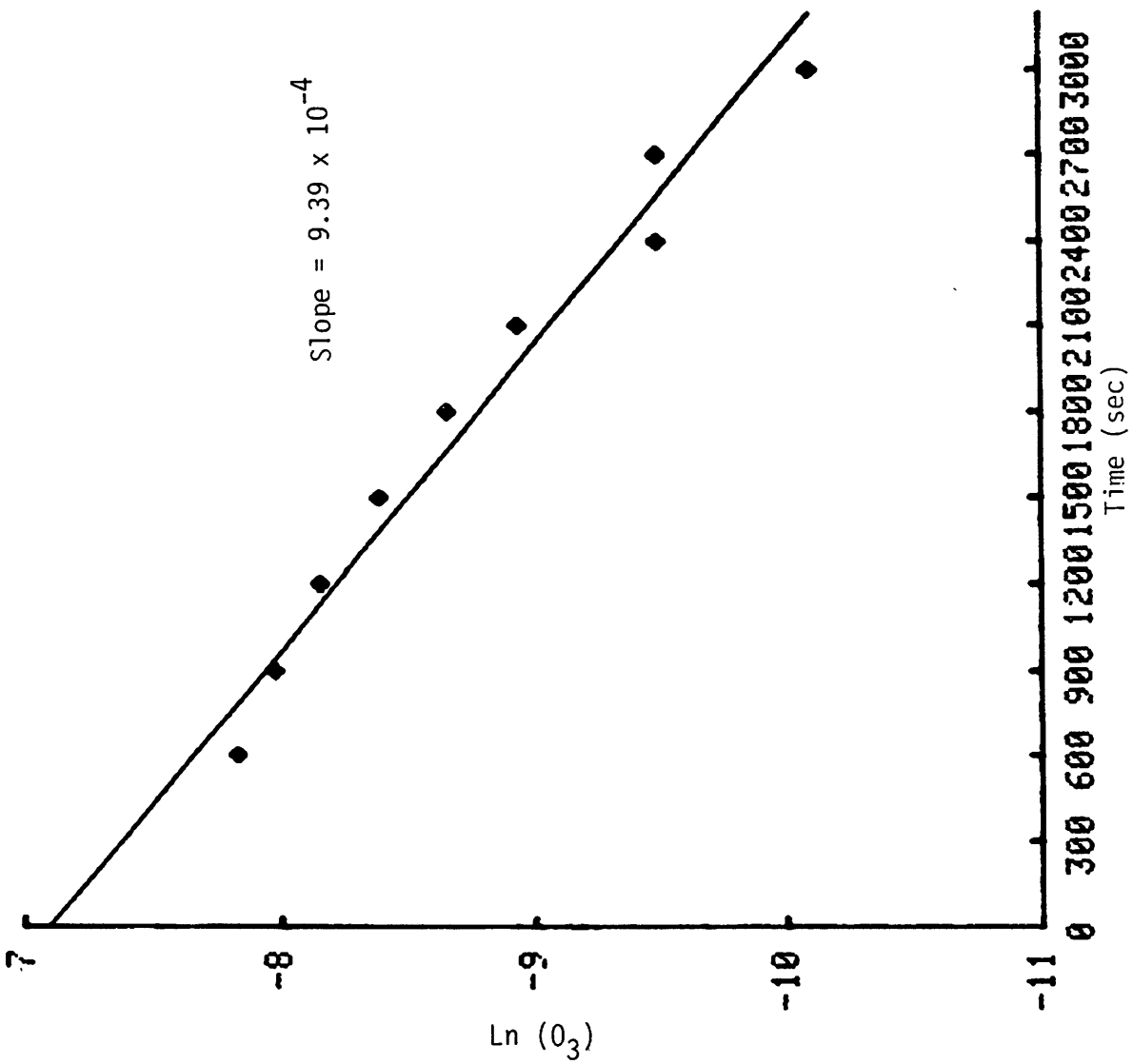

Figure 62. Graphic presentation of decomposition rate constant of O_3 in 1 M KCl using voltammetry.

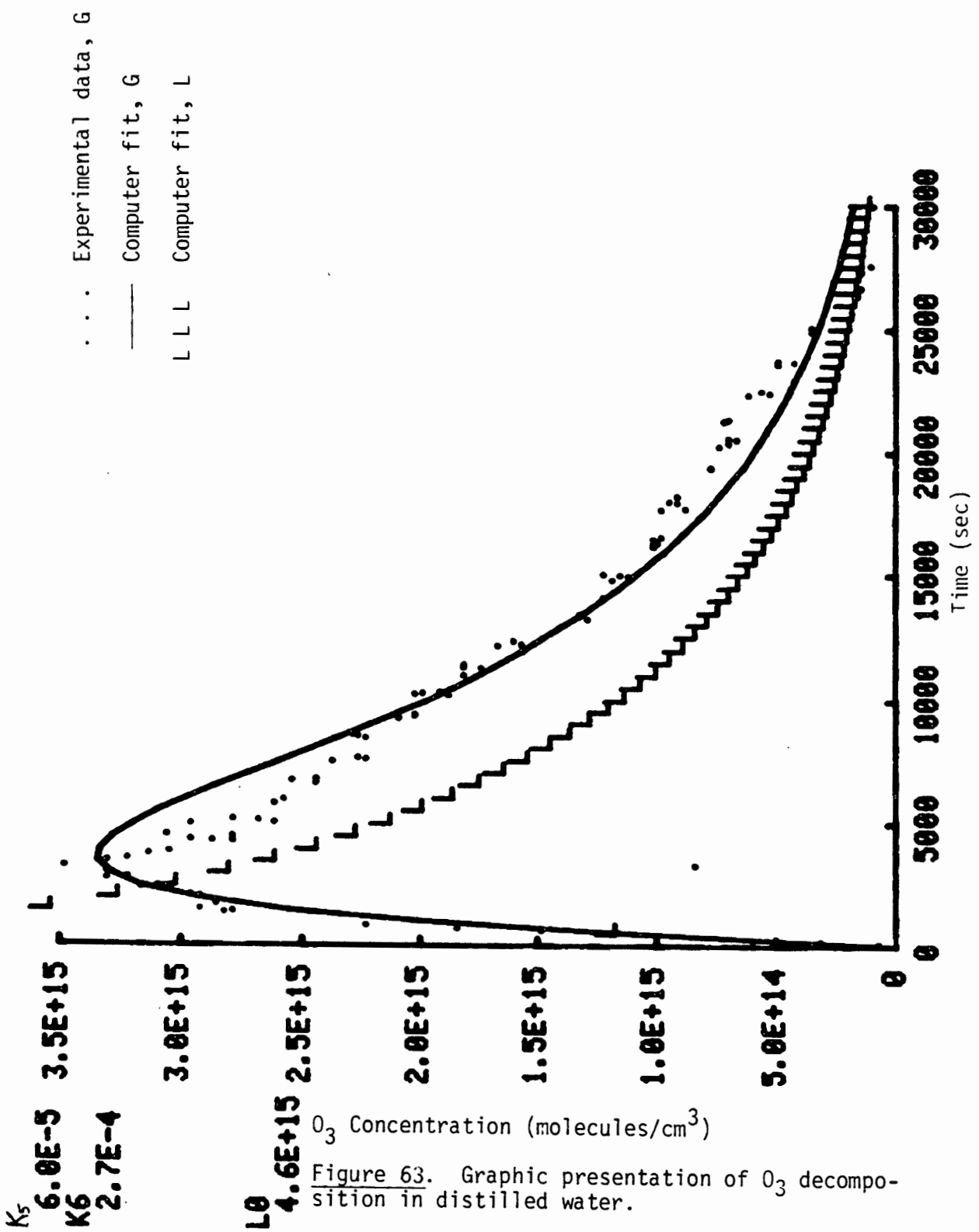

Figure 63. Graphic presentation of O_3 decomposition in distilled water.

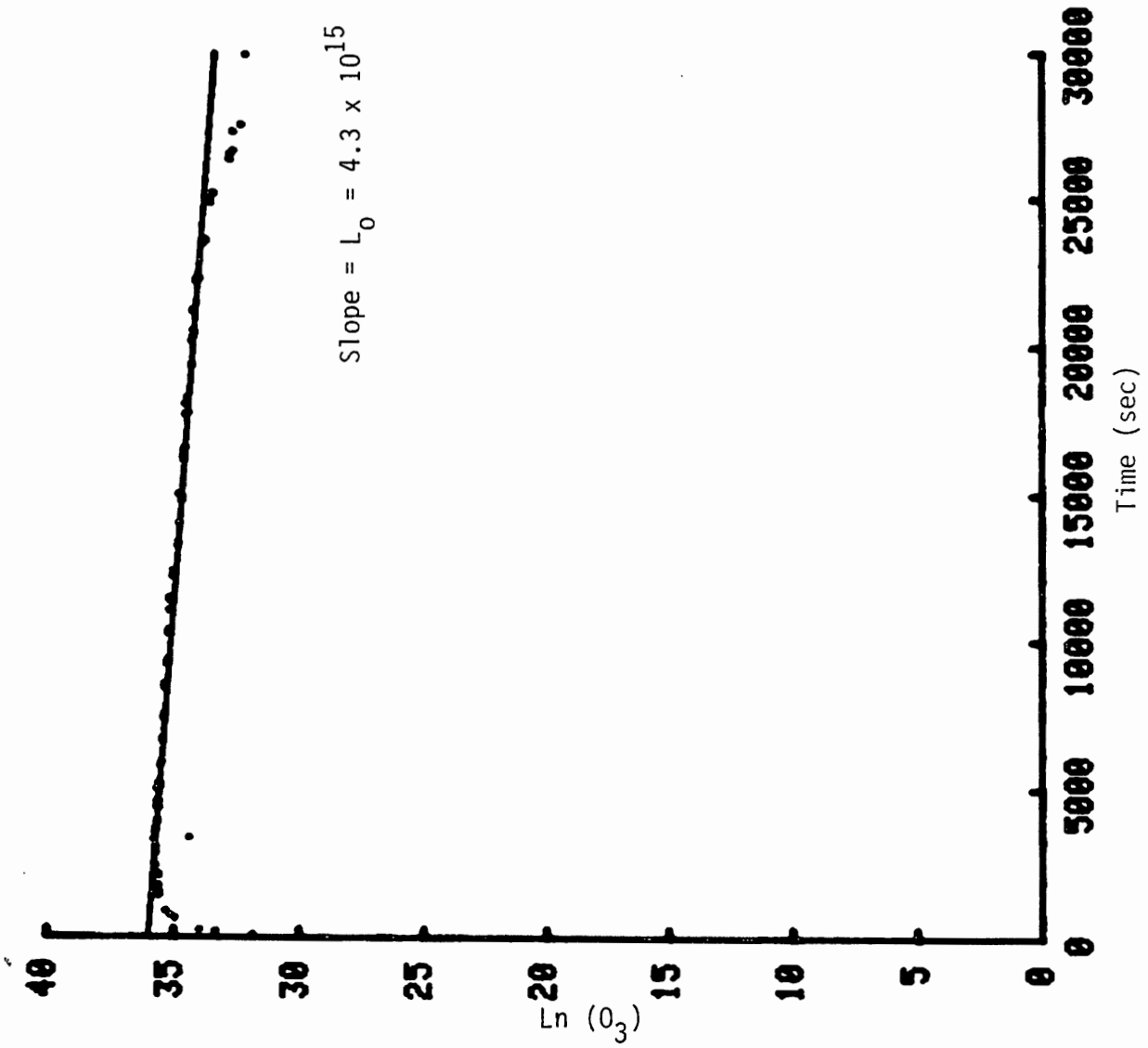

Figure 64. Extrapolate calculation of initial ozone concentration in solution.

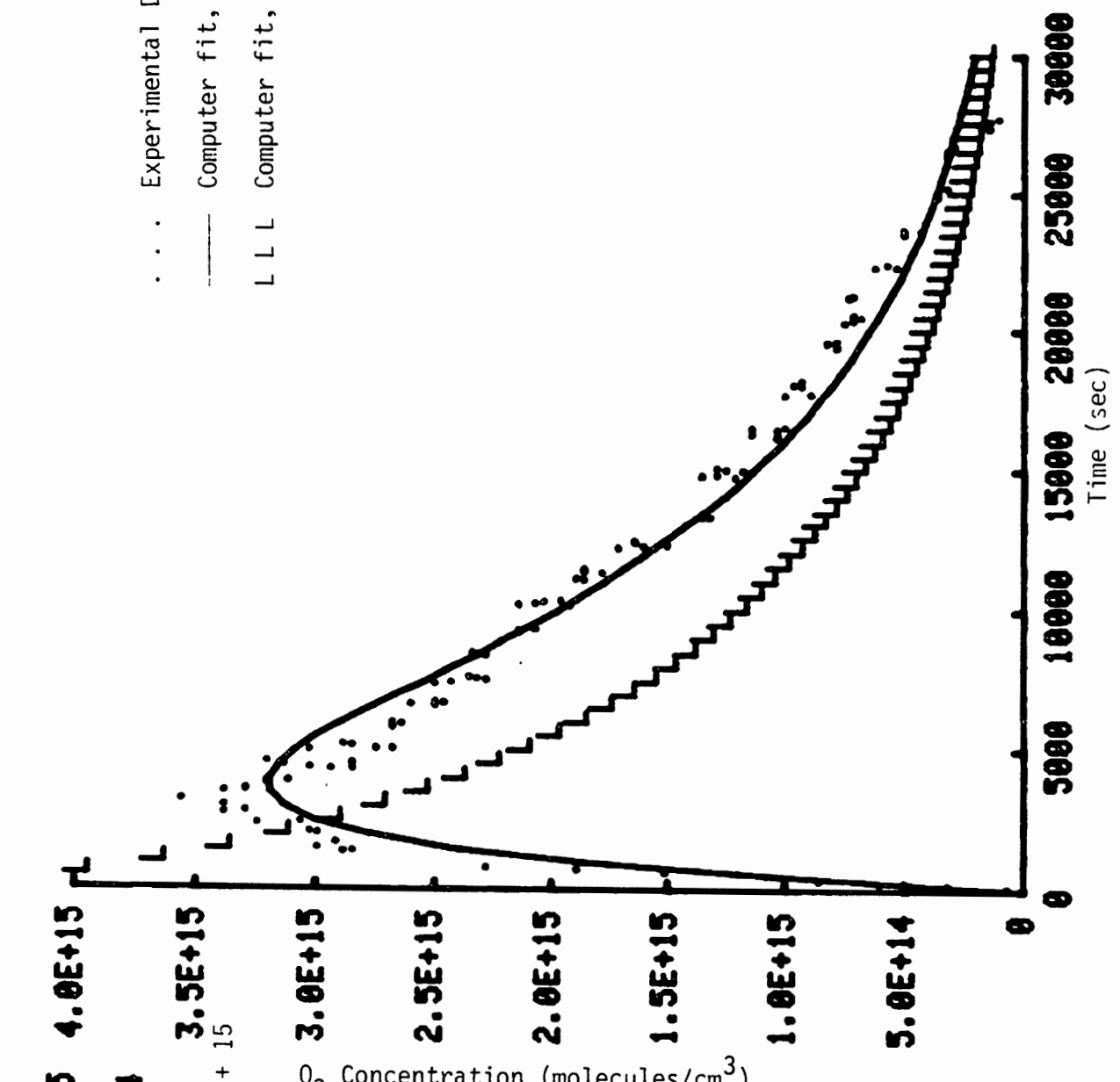

Figure 65. Graphic presentation of O_3 decomposition in distilled water.

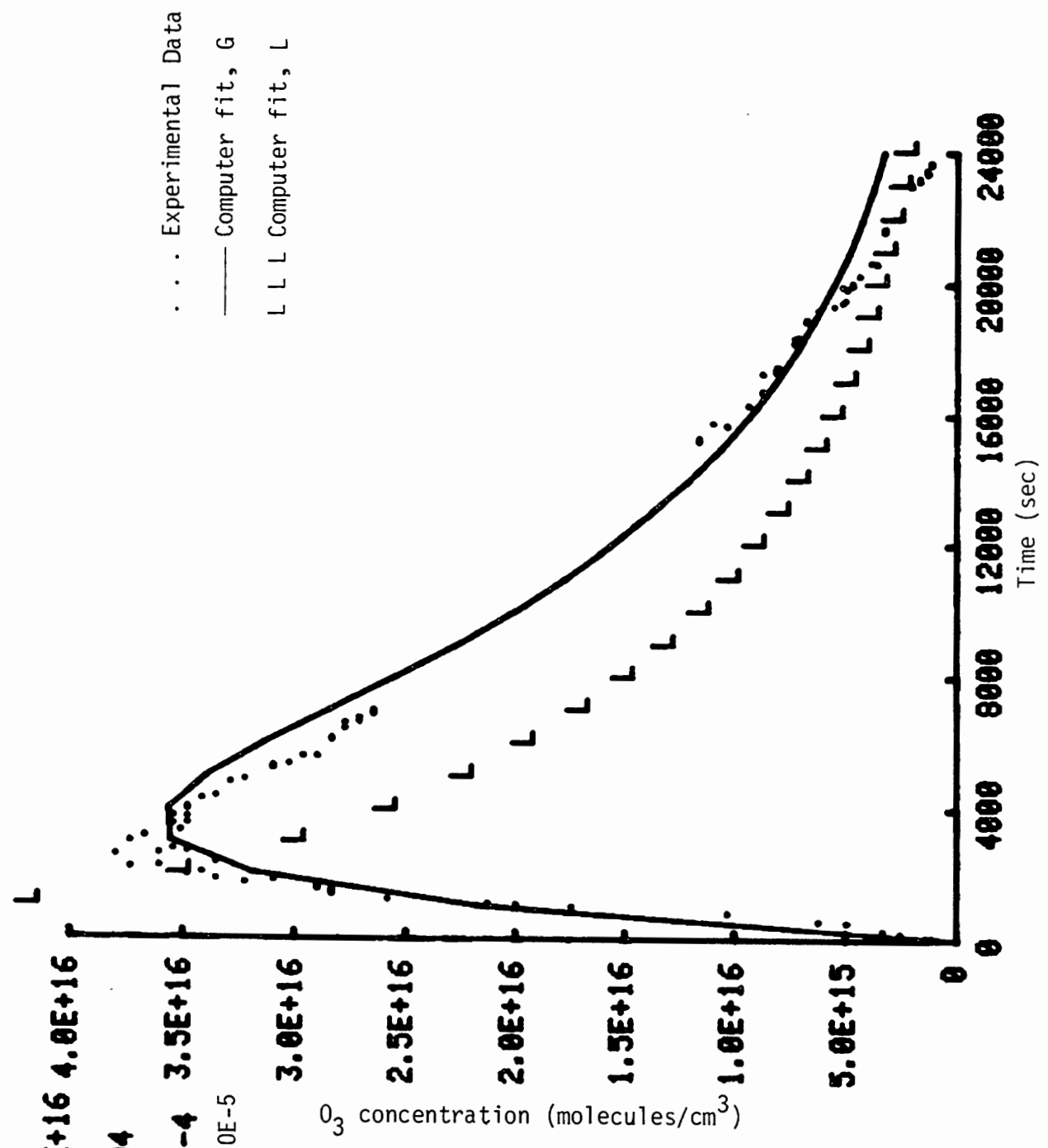

Figure 66. Graphic presentation of O_3 decomposition in distilled water.

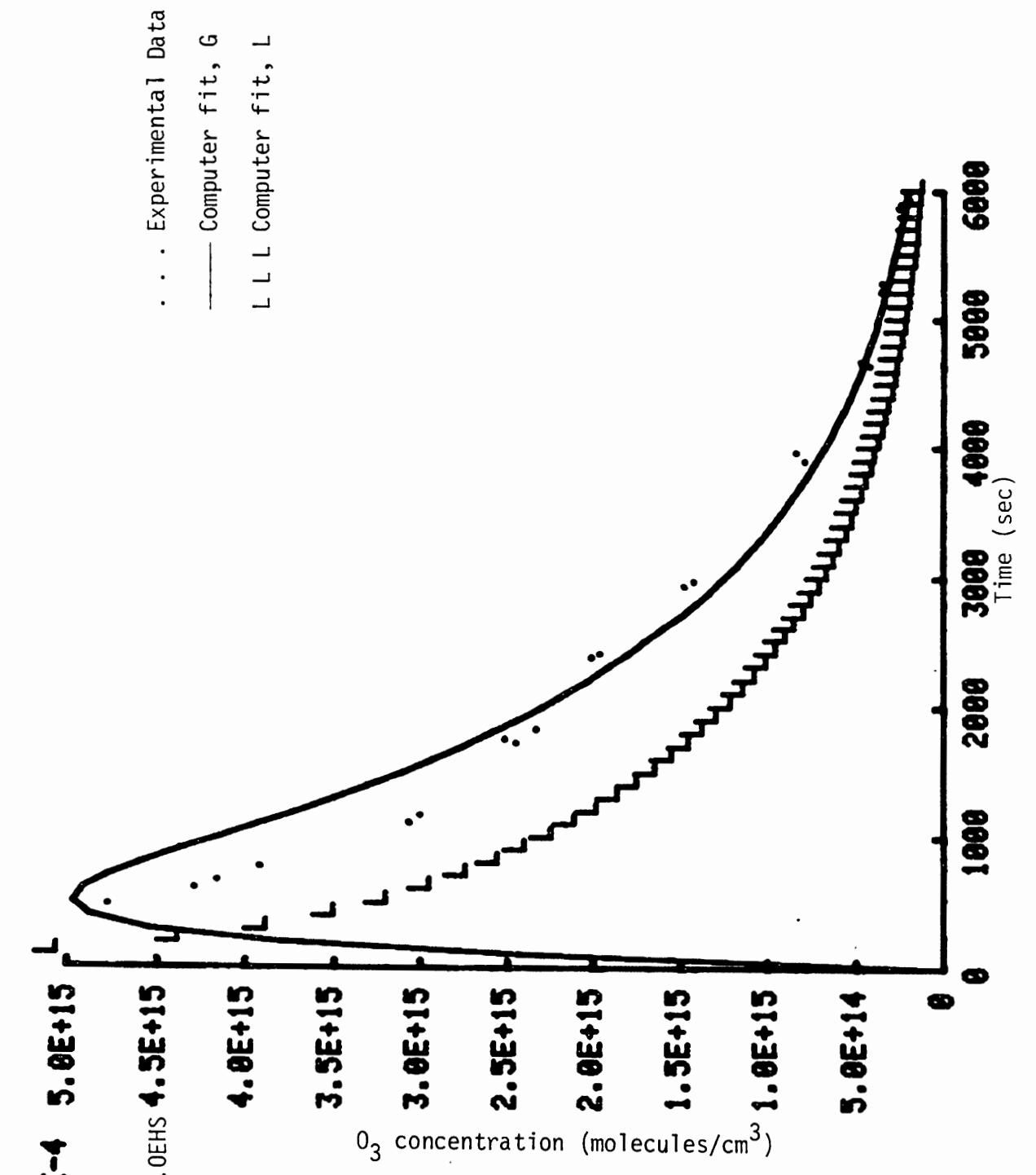

Figure 67. Graphic presentation of O_3 decomposition in ocean water (assuming O_3 decomposition first order).

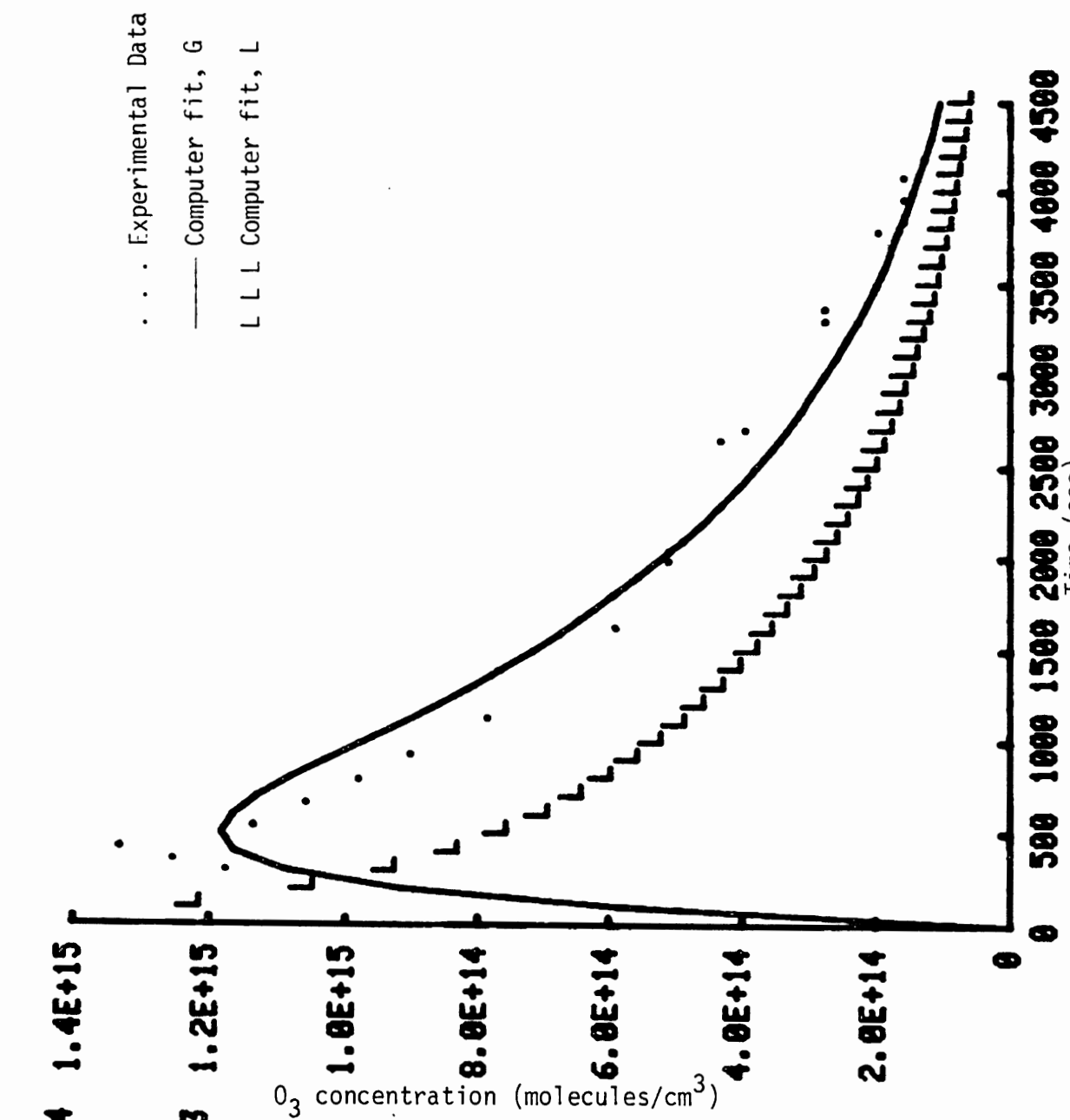

Figure 68. Graphic presentation of O_3 decomposition in ocean water (assuming O_3 decomposition first order).

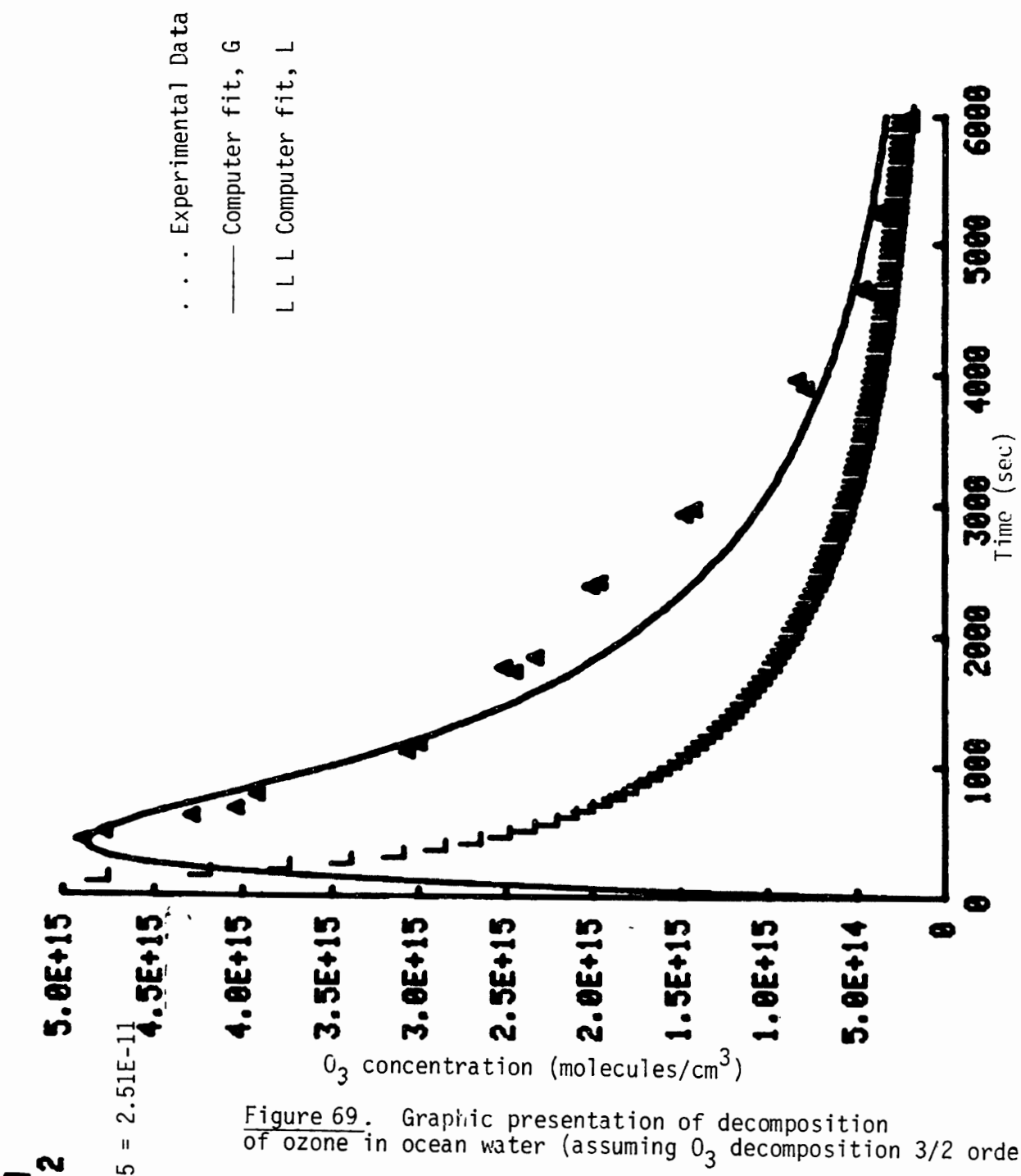

Figure 69. Graphic presentation of decomposition of ozone in ocean water (assuming O_3 decomposition 3/2 order).

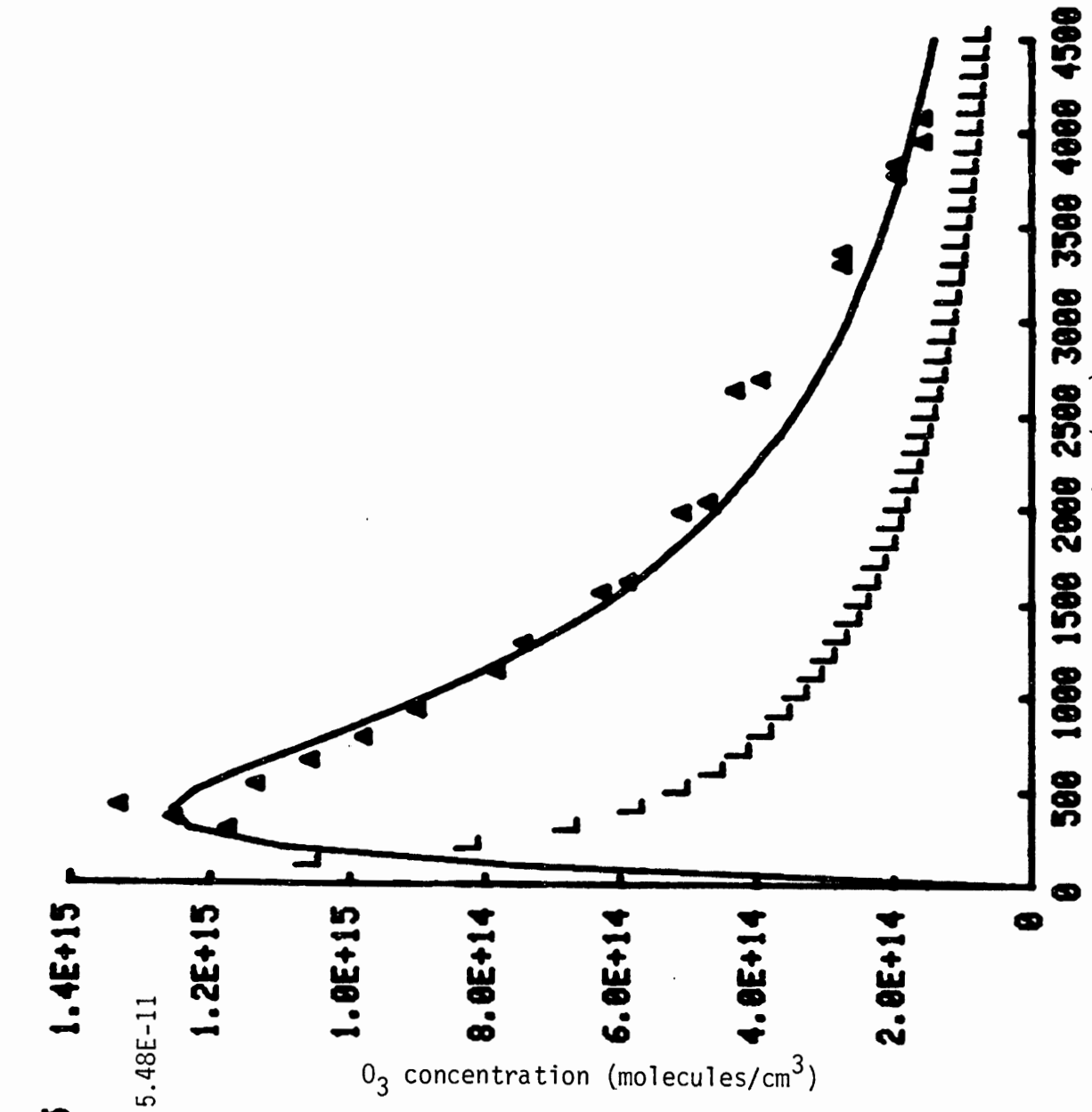

Figure 70. Graphic presentation of decomposition of ozone in ocean water (assuming O_3 decomposition 3/2 order).

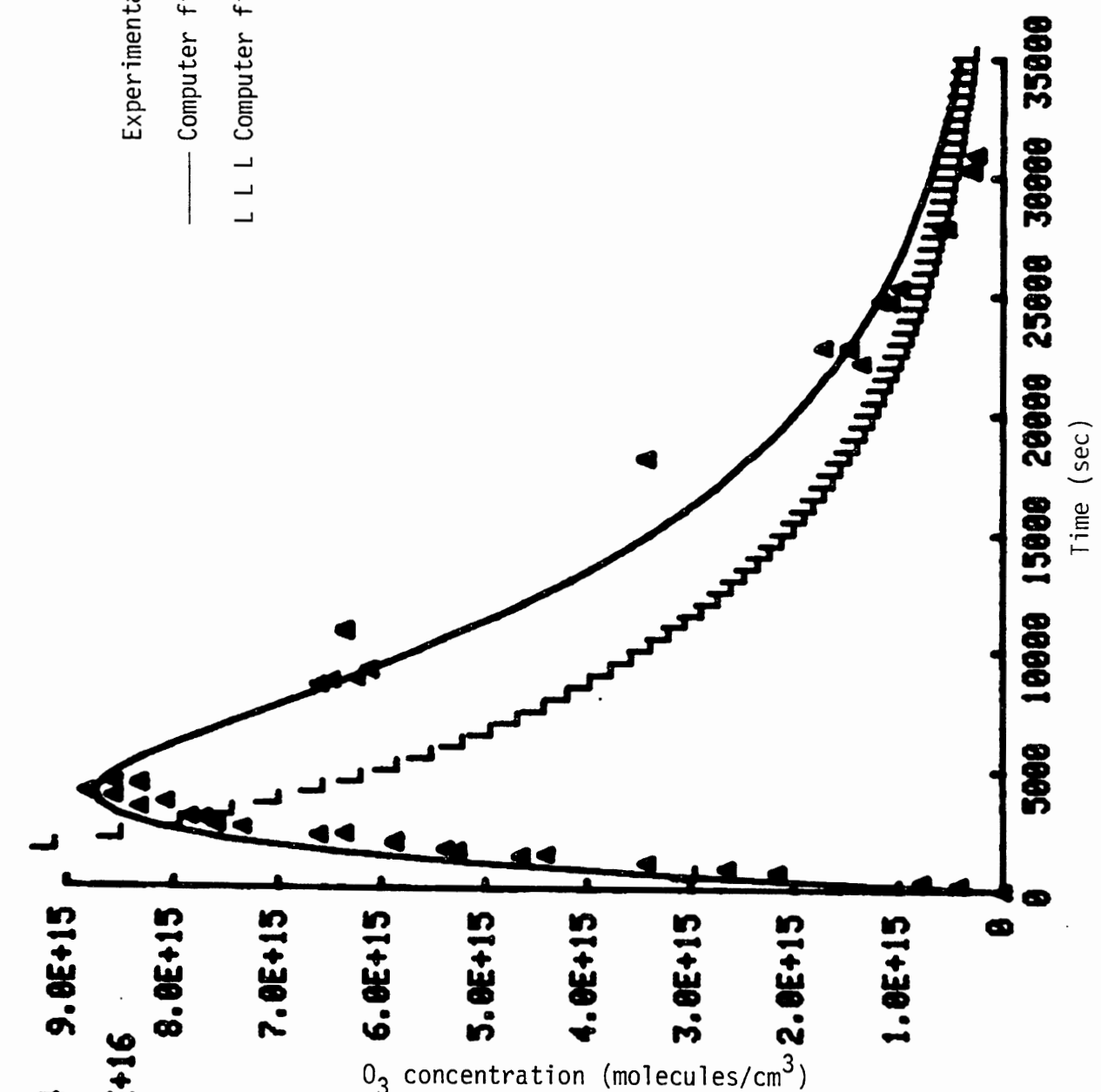

Figure 71. Decomposition of ozone in distilled water in room light.

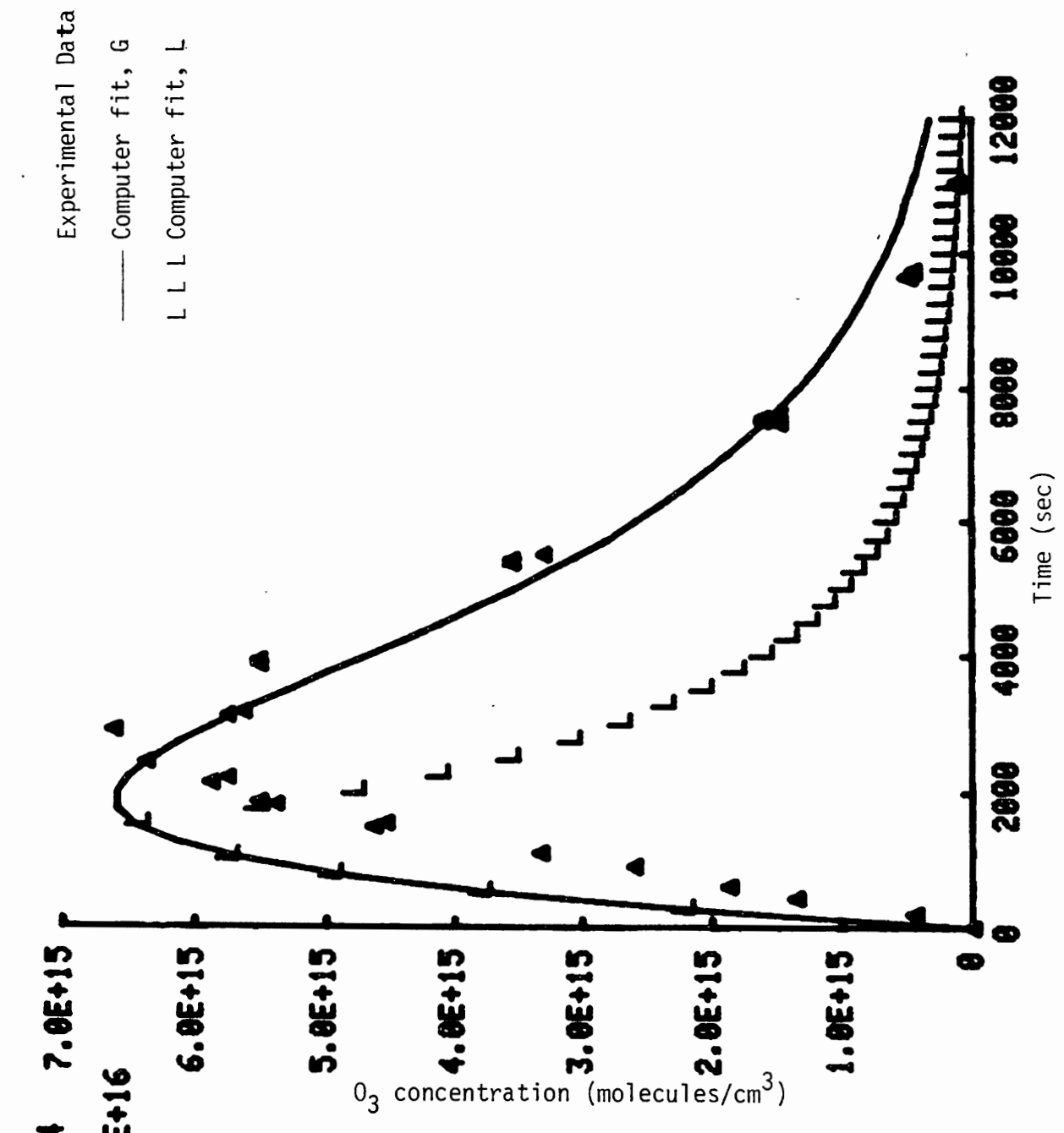

Figure 72. Decomposition of ozone in distilled water in room light.

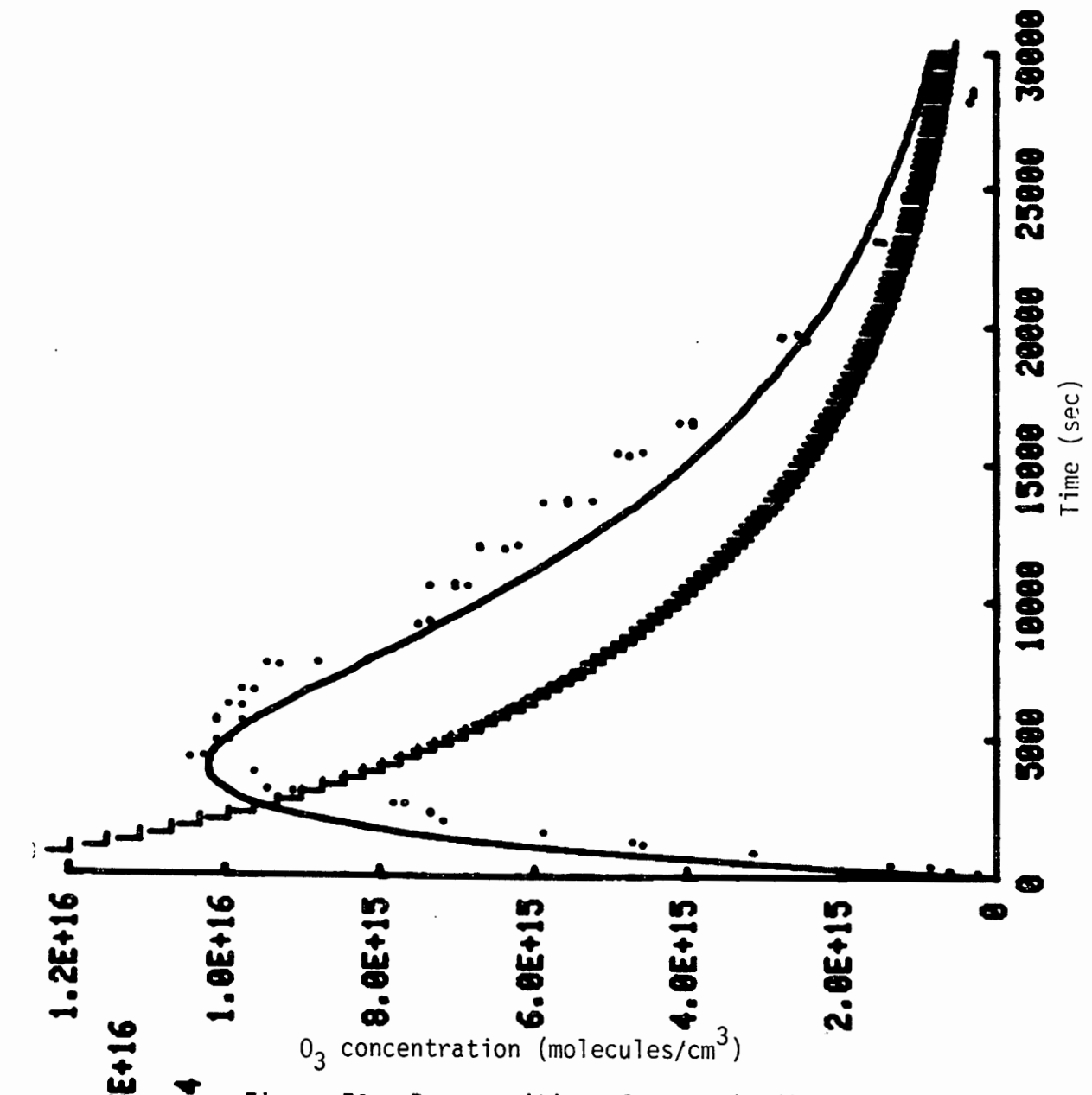

Figure 73. Decomposition of ozone in distilled water in darkness.

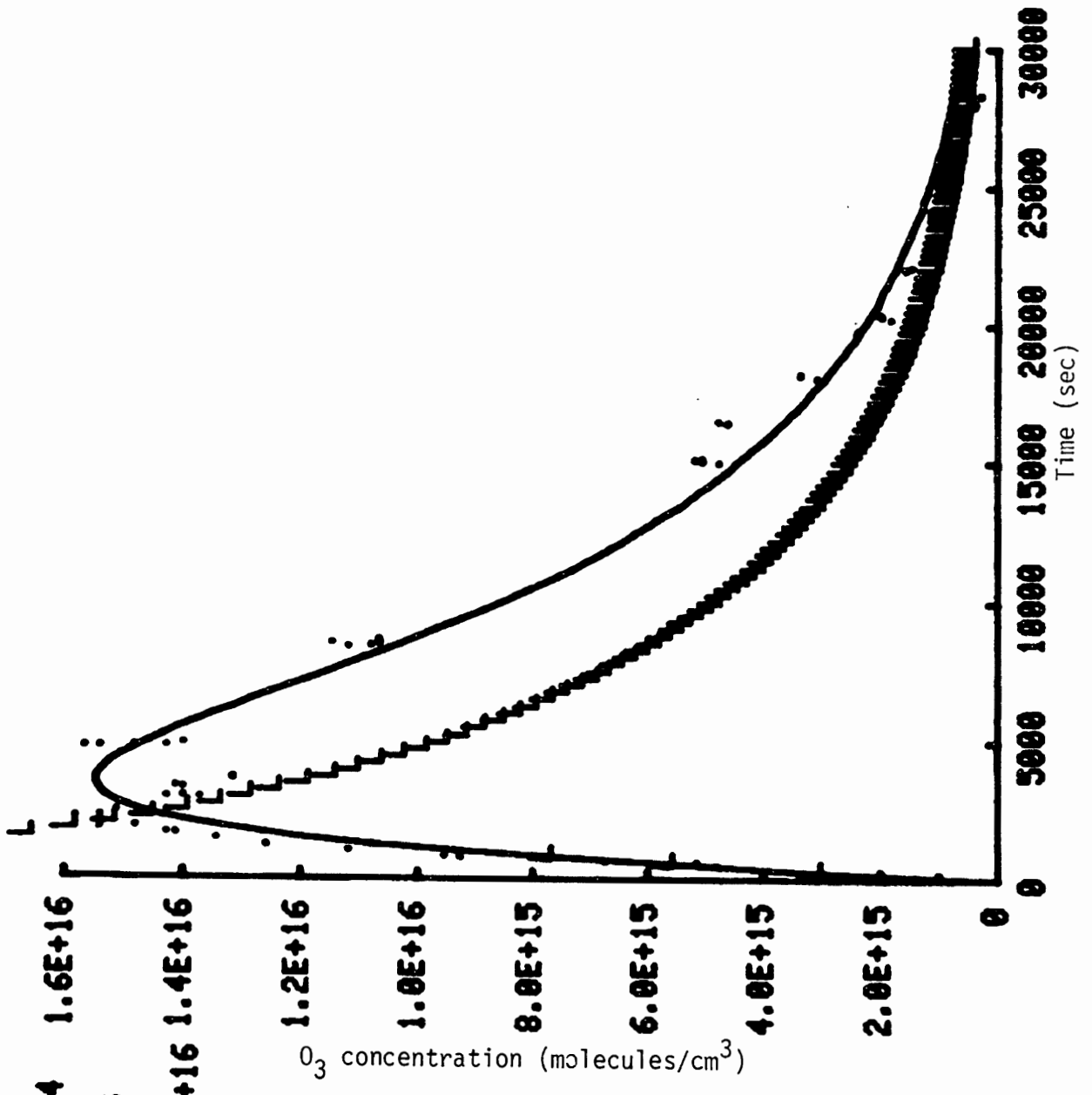

Figure 74. Decomposition of ozone in distilled water in darkness.

APPENDIX B

COMPUTER FILE

File 36

```
8020    V1 = 70
8030    V2 = 5000
8040    A = 10.2
8050    K6 = 2.7E-4
8060    H1 = V1/A
8070    H2 = 30
8080    M = -C2/H/H1
8090    N = C2/H/H2
8100    G = G0
8110    I = 0
8120    L = L0
8121    Move 0, 0
8130    For J = 1 to 10
8140        G = G+(M*(G-H*L)-K6*G)*I9
8150        L = L+(N*(G-H*L)-K5*L)*I9
8160        I = I+I9
8170    Next J
8180    Draw I, G
8181    Move I, L
8190    Print "L"
8200    Move I, G
8220    If I = T(7)  then 8240
8230    Go to 8130
8240    Home
8250    End
```

Lines 8020 through 8250 listed.

APPENDIX C

CONTROLLER

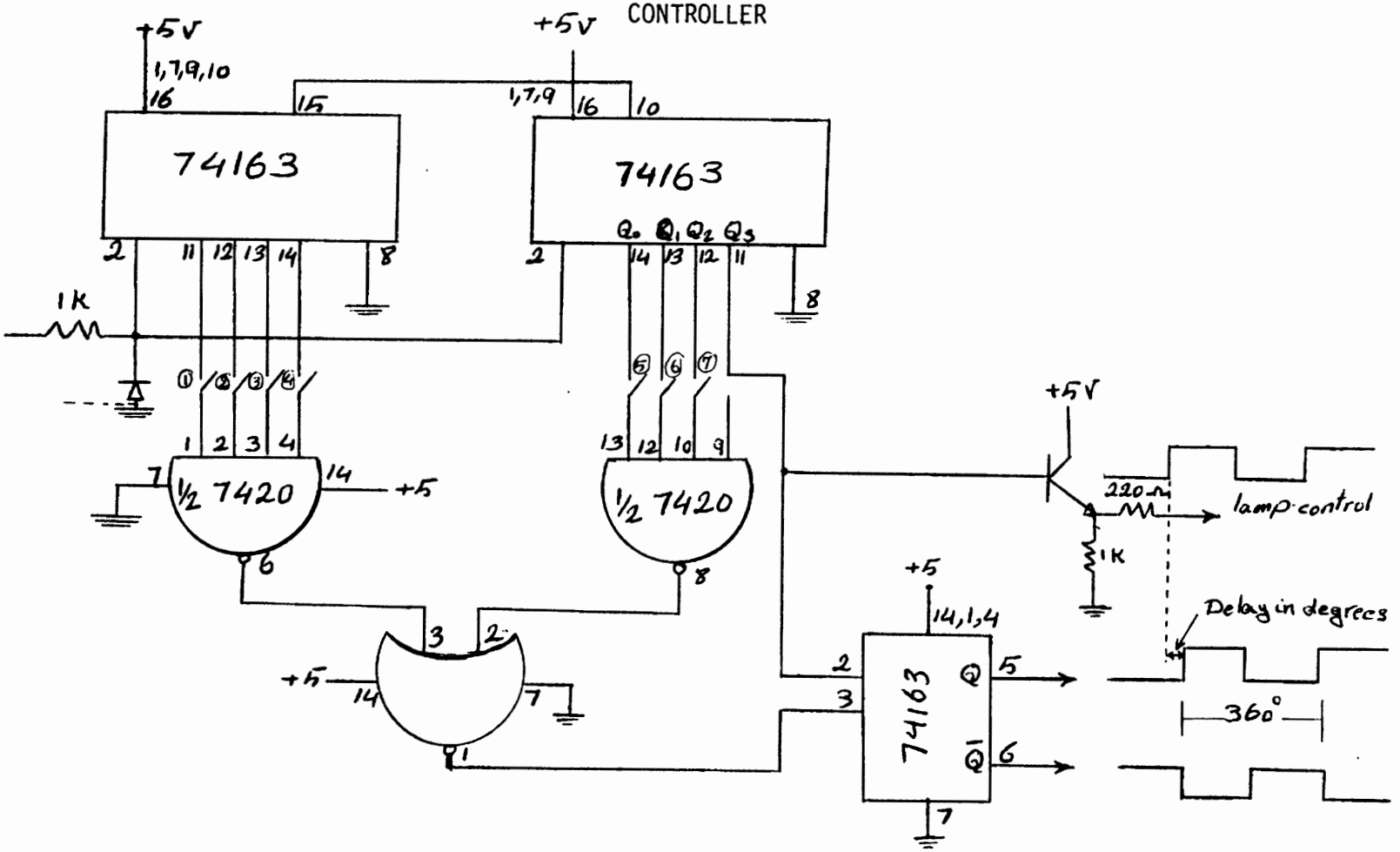

APPENDIX D

POWER APPARATUS

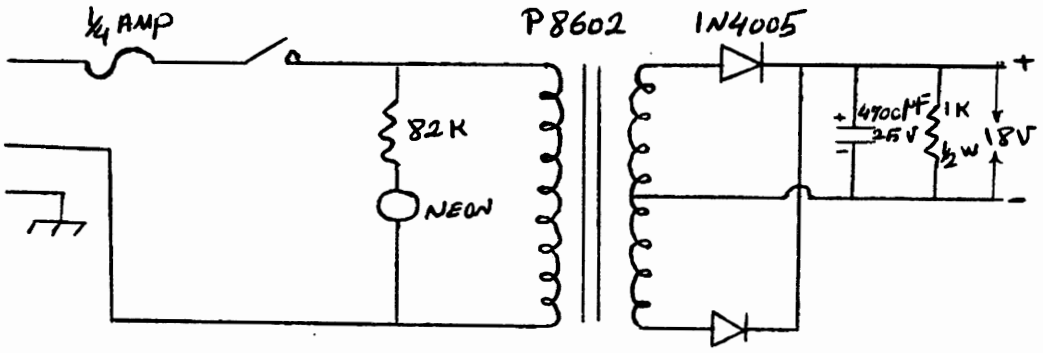

18 V Power Supply (20 Nominal)

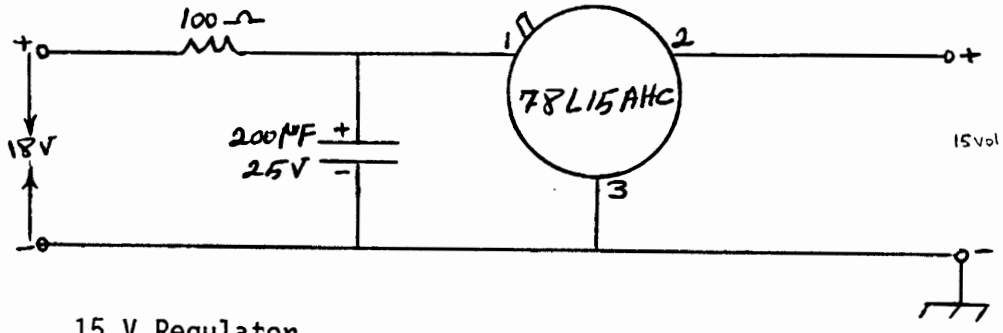

15 V Regulator

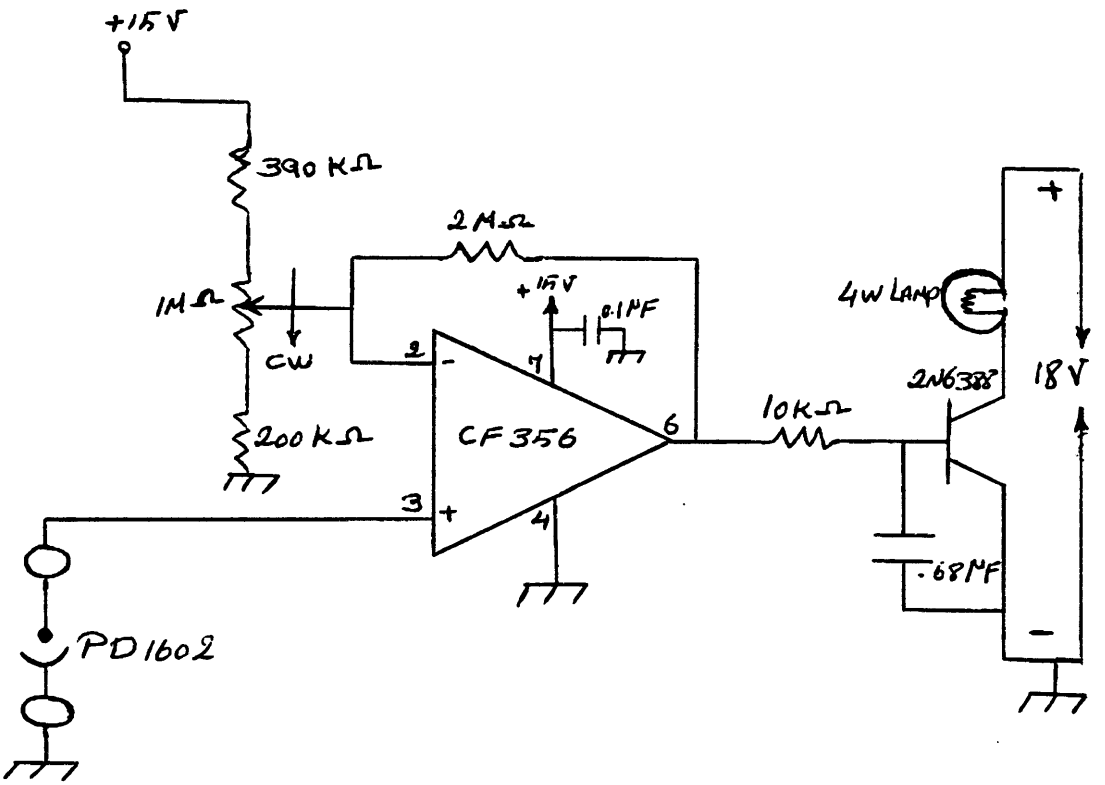

Photocell amplifier